Chem. Rev. 1989, 89, 1713–1747

Carbon Molecules, Ions, and Clusters

WILLIAM WELTNER, JR.,* and RICHARD J. VAN ZEE

Department of Chemistry and Chemical Physics Center, University of Florida, Gainesville, Florida 32611

Received November 16, 1988 (Revised Manuscript Received April 20, 1989)

Contents

I. Introduction

In recent years there has been increasing interest in pure carbon molecules, sometimes referred to as polycarbons. This is due principally to (1) the development of methods for the production of cold cluster beams, containing species up to C_{200}, which are subject to mass spectrometric detection and mass-selected spectroscopy; (2) rapid improvement in the accuracy and the feasibility of theoretical calculations and the enthusiastic application of those techniques not only to structures and electronic states but to ionization potentials, oscillator strengths, vibrational frequencies, etc.; (3) the fascinating, and unexpected, complexities in the properties and spectroscopy of these C_n species (for example, quasi-linearity and large Renner effects in C_3, linear and rhombic isoenergetic isomers of C_4, monocyclic aromatic rings or unique, threefold axial structures for n = 10–23, and the provocative ultrastable spheroidal C_{60} cluster); (4) awareness of the possible astrophysical significance of these species as contributors to the formation of the long-chain cyanopolyynes, carbon dust, polycyclic aromatic hydrocarbons, and diffuse interstellar bands; and (5) involvement of large C_n clusters in the nucleation of carbon particles and formation of soot in hydrocarbon flames. Hence, the study of polycarbons and their ions has broad implications.

We will refer to all of these implications in this review, but our main theme is the consideration of where we now stand experimentally and, to a lesser extent, theoretically in the search for information on neutral and ionic carbon molecules. It will be seen that the present knowledge of C_n molecules and their ions is almost a monotonically decreasing function of n. We emphasize that our principal concerns are with their structural, electronic, and vibrational properties as deduced spectroscopically in the gas phase or solid state.

This literature survey extends up to November 1, 1988.

II. C_2 Molecule

C_2 occurs in a variety of chemical reactions and in a wide range of astrophysical objects. Energetic treatment of hydrocarbons, either by irradiation, by highly exothermic stripping reactions, or by exposure to high temperatures, invariably produces C_2 and often in an

0009-2665/89/0789-1713$06.50/0

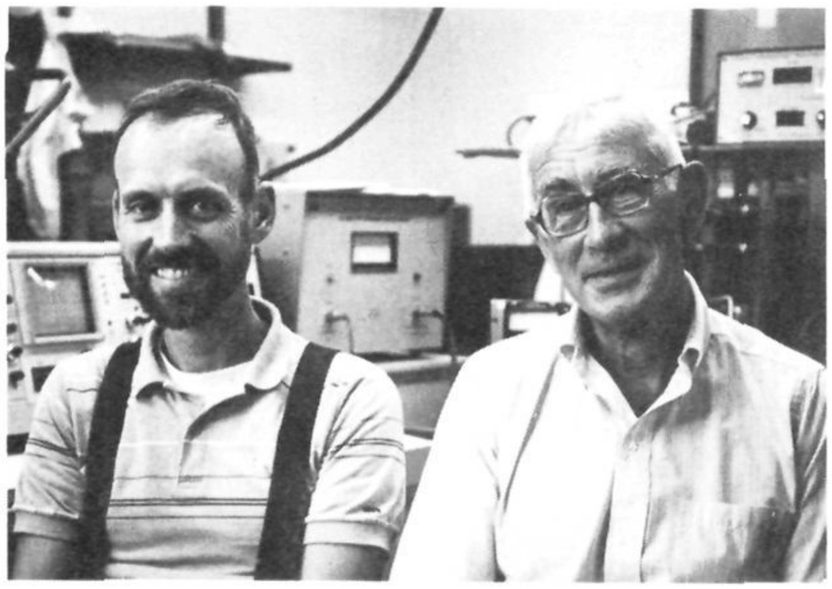

William Weltner, Jr. (right), was educated at The Johns Hopkins University and the University of California at Berkeley. Since 1966, he has been Professor of Chemistry at the University of Florida, Gainesville, FL. Richard J. Van Zee (left) was educated at Western Kentucky University and Michigan State University. He has been a Senior Research Associate in the Chemistry Department at the University of Florida since 1979. Their interests center around molecular spectroscopy and structure and electron spin resonance. The present emphasis is on small clusters, including metals.

emissive excited state.[1] C_2 appears in the atmospheres of carbon stars[2] and in the sun,[3] as well as in comets[4] and diffuse interstellar clouds.[5]

Huber and Herzberg[6] tabulated the electronic, structural, and vibrational properties of C_2 known as of about 1977. Every year since then there have been numerous papers identifying C_2 in some gaseous source and often adding to the detailed knowledge of its spectroscopy.

Presently about 17 electronic states of C_2 have been identified. The bands most often observed are the strong Swan system $d^3\Pi_g \rightarrow a^3\Pi_u$ at ~19 400 cm^{-1}. [Because of their prominence it was earlier assumed that the $^3\Pi_u$ state was the ground electronic state; this was also not in conflict with molecular orbital theory at the time.] Ballik and Ramsay[7] observed perturbations of the rotational levels in the $b^3\Sigma_g^-$ state (lying 5700 cm^{-1} higher than the $a^3\Pi_u$ state) indicating interaction with the rotational levels of a low-lying $^1\Sigma_g^+$ state, which was subsequently assigned as the ground state. These perturbations have recently been more thoroughly analyzed by Roux et al.[8] The $a^3\Pi_u$ state was found to lie only 716 cm^{-1} above the $X^1\Sigma_g^+$ state. Well-known band systems involve transitions to this lowest state: the Phillips bands $A^1\Pi_u$–$X^1\Sigma_g^+$ at 8268 cm^{-1} and the Mulliken bands $D^1\Sigma_u^+$–$X^1\Sigma_g^+$ at 43 227 cm^{-1}. Improved molecular constants have recently been derived for the $A^1\Pi_u$ and $X^1\Sigma_g^+$ states by reanalysis of the infrared part of the Phillips system by Douay, Nietmann, and Bernath.[9]

There are then three very low lying excited states above the $X^1\Sigma_g^+$ ground state beginning with the $a^3\Pi_u$ state at 716 cm^{-1}, then the $b^3\Sigma_g^-$ state at 6434 cm^{-1}, and then the $A^1\Pi_u$ state at 8391 cm^{-1}. The electronic configurations corresponding to these states are

$X^1\Sigma_g^+$	$KK(\sigma_g2s)^2(\sigma_u2s)^2$	$(\pi_u2p)^4$
$a^3\Pi_u$, $A^1\Pi_u$	...	$(\pi_u2p)^3(\sigma_g2p)$
$b^3\Sigma_g^-$, $B^1\Delta_g$, $B'^1\Sigma_g^+$	...	$(\pi_u2p)^2(\sigma_g2p)^2$

The missing $B^1\Delta_g$ and $B'^1\Sigma_g^+$ states arising in the last configuration have recently been found by Douay, Nietmann, and Bernath[10] by detection of the $B^1\Delta_g$–$A^1\Pi_u$ and $B'^1\Sigma_g^+$–$A^1\Pi_u$ transitions in infrared emission of hydrocarbon discharges (see Figure 1). These states had been predicted earlier by ab initio calculations.[11] The next higher state which is still at quite low energy is the $c^3\Sigma_u^+$ state, with T_e = 9227.4 cm^{-1}, derived from the configuration

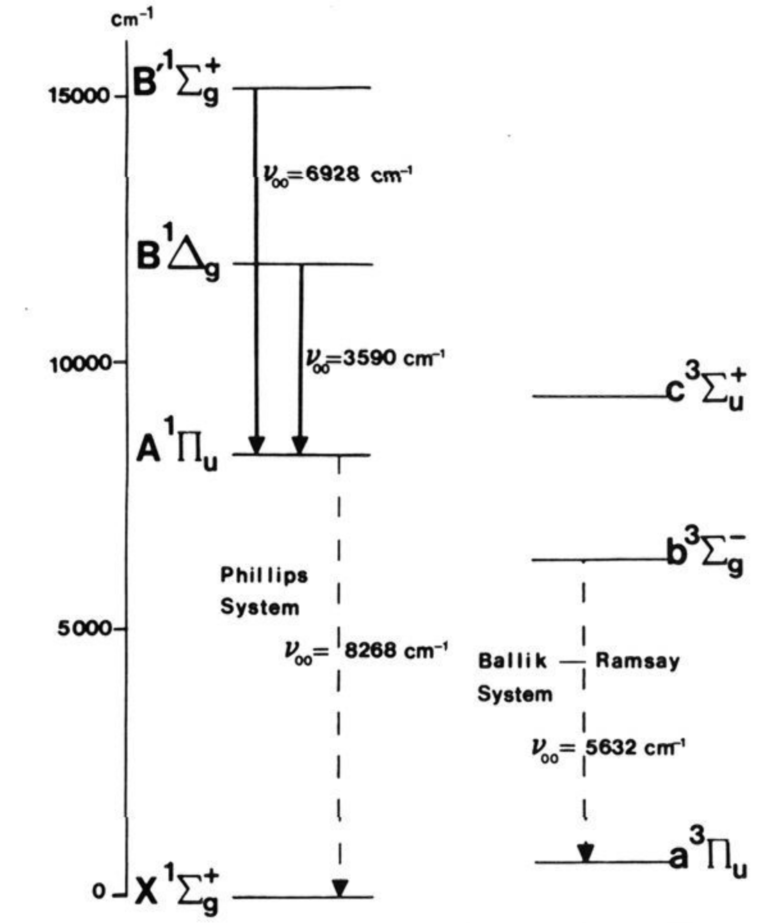

Figure 1. Lowest electronic states of the C_2 molecule. Transitions from the $B^1\Delta_g$ and $B'^1\Sigma_g^+$ states have recently been observed by Douay, Nietmann, and Bernath. (Reprinted from ref 10; copyright 1988 Academic Press, Inc.)

$$KK(\sigma_g2s)^2(\sigma_u2s)(\pi_u2p)^4(\sigma_g2p)$$

This was corrected by the infrared studies of Chauville, Maillard, and Mantz[12] from the previously accepted value of 13 310 cm^{-1}.[6]

Recent spectroscopic studies of Davis et al. have measured improved molecular parameters of $^{12}C_2$.[13] Pesic et al.[14] observed the Swan bands of $^{13}C_2$ and $^{12}C^{13}C$ and determined isotope effects upon band origins and molecular vibrational and rotational parameters. A series of high-resolution Fourier transform spectroscopic studies of $^{12}C_2$, $^{13}C_2$, and $^{12}C^{13}C$ were made by Amiot and co-workers. Amiot, Chauville, and Maillard[15] restudied the Ballik–Ramsay system of $^{12}C_2$ in the 4850–9900-cm^{-1} range, determined molecular constants, and reduced the rotational perturbations. Amiot and Verges[16] recorded the (0–0) band of the Swan system of $^{12}C_2$, $^{13}C_2$, and $^{12}C^{13}C$ by Fourier spectroscopy and made a complete analysis for the $a^3\Pi$ and $d^3\Pi(v = 0)$ levels. Many perturbations were observed in the $d^3\Pi(v = 0)$ level, and their origins were discussed. The (0–0) and (1–0) bands of the Phillips system and the (0–0) band of the Ballik–Ramsay system of $^{13}C_2$ and $^{12}C^{13}C$ were similarly observed and analyzed with the high accuracy of the Fourier transform interferometer. More recently, Curtis and Sarre[17] analyzed the nuclear hyperfine structure of $^{13}C_2$ in the $d^3\Pi_g$ and $a^3\Pi_u$ states resolved by laser-induced fluorescence to yield the Fermi-contact parameter b_F as 656 (9) and 43 (10) MHz, respectively. This reflects the difference in s character in the $\sigma_u 2s$ vs the $\sigma_g 2p$ orbitals in the two states where configurations differ only by the occupation of these orbitals by one of the odd electrons.

$b^3\Sigma_g^- \leftarrow a^3\Pi_u$ Ballik–Ramsay transitions were observed in absorption for the first time using a color center laser and magnetic rotation spectroscopy by Yan et al.[18] Many semiforbidden satellite lines which would be weak in normal absorption were observed with intensity comparable to main-branch lines. Some improvement in the accuracy of fine structure constants, particularly the spin-doubling constants, was made relative to the parameters of Amiot et al.[15,16]

Two rovibronic bands at ~22 400 cm^{-1} were tentatively assigned to a transition from a previously unknown strongly bound upper $^3\Sigma_g^+$ state [perhaps with the configuration $KK(\sigma_g 2s)^2(\sigma_u 2s)(\pi_u 2p)^4(\sigma_g 3s)$] to the $c^3\Sigma_u^+$ state by van der Burgt and Heaven.[19]

A high-lying new $1^1\Delta_u$ state was discovered by Goodwin and Cool[20] at 57 719 cm^{-1} above the ground state by resonance-enhanced multiphoton ionization of C_2.

A. Recent Theoretical Calculations of Spectroscopic Constants

Ab initio calculations of equilibrium geometries (third-order Møller–Plesset (M–P) perturbation and CID (DeFrees et al.[21])), of excitation and dissociation energies (augmented coupled cluster (Raghavachari[22])), and of both geometries and spectroscopic constants (both M–P perturbation and CAS–CI (Rohlfing and Martin[23])) have been made. Density-functional methods were also applied testing the basis set composition on LCAO-Xα (Dunlap[24]) and analysis of the types of correlation (Dunlap[25]), the local spin-density approximation (LSDA (Painter and Averil[26,27])), discrete variational Xα with Gaussian quadrature (Fukushima et al.[28]), and completely numerical calculations in the local-density approximation (Becke[29]), and a semirelativistic variant of the scattered wave–Xα method was compared to the full relativistic calculations (Heera, Seifert, and Ziesche[30]). Full configuration interaction (FCI), single-reference SDCI, coupled-pair functional (CPF), and CASSCF/MRCI treatments have been compared for the three lowest states of C_2 where the spectroscopic constants are well-known (Bauschlicher and Langhoff[31]).

Franck–Condon factors have been calculated by several methods (Walvekar and Rama,[32] Brown,[33] Kuz'menko and Chumak[34]). Partition functions and thermodynamic functions in the range 1000–9000 K have been compiled from the available molecular data (Sauval and Tatum,[35] Rossi, Maciel, and Benevides-Soares[36]).

Photoionization cross sections have been calculated for ionization of the $2\sigma_g$, $2\sigma_u$, and $1\pi_u$ orbitals of the $X^1\Sigma_g^+$ ground state in the frozen-core Hartree–Fock approximation by Padial, Collins, and Schneider.[37] SCF + CI wave functions and potential energy curves of the $X^1\Sigma_g^+$ state and the first four $^1\Pi_u$ states and transition moments to those states have been computed by Pouilly et al.[38] Photodissociation cross sections for absorption into the second and third $^1\Pi_u$ states were calculated and the interstellar photodissociation probability was found to be 0.73×10^{-10} s^{-1}.

B. Radiative Lifetimes and Oscillator Strengths

Experimentally determined lifetimes ($\tau_{v'}$), oscillator strengths ($f_{v'v''}$), and/or electronic transition moments squared ($\sum|R_e(v'v'')|^2$) of the important systems of C_2 were reviewed at least partially in 1976 by Tatarczyk, Fink, and Becker[39] and by Cooper and Nicholls,[40] in 1979 by Brewer and Hagan,[41] and in 1988 by Naulin, Costes, and Dorthe.[42] Progress during that period in the measurement of lifetimes using laser techniques has presumably yielded more accurate data. Also in the 1980s ab initio theory has been increasingly applied to calculate these properties. A great advantage of these calculations is that they provide a clear indication of the variation of the transition moments with r_{CC}, the interatomic distance; this variation is often quite large. In general, the agreement between theory and experiment has been good, although there are some outstanding discrepancies that suggest the application of the newer experimental techniques to other band systems. Also, refinement of theory has been found necessary to adequately treat the $A^1\Pi_u$–$X^1\Sigma_g^+$ (Phillips) system. The prominent systems will be briefly considered here:

Swan System ($d^3\Pi_g \rightarrow a^3\Pi_u$). Measurements made since 1976,[39,43–46] and some earlier data,[41,47,48] appear to support a value of $\tau_{v'=0} = 120 \pm 10$ ns ($f_{00} = 0.025 \pm 0.002$), but in the past few years lower values have emerged: 92 (5),[49] 106 (15),[50] and 101.8 (4.2) ns.[42] The last named was obtained from the laser-induced fluorescence decay of supersonically cooled $C_2(d^3\Pi_g)$. That lifetime leads to revision of Cooper and Nicholls'[40] value of $\sum|R_e|^2 = 3.52$ (0.50) au to 4.3 au at the bond distance of 2.44 bohr, which is in better agreement with the theoretical values of 4.12,[51] 4.65,[52] and 4.10 au.[53] f_{00} would then be raised to 0.031 (1).

Phillips System ($A^1\Pi_u - X^1\Sigma_g^+$). A recent measurement of the radiative lifetimes of the $A^1\Pi_u(v' = 0, 3)$ states by laser-induced fluorescence has yielded values of 18.5 ± 3 and 11.4 ± 2 μs, respectively.[50] A corresponding f_{00} value is 1.5×10^{-3} (in excellent agreement with the value of 1.41×10^{-3} obtained in 1982 by Brault et al.[3] from high-resolution solar spectra). $\tau_{v'=0}$ is about twice other earlier values derivable from experiments, 9.9[45,48] ($f_{00} = 3.94 \times 10^{-3}$) and 7.1 μs,[45,54] and also twice the values obtained from three theoretical calculations[38,55–57] which yielded closely agreeing values of about 11 μs and $f_{00} = 2.7 \times 10^{-3}$. O'Neill, Rosmus, and Werner[58] addressed this discrepancy by an ab initio calculation with single and double excitations from state-averaged MC–SCF reference functions in MC–CI wave functions. They found $\tau_{v'=0} = 14$ μs and $f_{00} = 2.13 \times 10^{-3}$, which are in better but still not complete agreement with the later experiment. Remaining possible causes for error in the calculations were discussed.[58]

Ballik–Ramsay System ($b^3\Sigma_g$–$a^3\Pi_u$). Experimental values are $\tau_{v'=0} = 17.2$ μs,[48,56] $f_{00} = 1.18 \times 10^{-3}$, and $\sum|R_e|^2 = 0.65$ (15) au ($\Delta v = +2$).[48] Theoretical values are $\tau_{v'=0} = 16$ μs and $f_{00} = 1.23 \times 10^{-3}$.[56] [An earlier calculation[53] yielded a considerably smaller f_{00} value.]

Fox–Herzberg System ($e^3\Pi_g$–$a^3\Pi_u$). Experimental values of $\sum|R_e|^2$ for $\Delta v = 0$ are 0.45 (10)[59] and 0.55 au.[60] For $\Delta v = -2$, Cooper and Nicholls measured 0.40 (10) au and $f_{00} = 1.75 \times 10^{-5}$,[40,48] but the latter assumed constant $\sum|R_e|^2$. Theoretical calculations of $\sum|R_e|^2$ show a sharply peaked, bell-shaped variation with r_{CC}.[52] The best comparisons with experiment are made at $r_{CC} = 2.9$ bohr for $\Delta v = 0$ where $\sum|R_e|^2 = 0.5$ and at $r_{CC} = 2.8$ bohr for $\Delta v = -2$ where the value is 0.38, in good agreement with experiment. Theory would place f_{00} about 30% lower than the above value.[52]

Mulliken System ($D^1\Sigma_u^+ - X^1\Sigma_g^+$). The one theoretical calculation done by Chabalowski, Peyerimhoff, and Buenker[56] [$\tau_{v'=0-3} = 14.5$ ns, $\sum|R_e|^2 = 0.40$ au, $f_{00} = 0.054$] is in good agreement with the old experimental studies of Smith[61] [$\tau_{v'=0} = 15.6$ (1.5) ns, $f_{00} = 0.055$ (6)], in fair agreement with Curtis, Engman, and Erman[43] [$\tau_{v'=0-3} = 18.1$ (1.0) ns], but in poor agreement with Cooper and Nicholls[40,48] [$\tau \cong 40$ ns, $\sum|R_e|^2 = 0.13$ (5) au, $f_{00} = 0.0171$]. It was suggested that the large discrepancy between theory and the Cooper–Nicholls data may be due to an error in the estimate of C_2 molecules in the upper state.[56]

Deslandres–d'Azambuja System ($C^1\Pi_g - A^1\Pi_u$). There is considerable discrepancy here between the theoretical data[56] [$\tau = 27$ ns, $\sum|R_e|^2 = 2.2$ au, $f_{00} = 0.040$] and the only experimental results of Cooper and Nicholls[40,48] [$\tau = 65$ ns, $\sum|R_e|^2 = 0.92$ au, $f_{00} = 0.0267$]. Chabalowski et al.[56] implied that, because this system is the singlet counterpart of the Swan system and also has a relatively large transition dipole, the theoretical treatment is as adequate as was that for the Swan system. Later experiments (see above) brought the experimental results for the Swan system to even better agreement with theory, so that the Cooper–Nicholls data are probably suspect here.

Freymark System ($E^1\Sigma_g^+ - A^1\Pi_u$). Here only the Cooper–Nicholls data are available: for $\Delta v = -1$, $\sum|R_e|^2 = 2.26$ (1.13) au and $f_{00} = 0.0464$.

C. Quadrupole and Intercombination Transitions

For interstellar and cometary C_2 radiative transitions between vibration–rotation levels of the same electronic state can occur only as slow, electric quadrupole transitions.[62] Excited vibrational states of $X^1\Sigma_g^+$ can also decay to lower levels of $a^3\Pi_u$ via spin–orbit interaction and subsequently relax by intercombination transitions[62–65] back to the lowest levels of the ground state. A corresponding mechanism occurs in the Swan bands of comets where vibrational transfers within the lower $a^3\Pi_u$ state can occur via a cascade through the $b^3\Sigma_g^-$ state levels. Both of these mechanisms have been examined by theoretical calculations.

The calculation of the quadrupole transition probability requires knowing the quadrupole moment Q as a function of internuclear distance. At $R_e = 1.24$ Å, the quadrupole moment Q in the $X^1\Sigma_g^+$ state was calculated (older to newer) to be 2.26 (10),[62] 2.35 (10),[63] ~1.94,[38] and 2.26 au[58] (multiply by 1.3450×10^{-26} to obtain esu cm^2). At shorter internuclear distances Q varies almost linearly with R, with a slope of about +2.3 au/bohr. At larger distances Q reaches a peak at ~1.3 Å and drops abruptly to negative values between 1.4 and 1.6 Å. The latter behavior is apparently due to an avoided crossing near 3.0 bohr which changes the dominant configuration contributing to the $X^1\Sigma_g^+$ wave function. Lifetimes for quadrupole decay in the $X^1\Sigma_g^+$ state were calculated by O'Neil et al.[58] and by van Dishoeck and Black[62] and agree within 5%. For example, the $(v' = 0, J' = 2) \rightarrow (v'' = 0, J'' = 0)$ lifetime is about 5.9×10^{16} s. O'Neil et al.[58] also calculated Q for the excited $A^1\Pi_u$ state as a function of R and found at $R_e = 1.32$ Å a value of about −0.4 au.

Intercombination transitions involving electric dipole radiation through spin–orbit coupling between states of C_2 was first treated by Lambert and Danks[65] and by Pouilly.[66] Although considered by the authors, Le Bourlot and Roueff,[67] to be still preliminary, new quantitative computations were carried out on the intercombination transition probabilities between the $a^3\Pi_u$ and $X^1\Sigma_g^+$ levels. The inclusion of the $b^3\Sigma_g^-$ state was shown not to be negligible. Experimental observation of intercombination lines is feasible and would allow evaluation of the theory.[62,67] Overall, in the purely radiative case, the indications are that depopulation of high vibrational levels in each of these states through intercombination transitions is much more effective ($\tau \cong 10^{-3}$ s^{-1}) than quadrupole transitions ($\tau \cong 10^{-7}$ s^{-1}) in achieving statistical equilibrium.[65,67]

D. High-Pressure Bands

An electrical discharge through CO at a relatively high pressure of ~0.1 atm produced the single $v' = 6$ progression of the $d^3\Pi_g \rightarrow a^3\Pi_u$ Swan system. This specific emission spectrum continues to be called the high-pressure bands[68–71] even though they are found to be produced under a wide variety of conditions including irradiation of graphite by a ruby laser focused off the surface,[72] in a carbon arc in the presence of a flowing mixture of He, N, and N_2,[73] in α-particle bombardment of He–CO mixtures at atmospheric pressure,[74] even in discharges[75] and afterglows[76] at lower CO pressure, and in the emission following UV fragmentation of CO.[77] Several mechanisms have been proposed for this intriguing enhancement of transitions with $v' = 6$ beginning with Herzberg's,[78] which involved the formation of excited C_2 from free carbon atoms. Setser and Thrush[79] suggested that formation occurs through the $b^3\Sigma_g^-$ state, which then populates the $d^3\Pi_g(v = 6)$ level. Other mechanisms involving metastable C_3, nitrogen atoms and intermediate C_2O have been proposed. Little and Browne[80] offered objections to all of these mechanisms and argued that the observation of the high-pressure bands under such a variety of experimental conditions requires a generally applicable mechanism. They proposed that the unobserved, but theoretically predicted (Kirby and Liu[81]), $^5\Pi_g(v = 0)$ state crosses at the $v = 6$ level of the $d^3\Pi_g$ level and emission occurs overwhelmingly from that level.

III. C_2^- Ion

A. Electron Affinity of C_2

Although recent calculations have predicted the spectroscopic constants of the low-lying states of C_2 and C_2^- very well,[82,83] it has been more difficult for theory to yield an accurate value of the electron affinity (EA) of C_2. Dupuis and Liu[84] specifically addressed this problem by examining various levels of CI but obtained values of the EA varying from 2.84 to 3.75 eV, compared to the experimental bounds 3.374–3.408 eV derived by Nichols and Simon.[85] This C_2/C_2^- system is particularly hard because of the large electron correlation effects involved. Again, Zeitz, Peyerimhoff, and Buenker[82] using MRDCI and Rosmus and Werner[83] using MCSCF-SCEP found it difficult to place the C_2^- states relative to the C_2 states required for determining the adiabatic EA of C_2. Nichols and Simons[85] used multiconfigurational self-consistent field (MCSCF)/electron propagator (MCEP) methods, limiting themselves primarily to the $X^2\Sigma_g^+$ and $B^2\Sigma_u^+$ states of C_2^- and the $X^1\Sigma_g^+$ and $a^3\Pi_u$ states of C_2 but over a wide range of bond lengths. If the anion states are shifted downward by approximately 0.3 eV (such an error in calculated EAs is not unusual), good agreement is obtained between calculated and experimental C_2–C_2^- energy differences. It is clear that this is a difficult theoretical calculation requiring further exploration.

B. Background

Besides intrinsic interest, C_2^- is noteworthy because it is one of few negative ions to have bound valence states (as opposed to Rydberg-like excited states)[86] below the continuum onset determined by the electron affinity of C_2 at 3.4 eV.

This ion may be present in carbon stellar atmospheres[87,88] or in the interstellar medium,[89] but it has not been detected as yet. The known stabilities of dicarbide molecules in the vapor over metal carbides and the presence of C_2 units in solid ionic carbides suggest that there is an analogy between the C_2 unit and an O atom.[90-93] Thus, M–C_2 bonding has similarities to that in the corresponding M–O diatomic oxide molecules. The treatment of C_2 as a pseudo-oxygen is not without precedence since it corresponds to the longstanding consideration among chemists of CN as a pseudo-halogen.

The first observation of this molecule was probably made by Honig[94] when he sampled the negative ions emitted by heated graphite at temperatures up to ~ 2600 K using mass spectrometric techniques. C_2^-, C_4^-, and C_3^- were the most abundant species, in that order. However, the molecule was first observed by optical spectroscopy by Herzberg and Lagerqvist.[95] They measured absorption and emission spectra of transitions (530–545 nm) between the ground $X^2\Sigma_g^+$ state and the excited $B^2\Sigma_u^+$ state when C_2^- was formed in a flash discharge of methane, although at the time the identification was not positive. Additional evidence that these bands were due to C_2^- was provided by the rare-gas matrix work of Milligan, Jacox, and Abouaf-Marguin[96,97] and conclusive proof was obtained from two-photon detachment of the negative ion in a mass-selected beam.[98] In this way Lineberger and co-workers confirmed the assignment to C_2^- and in fact, in later work, supplied much of the detailed gas-phase data, culiminating in their detection, via perturbations, of the missing $A^2\Pi_u$ state.[99-103] Rehfuss et al.[104] recently reported direct observation of the high-resolution infrared spectrum of the $A^2\Pi_u \leftarrow X^2\Sigma_g^+$ transition and gave molecular constants for the upper state.

The configurations providing the three observed electronic states are, in analogy with the isoelectronic molecules N_2^+, CN, and BO

$$X^2\Sigma_g^+ \quad 1\sigma_g^2 1\sigma_u^2 2\sigma_g^2 2\sigma_u^2 1\pi_u^4 3\sigma_g$$

$$A^2\Pi_u \quad 1\sigma_g^2 1\sigma_u^2 2\sigma_g^2 2\sigma_u^2 1\pi_u^3 3\sigma_g^2$$

$$B^2\Sigma_u^+ \quad 1\sigma_g^2 1\sigma_u^2 2\sigma_g^2 2\sigma_u^1 1\pi_u^4 3\sigma_g^2$$

TABLE I. Dunham Constants (cm^{-1}) for the Σ and Π States of the C_2^- Molecule[a]

constant	$X^2\Sigma_g^+$	$A^2\Pi_u$[b]	$B^2\Sigma_u^+$
T_e	0	4064 (91)	18390.723 (35)
Y_{00}	0.086	0.010	−0.2
Y_{10} (ω_e)	1781.202 (20)	1656 (10)	1969.542 (84)
Y_{20} ($-\omega_e x_e$)	−11.6716 (48)	−10.80 (26)	−15.100 (57)
Y_{30} ($\omega_e y_e$)	−0.00998 (28)		−0.135 (16)
Y_{40} ($\omega_e z_e$)			−0.0153 (17)
Y_{50}			$-(4.1 \pm 0.7) \times 10^{-4}$
Y_{01} (B_e)	1.74649 (16)	1.630 (5)	1.87718 (27)
Y_{11} ($-\alpha_e$)	−0.016557 (76)	−0.0152	−0.01887 (28)
Y_{21} (γ_e)	$-(3.2 \pm 0.7) \times 10^{-5}$	-2.4×10^{-5}	$(1.15 \pm 0.67) \times 10^{-4}$
Y_{31}		-1.1×10^{-7}	$-(5.4 \pm 0.5) \times 10^{-5}$
r_e	1.2684	1.313	1.2234

[a] Values in parentheses represent one standard deviation. Reproduced with permission from ref 103; copyright 1985 American Institute of Physics. [b] Restricted to values characteristic of a Morse potential. The vibrational energy expression for such a potential truncates after $\omega_e x_e$, while the rotational coefficients constitute an infinite series of constants with rapidly decreasing magnitude.

C. Theory and Gas-Phase Spectroscopy

Ab initio theory has been applied to confirm the assignment of the B state and to predict the energy of the A state and also of the lowest quartet states.[82,83,105-107] The most recent calculations of Zeitz et al.[82] and Rosmus and Werner[83] yield potential energy curves for all three doublet states in excellent agreement with experiment[103] and also an electron affinity of C_2 of 3.43 eV,[82] also in accord with the measured values.[99,108] (Green's function method has also been used to calculate the electron affinity of C_2.[109]) Zeitz et al.[82] found that the two quartet states, resulting from the electronic configuration $^4\Sigma_u^+$, $^4\Delta_u$ $1\sigma_g^2 1\sigma_u^2 2\sigma_g^2 1\pi_u^3 3\sigma_g 1\pi_g$, lie at considerably higher energies (3.70 eV for the $^4\Sigma_u^+$ state) and longer bond lengths. This is important since earlier theory[106] and experiment[110] had mistakenly inferred that the $^4\Sigma_u^+$ state had almost the same energy as the $B^2\Sigma_u^+$ state, and it was therefore used to account for perturbations observed in the B ← X spectrum.[95,103] The calculations of Rosmus and Werner,[83] utilizing highly correlated wave functions, yield lower energies for the bound doublet states, but the spectroscopic constants of both calculations are in good agreement.

Lineberger's group[98-103] has clearly made the major experimental contributions to the understanding of the electronic properties of C_2^-, beginning with the observation of two-photon detachment in a mass-selected negative ion beam. There, resonances were observed in the C_2^- photodetachment cross section at wavelengths corresponding to the Herzberg–Lagerqvist bands, caused by resonant excitation of C_2^- from the X state to the B state, followed by photodetachment of the excited state. That work has been followed over the past 15 years by a series of definitive papers utilizing increasingly sophisticated experimental procedures resulting in the following:

(a) The electron affinity of C_2 was established as being between 3.37 and 3.40 eV, in place of the earlier value of 3.54 eV.[108]

(b) Rotational and vibrational constants (including centrifugal distortion and spin rotation) were determined for the B and X electronic states, allowing accurate potential curves to be constructed (see Table I and Figure 2).

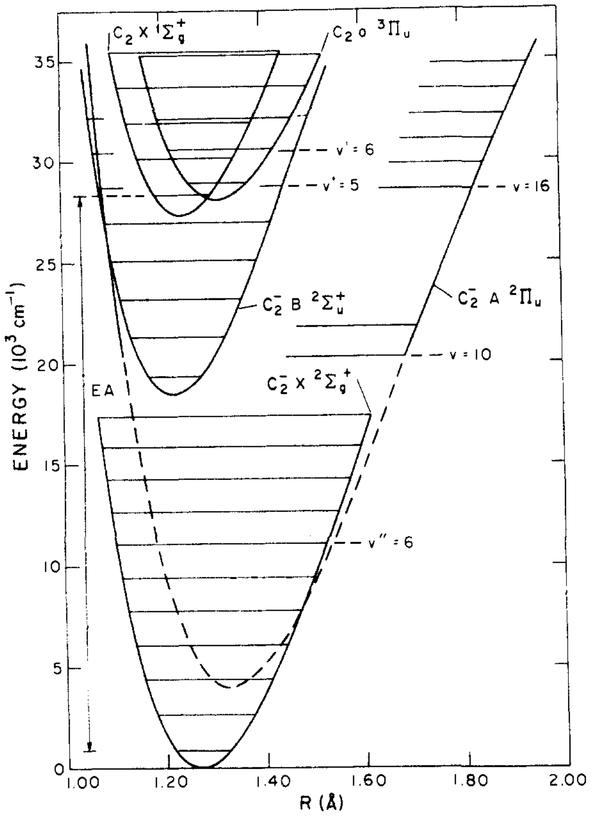

Figure 2. Potential curves for the X, A, and B states of C_2^- and the X and a states of C_2. (Reprinted from ref 103; copyright 1985 American Institute of Physics.)

(c) Lifetimes for the B state autodetaching levels for υ = 6–9 were measured and found to be very dependent upon rotation and vibrational level. These compared well with the measurements of Leutwyler, Maier, and Misev[111] and calculations of Rosmus and Werner.[83]

(d) Approximate molecular constants were obtained for the low-lying $A^2\Pi_u$ state from high-resolution photodetachment data on the perturbations in the B–X bands.

As already mentioned, Oka and co-workers[104] have recently observed the $A^2\Pi_u \leftarrow X^2\Sigma_g^+$ high-resolution spectrum in the infrared and have given accurate values of the energy of the A state and molecular constants in both states. The (0,0), (0,1), and (1,1) bands at 3929, 3816, and 2171 cm^{-1} in the electronic transition were detected and analyzed. The results of that analysis are given in Table II where a comparison is also made with the Mead et al.[103] results obtained from perturbations in the B state. Theoretically calculated parameters by Zeitz et al.[82] and Rosmus and Werner[83] are also given.

Leutwyler et al.[111] obtained an oscillator strength of f_{00} = 0.044 ± 0.004 for the B–X system by measuring the lifetimes in selected rotational levels in the υ' = 0 and υ' = 1 levels of the B state. Specifically they found the mean lifetime in these levels to be 77 ± 8 and 73 ± 7 ns, respectively. This was essentially corroborated by the radiative lifetimes measured by Bondybey and Brus[110] in matrices where a variation from 34 to 64 ns occurred in environments of solid Xe to Ne. The gas-phase oscillator strength is, however, about 3 times larger than that calculated from shock tube data.[112] Theory has yielded a mean radiative lifetime of 67 ns,[82] and, more recently, Rosmus and Werner have calculated from highly correlated MCSCF–SCEP wave functions a value of 76.5 ns for the $B^2\Sigma_u^+(\upsilon' = 0)$ level, in excellent agreement with experiment.[83] These latter authors also found that the transition dipole for the A–X transition is exceedingly large, leading to a radiative rate of spontaneous emission of 19111 s^{-1}. This is much larger than the rates of vibrational transitions expected within one electronic state. Thus, C_2^- is a strong emitter in the IR. Specifically, the radiative lifetime of the $A^2\Pi_u(\upsilon' = 0)$ state is predicted to be 49.9 μs.

TABLE II. Equilibrium Molecular Constants of C_2^- (cm^{-1})[a]

$A^2\Pi_u$ State

constant	RLDJHCO[104]	MHSL[103]	ZPB[82]	RM[83]
T_e	3985.83 (50)	4064 (91)	3250	3550[b]
ν_e	1666.4 (10)	1656 (20)	1653	1646
$\nu_e x_e$	10.80 (26)	10.80 (26)		11
B_e	1.64305 (334)	1.630 (5)		1.619
α_B	0.01601 (44)	0.0152		
A_e	−25.009 (15)	−24 (1)		
α_A	−0.048 (22)			
r_e	1.30768 (13)	1.313	1.318	1.318

$X^2\Sigma_g^+$ State

constant	value	constant	value	constant	value
ν_e	1781.189 (18)	$\nu_e x_e$	11.6717 (48)	$\nu_e y_e$	0.00998128
B_e	1.74666 (32)	α_e	0.01651 (46)	r_e	1.26831 (13)

[a] Reproduced with permission from ref 104; copyright 1988 American Institute of Physics. [b] Converted from their value of 0.44 eV to wavenumber units.

D. In Matrices

Another aspect of these gas-phase studies of C_2^- enters when matrix or crystal environments are considered. Then the surroundings and, more importantly, the countercation interactions may be significant, as suggested by the matrix lifetime measurements mentioned above. C_2^- was prepared in argon matrices by photolysis of 1% C_2H_2 at 4 K by Milligan, Jacox, and Abouaf-Marguin[96,97] and by X-irradiation of C_2H_2 trapped in solid Ar, Kr, and Xe by Frosch.[113] A progression with the (0,0) band at 19107 cm^{-1} (5208 Å), corresponding to the B ← X absorption, was observed in argon with $\Delta G'_{1/2}$ = 1955 cm^{-1} as compared to 18280.9 cm^{-1} (5470 Å) and 1940 cm^{-1} in the gas phase. These are normal matrix shifts for such an ion.[114] The counterion in the matrices with this preparation procedure has not been identified, but Brus and Bondybey[115] reasonably suggest $C_2H_2^+$. They also rationalize the formation of C_2^- with 1216-Å (10.2-eV) photolysis, when the gas-phase ionization potentials of the species present are all greater than 11.4 eV, by considering the dielectric solvation energies and the screened Coulomb potential acting on the transferred electron.

Milligan and Jacox[97] found that the addition of a small amount of alkali metal atoms to the rare-gas matrices enhanced the intensity of the C_2^- spectrum. However, if the metal concentrations were brought to 5–10%, Graham, Dismuke, and Weltner[116] observed new progressions to also appear, shifted depending upon the alkali metal used. The (0,0) band then varied from 4771 Å (Li^+) to 5002 Å (Cs^+). This is presumably due to intimate ion pairs $M^+C_2^-$ formed in the matrices. Electron spin resonance (ESR) spectra, with ^{13}C substitution, confirmed this by exhibiting metal and carbon hyperfine splittings (hfs).[116] Orthorhombic **g** tensors indicated $^2A_1$ ground states with C_{2v} symmetries for the ion pairs containing two equivalent carbon atoms. The ESR of the C_2^- ion in the absence of alkali metal was not observed, which was a subject of some speculation.[115,116]

It is interesting to note that implantation of 250-keV C^+ ions into alkali metal halide single crystals at low temperatures yielded C_2^- ions.[121] Herzberg–Lagerqvist spectra (B ← X) of highly resolved bands were observed, the energy of which depended upon the respective matrix. As in the rare gases, blue shifts were observed relative to the gas-phase spectrum.

Vibrational relaxation times have been the subject of study by several authors using pulsed laser fluorescence.[117-120] They were found to be very dependent upon C_2H_2 concentration but not determined by lattice phonon interaction. As mentioned above, it appears that excited quartet states of C_2^- have not been identified so that vibrational relaxation mechanisms involving them, although possible, can only be speculated upon at present.

IV. C_2^+ Ion

A. Ionization Potential of C_2

Two experimental values of ostensibly the ionization potential (IP) of C_2 have been obtained and are in essential agreement. A mass spectrometric measurement of the appearance potential for C_2 in carbon vapor was measured by Drowart et al.[122] to be 12.0 ± 0.6 eV. Dibeler and Liston[123] derived this IP from the photoionization of C_2N_2 as 12.15 ± 0.05 eV. However, the potential curves of C_2 and theoretically derived ones for C_2^+ suggest that some ionization could be occurring from the low-lying $a^3\Pi_u$ state of C_2 at the temperatures of the experiments and also that the ion could be readily formed in its low-lying $1^2\Pi_u$ state.[124] The unfavorable Franck–Condon factors ($r_e = 2.384a_0$ in C_2 to $2.67a_0$ in C_2^+) make it unlikely that the transition involving both ground states will be observed experimentally. The adiabatic IP estimated from theory is 11.35 eV.[124]

B. Theoretical and Experimental Data

Until recently, there has been no valid spectroscopic information on this ion in spite of its probable importance in plasmas and interstellar chemistry. It remains undetected in interstellar media except for identification in two comets via in situ mass spectrometry.[125] Its reactions have been of particular interest in studies of the formation of molecules in space. In the laboratory, ion cyclotron resonance[126] and the selected-ion flow tube technique[127,128] have been applied principally to reactions with H_2 and CH_4 but also with C_2N_2[128] and HCN.[129] It now seems probable that its spectroscopic observation has been hampered in the past by the fact that its most accessible electronic band system is overlapped by the intense C_2 Swan bands. Much earlier, Meinel[130] proposed a band system at 249 nm, produced in an acetylene discharge, to be a $^2\Sigma_g^- - ^2\Pi_u$ transition of C_2^+, but that assignment was rejected by ab initio theorists (however, see below).[124,131]

The status of knowledge of C_2^+ as of 1981 was given by Petrongolo et al.,[124] who made theoretical predictions of the potential curves for its 16 lowest lying electronic states correlating to the first dissociation limit, $C(^3P_g) + C^+(^2P_u)$. The ab initio calculations were carried out at the multireference double excitation configuration interaction (MRD–CI) level with similar accuracy to the authors' previous work on C_2 and C_2^-. The ground state is $^4\Sigma_g^-$ with r_e = 1.41 Å, and the first excited state is $^2\Pi_u$ at the shorter bond distance of 1.32 Å and 0.84 eV higher in energy. The next three states are $^4\Pi_g$ at 1.37 eV (1.27 Å), $^2\Delta_g$ at 1.46 eV (1.44 Å), and $^4\Sigma_u^-$ at 2.50 eV (1.35 Å).

In 1986 Rosmus et al.[131] calculated, using a variational MCSCF–SCEP procedure, the potential functions and spectroscopic constants of the ten lowest electronic states of C_2^+ and compared them with the MRD–CI results of Petrongolo et al.[124] The two methods are in good agreement: $\Delta r_e \cong 0.02$ Å, $\Delta\omega_e \cong 40$ cm^{-1}, and $\Delta T_e \cong 0.2$ eV; slightly lower total energies were obtained by Rosmus et al. Transition moments between the three lowest quartet states were derived (the $A^4\Pi_g - X^4\Sigma_g^-$ transition is symmetry forbidden): for example

$$B^4\Sigma_u^- - X^4\Sigma_g^-:\ T_0 = 20\,034\ \text{cm}^{-1},\ f_{00} = 1.56 \times 10^{-2},\ \tau_{00} = 148\ \text{ns}$$

$$B^4\Sigma_u^- - A^4\Pi_g:\ T_0 = 10\,054\ \text{cm}^{-1},\ f_{00} = 4.4 \times 10^{-4},\ \tau_{00} = 8.73\ \mu\text{s}$$

Thus, the B–A transition emission rates are about 100 times smaller than those for the B–X transition. Transition moments were also calculated for dipole-allowed transitions among doublet states; all are several orders of magnitude less than for the B–X transition.

The first positive experimental observation of C_2^+ was obtained from translational energy spectroscopy,[132] but it has a resolution of only about 100 meV (800 cm^{-1}). Although many transitions were observed, their analysis rested upon the relative intensities and the energy differences derived from theoretical calculations.[124] However, within those bounds, the authors made tentative assignments based on known selection rules which are essentially the optical ones. They assigned possibly eight signals to transitions initiating from the lowest doublet level ($^2\Pi_u$) or the ground state ($^4\Sigma_g^-$). The strongest signal at 2.5 eV is most probably the $B^4\Sigma_u^- \leftarrow X^4\Sigma_g^-$ transition, which is estimated to have the greatest intensity in the quartet manifold.

C_2^+ was subsequently observed in a neon matrix at 5 K by Rasanen et al.[132b] where it was trapped directly from the vapor over graphite during pulsed Nd-YAG laser heating. The same spectrum was observed by Forney, Althaus, and Maier,[133a] who, however, generated C_2^+ by photolysis of acetylene, halogenated acetylenes, and/or other precursors containing a C_2 group, followed by photoionization using Ne I (73.6 nm = 16.8 eV) radiation. A progression of three bands at 505.8, 470.3, and 439.8 nm were assigned to the 0–0, 1–0, and 2–0 absorptions of the $B^4\Sigma_u^- \leftarrow X^4\Sigma_g^-$ transition of C_2^+. [The C_2 Swan bands cannot be observed in absorption in a matrix at 5 K since the lowest state ($a^3\Pi$) of that system is not thermally occupied.] Other signals in the matrix spectra could be identified as due to C_2^- or other precursor products. ν_{00} = 19765 (4) cm^{-1} and the vibrational frequencies in the upper state are 1491 cm^{-1} (v' = 1–0) and 1475 cm^{-1} (v' = 2–1), yielding ω_e' = 1507 (4) and $\omega_e x_e'$ = 8 (4) cm^{-1} in the neon matrix. The assignment to the B ← X transition was based upon the theoretical predictions of wavelength of the transition

TABLE III. Spectroscopic Constants (cm^{-1}) of $^{12}C_2^+$ and $^{13}C_2^+$ [a]

constant	$\tilde{X}^4\Sigma_g^-$		$\tilde{B}^4\Sigma_u^-$	
	$^{12}C_2^+$	$^{13}C_2^+$	$^{12}C_2^+$	$^{13}C_2^+$
T_e	0	0	19652.2 (4)	19653.2 (4)
ω_e	1351.2 (5)	1297.8 (5)	1508.1 (5)	1447.7 (5)
$\omega_e x_e$	12.06 (2)	11.08 (15)	12.69 (15)	11.39 (15)
B_3	1.3651 (5)		1.4871 (8)	
B_2	1.3824 (5)	1.2787 (5)	1.5048 (5)	1.3908 (5)
B_1	1.3996 (5)	1.2940 (5)	1.5223 (5)	1.4069 (5)
B_0	1.4181 (5)	1.3097 (5)	1.5383 (6)	1.4215 (5)
B_e	1.4266 (5)	1.3174 (4)	1.5474 (6)	1.4294 (5)
α_e	0.0176 (10)	0.0155 (10)	0.0171 (10)	0.0154 (10)
D_e	6.3 (5) × 10^{-6}	5.4 (5) × 10^{-6}	6.5 (5) × 10^{-6}	5.5 (5) × 10^{-6}
r_e, pm	140.34 (5)	140.31 (5)	134.75 (6)	134.70 (5)

[a] Values in parentheses represent two standard deviations. Reproduced with permission from ref 133c; copyright 1988 American Institute of Physics.

TABLE IV. Lifetimes of $C_2^+(\tilde{B}^4\Sigma_u^- v')$ and the Oscillator Strengths for the $\tilde{B}^4\Sigma_u^-$–$\tilde{X}^4\Sigma_g^-$ Transition[a]

v'	$\tau_{v'}$, ns	v''	$f_{v',v''}$
0	113 (12)	0	0.023 (3)
		1	0.010 (2)
		2	0.0027 (3)
		3	0.0006 (2)
1	127 (10)	0	0.0062 (7)
		1	0.0076 (8)
		2	0.012 (2)
		3	0.0053 (6)
2	134 (28)	0	0.0004 (1)
		1	0.0082 (8)
		2	0.0016 (2)
		3	0.0098 (9)

[a] Values in parentheses represent 2σ uncertainty. Reproduced with permission from ref 133c; copyright 1988 American Institute of Physics.

and the vibrational frequency in the upper state.[124,131] A less definite fluorescence band at 502.4 nm (1-1 transition) yielded $\nu''(1-0) = 1359$ (6) cm^{-1}.

With these experiments providing an approximate location of the 0–0 band in the gas phase, Rösslein, Wyttenbach, and Maier[133b] were able to observe the high-resolution spectrum of the free C_2^+ molecule using laser excitation spectroscopy with ^{13}C substitution as proof of the carrier. Cutoff filters were used to discriminate the C_2 Swan band signals. The rotational pattern was in accord with the symmetry of a $^4\Sigma_u^-$–$^4\Sigma_g^-$ transition with the band origin at 19 730.6 cm^{-1}, about 30 cm^{-1} from that in the matrix. Subsequently a complete rotational and vibrational analysis of ten vibronic bands of $^{12}C_2^+$ and seven bands of $^{13}C_2^+$ was made by Maier and Rösslein.[133c] Molecular constants of the $X^4\Sigma_g^-$ and $B^4\Sigma_u^-$ states were obtained for both isotopic molecules and are given in Table III. Some spin splittings were resolved (also see ESR results below). Lifetimes in the B state for various v', v'' transitions were also determined and oscillator strengths for the B–X transition were calculated with the aid of the ab initio potentials (see Table IV). The measured lifetimes are approximately 20% shorter than the theoretically calculated values.[131] f_{00} was found to be 0.023 (3) compared to a calculated value of 0.0169 (from the above theoretical value of 0.0156, corrected for the experimental r_e).

It is interesting that these authors also point out that the spectroscopic constants of the $^2\Pi_u$ state assigned by Meinel[130] to C_2^+ are in good agreement with the low-lying $^2\Pi_u$ state calculated theoretically.[124,131] They imply that the 249-nm band observed by Meinel may be a $^2\Sigma$–$^2\Pi_u$ transition of C_2^+ or possibly a Rydberg transition of C_2 converging to the ion state.

The most recent study is that of Knight, Cobranchi, and Earl,[134] who measured the electron spin resonance (ESR) spectra of $^{12}C_2^+$ and $^{13}C_2^+$ in neon matrices. Here the C_2^+ was generated by pulsed laser vaporization of graphite with simultaneous irradiation at 16.8 eV from a neon resonance lamp during the formation of the matrix at 4 K. The results confirm the $^4\Sigma_g^-$ ground electronic state and also provide a zero-field-splitting parameter of $|D| = 3668$ (3) MHz = 0.1223 (1) cm^{-1} in that state. (This value is expected to be perhaps 2% lower than the gas-phase value.[135]) The **g** tensor was almost isotropic with components close to $g_e = 2.0023$ as expected for little orbital angular momentum mixed into the ground state; i.e., theory indicates that the lowest excited $^4\Pi$ state is at ~1.37 eV.[124,131] The ^{13}C hyperfine splitting parameters $|A_\parallel| = 99.4$ (8) and $|A_\perp| = 95.2$ (5) MHz yield isotropic (A_{iso}) and dipolar (A_{dip}) contributions to the hf tensor of 95 (1) and 2 (1) MHz, respectively. Using the ^{13}C atomic parameters as a basis leads to an interpretation of the wave function of the unpaired spins (choosing positive signs for the hf components) as 2.5% $2s\sigma$, 16.4% $2p\sigma$, and 31% $2p\pi$ character at each carbon atom. This is consistent with a dominant configuration of $...p\sigma^1 p\pi^2$ for the $^4\Sigma_g^-$ ground state.

The uncertainty in the IP of C_2 (see section IV.A) results in corresponding uncertainties in the calculation of the dissociation energy (D_e) of C_2^+ since $D_e(C_2^+) = D_e(C_2) + IP(C) - IP(C_2)$, where $D_e(C_2) = 6.32$ (0.16) eV and IP(C) = 11.26 eV. There appear to be no direct measurements of this quantity. Theory, at the estimated full CI level, yields 5.62 eV.[124]

Passing from C_2^+ $\tilde{X}^4\Sigma_g^-$ to C_2 $\tilde{a}^3\Pi_u$ to C_2^- $\tilde{X}^2\Sigma_g^+$ involves successive additions of electrons to the π_u bonding orbital with an expected decrease of r_e and increase in ω_e. As Maier and Rösslein[133c] point out, this is observed:

	C_2^+ $\tilde{X}^4\Sigma_g^-$	C_2 $\tilde{a}^3\Pi_u$	C_2^- $\tilde{X}^2\Sigma_g^+$
r_e, pm	140.34	131.19	126.82
ω_e, cm^{-1}	1351	1641	1781

Thus, in a very short span of time a rather complete picture of the lowest quartet states of the C_2^+ ion has emerged. Hopefully it will now be possible to detect it in stellar and interstellar atmospheres.

V. C_3 Molecule

A. Early Research

The spectrum of C_3 beginning at 4050 Å was seen in emission from comets at least as early as 1882,[136] but it remained unidentified until the work of Douglas in 1951. Besides observations in comets[137] these bands are also seen in absorption in the atmosphere of cool carbon stars[138,139] and supergiant circumstellar shells;[140] however, recent attempts by Clegg and Lambert[141] to detect them in diffuse interstellar clouds were not successful. In any hot source and especially the emission from a graphite tube furnace or an acetylene–oxygen flame,[142] these bands are observed on top of a strong underlying continuum. Brewer and Engelke[143] early considered this continuum as derived from the overlapping of many bands of C_3 excited at the high temperatures of these sources.

The C_3 bands (sometimes referred to as Swings bands[137]) were first produced in the laboratory by Herzberg[144] in electrodeless discharge through methane, and the emitter was established as C_3 by the further work of Monfils and Rosen,[145] Douglas,[146] and Clusius and Douglas.[147] From the analysis of the rotational structure of the 4050-Å band, Douglas found that the molecule was linear in both states with the C–C bond distance increasing from 1.281 Å in the lower state to 1.305 Å in the upper state.[146] Preparation of C_3 enriched in ^{13}C confirmed this analysis.[146,147] Attempts were made to carry the analysis of the rotational structure of the 4050-Å band and another strong band at 4072 Å to higher J values by Kiess and Bass[148] and by Kiess and Broida,[149] but there were complexities in the spectrum that defied a straightforward interpretation. A resolution of this was provided by Gausset, Herzberg, Lagerqvist, and Rosen (GHLR),[150] who obtained a relatively low temperature absorption spectrum of C_3 from the flash photolysis of diazomethane. Two important conclusions result from the analysis of the spectrum, which also established that it was a $^1\Pi_u \leftarrow {}^1\Sigma_g^+$ transition: C_3 has a very low bending frequency ($\sim$60 cm^{-1}) with considerable anharmonicity in the ground electronic state, and there is a strong vibronic Renner–Teller effect in the $^1\Pi$ upper state.

From rotational analysis, GHLR[150] found that absorptions at 4049.8, 4072.6, and 4099.1 Å all corresponded to $\Pi_u \leftarrow \Sigma_g^+$ vibronic transitions (see below) which were assigned, respectively, as absorptions from the 000 level and from two low-lying levels 132 and 286 cm^{-1} above the 000 level. These spacings were assigned to $2\nu_2''$ and $4\nu_2''$, indicating a low anharmonic bending frequency in the ground state. Four other bands had the same lower 000 state but all other transitions were "hot" bands originating from quanta $(0v_2^l0)$ of this low-frequency bending with splittings due to l-type doubling. The spacing of the observed bending levels was analyzed to yield $\nu_2'' = 63.1$ cm^{-1}. The later work of Merer[151] added the observation of the $\nu_2'' = 6$, $l = 0$ level at 458.2 cm^{-1} as well as further transitions involving the symmetric stretching vibrations. From B''_{000},[150] r_0''(C–C) was found to be 1.277 Å.

Bending in a doubly degenerate electronic state of a linear molecule leads to resolution of the degeneracy so that so-called vibronic interaction is involved, i.e., breakdown of the Born–Oppenheimer approximation. This effect was first recognized by Teller and analyzed by Renner.[152] In the upper $^1\Pi_u$ electronic state of C_3 the observed absorptions again terminate on vibronic levels involving quanta of the bending frequency, which, however, is now much larger ($\nu_2' = 307.9$ cm^{-1}). These upper levels are very irregularly spaced due to the Renner–Teller effect, and a Renner parameter $\epsilon = +0.537$ was derived. Deviations from values predicted with Renner's relationships were found to increase with increasing K and v_2, as expected from the effect of anharmonicity and neglected terms in that theory (see below). From B'_{000}, GHLR[150] found r_0'(C–C) = 1.305 Å, and the symmetric stretching frequency in the upper state was $\nu_1' = 1085.9$ cm^{-1}.

The absorption spectrum of C_3 was also observed in solid neon, argon, and xenon matrices by Barger and Broida,[153] Weltner et al.,[154-157] and Bondybey and English.[158] The assignments of GHLR were verified by Weltner et al.[155-157] in neon and argon at 4 K. At that temperature all absorption takes place from the lowest vibrational level of the ground electronic state. (No experimental evidence of rotation of the C_3 molecules in these matrices was found.) One then expects, with the Renner effect, only $\Pi^\pm \leftarrow \Sigma$ vibronic transitions to be observed. In neon matrices a very long progression in the upper state bending vibration is observed with the $K = 1$ levels of the $A^1\Pi_u$ state appearing up to $v = 10$ (+) and $v = 20$ (−) where the classical turning point of the vibration corresponds to a bond angle of 110°.[156,158,159] The neon matrix work thus supported the analysis in the gas phase (including yielding $\nu_1' = 1092$ cm^{-1}) and also extended it to the shorter wavelengths where the high-temperature C_3 bands appear. The gas-phase spectrum there is too complex for satisfactory analysis.

The matrix work also provided information about the remaining unknown stretching frequencies $\nu_1'' = 1226$ cm^{-1}, $\nu_3'' = 2040$ cm^{-1}, and possibly $\nu_3' = 840$ cm^{-1}. Merer later confirmed the matrix value of ν_1'' by finding $\nu_1'' = 1224.5$ cm^{-1} in his study of a particularly strong spectrum of C_3 produced by the flash photolysis of diazopropyne.[151] In the infrared spectra of matrices containing graphite vapor, the asymmetric stretching frequency, $\nu_3'' = 2042$ cm^{-1} in neon and 2038 cm^{-1} in argon, appears intensely.[155,156,160] The vaporization of partially ^{13}C-enriched carbon, similar to the gas-phase work of Douglas,[146] leads to the formation of six isotopically substituted C_3 molecules which produce their individual ν_3'' bands, thus proving the assignment.[156]

Weltner and McLeod[157] tentatively assigned two bands in the neon matrix spectrum to transitions to upper vibronic levels (002) and (102), yielding the asymmetric stretching frequency in the $^1\Pi_u$ state as $\nu_3' = 840$ cm^{-1}. This low frequency was rationalized at the time by comparison of the derived anomalous interaction force constant with those for BO_2 and CNN. Some support for this low value was also provided by Clusius and Douglas' observed isotopic shifts[147] which indicated that $\nu_3' - \nu_3'' \simeq -1150$ cm^{-1} so that $\nu_3' \cong 900$ cm^{-1}.[157] Brown has shown from the K-type doubling[159,162] (see below) dependence on the energy denominator $\omega_3' - \omega_2'$ that ω_3' had to be in the region of 650 cm^{-1} in order to fit the GHLR data. Jungen and Merer[163] found that such a term, in their formalism (see Table VII), also improves the agreement with experiment. Although the 650-cm^{-1} frequency was not as effective in making a good fit, they nevertheless concluded that "ω_3' has to be quite small in the $A^1\Pi_u$ state".

The π_g molecular orbital is not occupied in the C_3 molecule in the ground electronic state whereas excitation from the σ_u into that orbital occurs in the $^1\Pi_u$ level:

$$\mathrm{KKK}\ 1\sigma_g^2 1\sigma_u^2 2\sigma_g^2 1\pi_u^4 2\sigma_u^2\ \ X^1\Sigma_g^+ \rightarrow$$
$$\mathrm{KKK}\ 1\sigma_g^2 1\sigma_u^2 2\sigma_g^2 1\pi_u^4 2\sigma_u 1\pi_g\ {}^1\Pi_u\ (\text{and } {}^3\Pi_u)$$

The corresponding abrupt rise in the bending frequency from 63 cm^{-1} to 308 cm^{-1} is attributed to the occupation of this antibonding π_g orbital[150,164] having a strong stabilizing influence on the linear conformation. The addition of further electrons to this orbital leads to steadily increasing ν_2 frequencies in the series of mol-

TABLE V. **Molecular Constants of C_3 (cm^{-1})[a]**

	ν_3 (0,0,1)	ground (0,0,0)
B_v	0.435565 (37)	0.430445 (37)
D_v	3.663 (62) × 10^{-6}	0.742 (66) × 10^{-6}
H_v	0.111 (33) × 10^{-9}	−0.943 (28) × 10^{-9}
L_v	−0.2214 (108) × 10^{-12}	
M_v	0.2176 (160) × 10^{-16}	
band origin	2040.0198 (8)	

[a] Values in parentheses denote one standard deviation. Reproduced with permission from ref 161a; copyright 1988 American Institute of Physics.

ecules CCN, NCN, BO_2 and CO_2.[150,165–167] With a filled $...\pi_g{}^4$ orbital in CO_2, the frequency has risen to 667 cm^{-1}. (This reasoning has been extended to pentatomic molecules by Smith and Leroi[167] and will be considered again when longer carbon chains are discussed.)

The low bending frequency of C_3 and its anharmonicity were found to have significant effects in the understanding of the thermodynamics of vaporization of carbon. The initial effusion studies of Brewer et al. in 1948[168] were followed by other similar research[169,170] and the increasing use of mass spectrometry to establish the vapor pressure of the individual vaporizing molecules during thermal[94,122,171–176] and laser heating.[177] Chupka, Inghram, Drowart et al.[122,171,173] established that C_3 is the dominant (~60 mol %) vapor species over graphite at 2500 K with an average C–C bond strength of 160.4 kcal/mol. However, the very low bending frequency in the $X^1\Sigma_g{}^+$ state, if treated as harmonic, was found to lead to large discrepancies in the second- and third-law values of $\Delta H_0°$ for the sublimation of C_3.[156] (An informative and interesting review of the efforts made up to 1955 to establish the heat of sublimation of carbon is given by Kern.[175]) Strauss et al.[178,179] first considered the anharmonicity of this bending and its effect upon the thermodynamics of C_3 vapor. Strauss and Thiele[179] considered a quadratic–quartic potential function for the bending and also included the interaction between the bending vibration and overall rotation. These contributions were found to be important in accounting for the thermodynamic data at high temperatures. These matters were discussed at some length in a critical review by Palmer and Shelef.[180]

B. Vibrational and Rotational Properties in the Ground State

Two recent papers have determined the gas-phase value of ν_3'', the rotational parameters B_{000} and B_{001}, and higher rotational constants in the ground state. Matsumura et al.[161a] produced C_3 by 193-nm photolysis of hydrocarbons and detected a diode laser beam in absorption through a multipass cell. Vibrational–rotational analysis of the strong band at 2040 cm^{-1} was analyzed according to

$$\nu(J'–J'') = \nu_0 + F_3(J') - F_0(J'')$$

with $F_v(J') = B_{v}f - D_vf^2 + H_vf^3 + L_vf^4 + M_vf^5$, where $f = J(J + 1)$, v is 0 or 3 for the ground and ν_3 states, and ν_0 denotes the band origin. The results are given in Table V. The band origin at 2040.0198 (8) cm^{-1} is in good agreement with the matrix value of 2040 cm^{-1}.[156] The B_{000} value agrees well with Gausset et al.,[150] but D_0 is different, probably because of the higher terms in f in the above equation. The authors also point out that the centrifugal distortion constant calculated from $D = 4B_0{}^3/\omega_1{}^2$ (with $\omega_1 = 1224.5$ cm^{-1} here) which usually holds for linear YXY molecules is much smaller than the observed values in Table V. This situation also arises in the C_3O_2 molecule where quasi-linearity has been proposed (see section C). Also the vibrational dependence of the rotational constant is unusually negative [−0.005120 (52) cm^{-1}], similar to the asymmetric C–C stretch in C_3O_2 at 2290 cm^{-1}, where it was accounted for by the potential barrier to linearity in the ν_3 state being larger than in the lowest state.

Concurrently with the study of Matsumura et al.,[161a] Hinkle, Keady, and Bernath[161b] detected the vibration–rotation spectrum of C_3 near 2040 cm^{-1} in the circumstellar spectrum of the carbon star IRC+10216 (see below). Their band origin at 2040.02113 (62) cm^{-1} is, within experimental error, the same as that in Table V, and their independent analysis yielded essentially the same spectroscopic parameters for C_3.

C. Is C_3 Quasi-linear in the $X^1\Sigma_g{}^+$ State?

Gausset et al.[150] mentioned the possibility that C_3 might not be linear in the ground state, but if there is a slight potential maximum, it must be less than ν_2''. In the latter case the molecule is called quasi-linear since as a bent molecule it only becomes linear by vibration.[183,184] The questions then arise as to whether a potential function could be derived from ab initio theory or modeled to fit the known rotational and vibrational properties of C_3, and what inferences could be made from such considerations about its structure and excursions from linearity in the ground state. On the basis of a criterion suggested by Yamada and Winnewisser,[184,185] C_3 has a quasi-linearity parameter of −0.89, which indicates "weak" quasi-linearity; a well-behaved linear molecule would have a value between −1.02 and −0.98.[185]

The low bending frequency of C_3 leads to large-amplitude vibrational motion with bending angles up to 60° and therefore to deviations from normal-mode small-amplitude models. Experiment indicates that the moment of inertia decreases as the quantum number v_2'' increases,[150] and the actual bond length is noticeably larger than that deduced from the moment of inertia via the rotational constant. This variation in B_v is not due to a variation of C–C bond length with angle but is a consequence of the large anharmonicity and large-amplitude motion.

Following the initial studies of Strauss et al.[178,179] there have been many theoretical efforts to improve the model for bending or to establish the bending potential function from ab initio calculations. Hansen et al.[186,187] considered the effects of curvilinear bending motion and a square-well potential on the vibrational eigenvalues. Early theoretical studies[188–191] generally agreed on an electronic structure of the form :C=C=C: where C_3 was assumed linear. However, it is interesting to note that in 1966 Hoffmann[192] using extended-Hückel theory calculated that C_3 was nonlinear with an equilibrium CCC angle of ~160° and a very small barrier of ~65 cm^{-1} at the linear geometry. But the experimental evidence at that time caused him to write "since the molecule is linear one should add C_3 then to the list of failures of the extended-Hückel theory; the failure, however, is not great here—the deviation from linearity is small and in fact the molecule does bend easily". As will be seen, Hoffmann underrated his theory! Liskow, Bender, and Schaefer,[193] also motivated partly by the discrepancy in the entropy of C_3, made an ab initio SCF calculation, with the inclusion of d orbitals in the basis set, which yielded a small bending frequency (69 cm^{-1}) and quite anharmonic behavior. However, the square well with a "dimple" (toward *lower* energy) between 160° and 180° constituted an unusual bending potential. Perhaps the important point is that the d-function contributions, which cannot contribute to the SCF wave function in the linear case, become increasingly important with increased bending. A more extensive calculation by Perič-Radič et al.[194a] utilizing MRD–CI with a basis set of double ζ plus polarization but including only s and p functions calculated all of the potential curves and vibrational frequencies of the ground state (and $^{3,1}\Pi_u$ states). The extremely flat bending surface in the ground state would not be expected to be adequately treated, and the calculated $\nu_2'' = 216$ cm^{-1} was much too high, not unexpected in view of the sensitivity of the calculated value to the basis set used and the assumption of uncoupled vibrational modes.[194a] (The two stretching frequencies calculated were in satisfactory agreement with experiment and were improved in the latter extended calculations:[195] 1245 and 2034 cm^{-1} vs the experimental 1225 and 2040 cm^{-1}.)

Jones[196] used the parameter-free local spin density approximation to calculate the energy surfaces of the ground state and low-lying excited states of C_3. The equilibrium ground state was found to be linear with a bending potential which when fitted to a quartic polynomial yielded $\nu_2'' = 75$ cm^{-1}. (The excitation energies calculated via the MRD–CI method were better than the local-density results, but otherwise the agreement was good.)

Carter, Mills, and Murrell in a series of papers developed a method of obtaining an analytical expression for the potential energy surface of a polyatomic molecule that approximates closely to the true surface over the whole $(3n - 6)$-dimensional space of the internuclear coordinates. Application to C_3[197] utilized the GHLR linear equilibrium structure and vibrational frequencies from the gas phase and matrices, in addition to the ab initio calculations of energy as a function of nuclear configurations of Liskow et al.[193] and Romelt, Peyerimhoff, and Buenker.[195] The objective here was to have a functional form that exactly reproduced the energy, geometry, and force constants of the equilibrium configuration of C_3 as well as the dissociation energy and diatomic potential energy curves for atom + diatom dissociation products. For C_3 from energetic considerations the most likely channel of dissociation is

$$C_3(X^1\Sigma_g^+) \rightarrow C_2(a^3\Pi_u) + C(^3P)$$

The connecting surfaces were obtained by interpolation between equilibrium configurations. Their findings indicated a linear C_3 with large anharmonicity in the bending frequency, which was found to be roughly 106 cm^{-1}.

The background for a more exact treatment of the rotation–vibration problem in C_3 (i.e., beyond the rigid-rotor, harmonic-oscillator, Born–Oppenheimer approximation, with perturbation treatment of centrifugal distortion, Coriolis coupling; and anharmonicity) can probably begin with the development of the nonrigid bender Hamiltonian derived by Hougen, Bunker, and Johns in 1970[198] and followed by a series of refinements by Bunker and co-workers.[183,199,200] Other significant contributions were made by Dixon, Duxbury, and co-workers.[201] The theory was reviewed as it developed by Sorensen,[202] Buenker,[183] and Jensen.[203] It was first applied to C_3 by Sorensen.[202] He fit the rotation–bending levels of the ground state directly using a large-amplitude formalism with curvilinear coordinates and allowing for l uncoupling. The C–C bond length was found to be essentially independent of the bending angle, with $r_e(\rho = 0) = 1.295$ Å. (ρ is the amplitude of the bending motion displacement from the linear configuration.) The potential function of the bending up to $v_2 = 6$ was well determined, and C_3 was linear at equilibrium.

Jungen and Merer[163] derived a potential function for the ground state, containing terms up to ρ^6, which also fits the observed vibronic levels of GHLR quite well. Their purpose was to establish the ground-state function to the same degree of accuracy as that for the upper $^1\Pi_u$ state in order to calculate Franck–Condon overlap integrals for that transition (see section E). The bond length in their fitting was refined and then held fixed at 1.299 Å; variation of C–C bond length with angle was not required to obtain agreement. They reasoned that this is possibly because no π_g orbitals are occupied so that the molecule can bend without distorting the C–C bonds.

An improved version that explicitly derives the bending potential function in terms of the two stretching vibrational quanta v_1 and v_3 was calculated by Beardsworth et al.[204] applying the theory of Jensen and Bunker[200] on quasi-linear molecules. (The calculation for C_3 could be slightly simplified because $\nu_2 \ll \nu_1$ or ν_3, although these authors examined the accuracy of that simplification.) This work was preceded by an ab initio calculation by Kraemer, Bunker, and Yoshimine[205] of the ground electronic state potential energy surface at a large number of points with energies up to 12 000 cm^{-1} above equilibrium. Care was taken in the choice of the basis set since Liskow et al. had shown that the results were sensitive to the weighting of essential d functions.[193] Configuration interaction calculations were performed including all single and double excitations with reference to a single-reference Hartree–Fock state and with the Davidson estimate of higher excitations. The derived potential function yielded the equilibrium angle as 161.6° and $r_e = 1.2897$ Å in the $X^1\Sigma_g^+$ state. According to this calculation the molecule is quasi-linear with a barrier to linearity of 20 cm^{-1}. The rotation–vibration energies were calculated by using the nonrigid bender Hamiltonian with the results shown in Table VI.[205] The shape of the effective potential depends strongly on v_1 and v_3; the molecule is quasi-linear in the $v_1 = v_3 = 0$ state, linear in the $v_1 = 3, v_3 = 0$ state, and bent in the $v_1 = 0, v_3 = 3$ state.[205] As the molecule is bent, ω_1 increases (or conversely, with the excitation of ω_1 the bending requires more energy), whereas ω_3 behaves just the opposite.

A treatment of the bending problem in C_3 was made by Perič, Buenker, and Peyerimhoff[208] where the potentials and kinetic energy terms are represented by a

TABLE VI. Rotation–Vibration Energies and Constants (cm^{-1}) for $C_3(\tilde{X}^1\Sigma_g^+)$ Calculated Using the Nonrigid Bender Hamiltonian[a]

	calcd CI–SDQ	exptl[b]
B_0	0.433	0.4305
$B(\nu_1)$	0.428	
$B(2\nu_1)$	0.425	
$B(\nu_2)$	0.442	0.4422
$B(2\nu_2)$	0.451	0.4519
$B(\nu_3)$	0.436	
$B(2\nu_3)$	0.462	
q_2	0.0048	0.0055
ν_1	1260	1230[c]
$2\nu_1$	2504	
ν_3	2118	2040[d]
$2\nu_3$	4209	
ν_2	68	63.1
$2\nu_2$	159	132.7
$3\nu_2$	240	207.0
$4\nu_2$	321	286.5
$5\nu_2$	400	
$6\nu_2$	480	458.2[e]

[a] Adapted from ref 205. [b] Reference 150, except where otherwise stated. [c] Reference 157, matrix value. [d] Reference 155, matrix value. [e] Reference 163.

Fourier series and variationally solved in a basis of trigonometric functions. Comparison is made with other methods using polynomial representations of the energy terms and with data obtained by numerial solution of the Schrødinger equation. A basis of trigonometric functions is advantageous when transition probabilities between vibronic states are calculated. The convergence of the results is somewhat slower than when the vibrational basis functions are eigenfunctions of a two-dimensional harmonic oscillator, but the accuracy is comparable with that achieved with other approaches. Also the procedure is applicable to studies of the isomerization of a triatomic molecule, where other methods are not.

A nonperturbative approach using a Morse oscillator rigid bender internal dynamics (MORBID) rotation–vibration Hamiltonian developed by Jensen[206] was applied to C_3 by Jensen and Kraemer.[207a] Comparison with the nonrigid bender formalism using the ab initio data of Kraemer et al.[205] shows that the two approaches yield virtually identical results, which is a reassuring verification of the perturbation results for the rotation–vibration constants of C_3.

The most recent study is that of Jensen[207b] using the MORBID Hamiltonian to refine the potential energy function of C_3 in the ground electronic state by fitting the experimental data, including new bend–stretch term values $(v_1, v_2, v_3)^{l=0}$ = (0, 20, 0), (2, 4, 0), (0, 14, 2), etc., extending up to 5017 cm^{-1}, determined by Smith et al.[207c] These were generally fit to a few cm^{-1} with a maximum deviation of 11 cm^{-1}. It was necessary to account for both strong stretch–stretch and bend–stretch vibrational interactions, necessitating the use of many vibrational basis functions. The extent of this parameterization is indicated in Table VII. The $f_0^{(i)}$ specifically apply to the expansion of the potential energy for bending, $V_0(\bar{\rho})$, with the bond lengths fixed at their equilibrium values:

$$V_0(\bar{\rho}) = \sum_{i=1}^{8} f_0^{(i)}(1 - \cos\bar{\rho})$$

($\bar{\rho}$ is the instantaneous value of ρ.) Figure 3 shows the calculated effective bending potential $V_{\mathrm{eff}}^{(v_1,v_3)}(\rho)$ in the stretching states (v_1, v_3) = (0, 0) (1, 0), and (0, 1). Note that excitation of the symmetric stretching mode ν_1 removes the barrier to linearity while excitation of the asymmetric stretching mode ν_3 causes it to be higher (as in C_3O_2) and explains why the B constant then increases. This is shown in Table VIII where the observed rotational constants of C_3 are also compared with those predicted from theory.[207b]

TABLE VII. Values of the Potential Energy Parameters for the Electronic Ground State of C_3[a]

parameter	ab initio[b]	fitted
r_{12}^f/Å	1.289726	1.289726[c]
a_1/Å^{-1}	2.1	2.1[c]
$f_0^{(1)}/cm^{-1}$ [d]	−913	−777 (91)[e]
$f_0^{(2)}/cm^{-1}$ [d]	11966	10759 (414)
$f_0^{(3)}/cm^{-1}$ [d]	−38132	−38889 (866)
$f_0^{(4)}/cm^{-1}$ [d]	63289	67082 (105)
$f_0^{(5)}/cm^{-1}$ [d]	−42461	−49903 (2039)
$f_0^{(6)}/cm^{-1}$ [d]	17844	19146 (483)
$f_0^{(7)}/cm^{-1}$ [d]		−12519 (3892)
$f_0^{(8)}/cm^{-1}$ [d]		7252 (2720)
$f_1^{(1)}/cm^{-1}$	−2086	−902[f]
$f_1^{(2)}/cm^{-1}$		−5024[f]
$f_{11}^{(0)}/cm^{-1}$	62332	57391 (172)
$f_{11}^{(1)}/cm^{-1}$	−1857	−1857[c]
$f_{13}^{(0)}/cm^{-1}$	179	−1503 (290)
$f_{111}^{(0)}/cm^{-1}$	8036	8073[f]
$f_{1111}^{(0)}/cm^{-1}$	30239	30239[c]
ρ_e/deg[g]	18.18	17.5 (10)
H/cm^{-1} [h]	21	16.5 (36)

[a] Reproduced with permission from ref 207b. [b] Obtained in ref 207a from the ab initio data by Kraemer et al.[205] [c] Parameter constrained to the ab initio value. [d] Coefficients for the expansion in 1 − cos $\bar{\rho}$ given in the text. The ab initio values are calculated from the expansion coefficients (appropriate for an expansion in cos ρ_e − cos $\bar{\rho}$) given in Table VIII ref 207a. [e] Quantities in parentheses are one standard error in units of the last digit. [f] Constrained to value determined in a preliminary least-squares fit. [g] Equilibrium value of $\bar{\rho}$. The fitted value is calculated from the fitted values of the parameters $f_0^{(i)}$ (i = 1, ..., 8). [h] Barrier to linearity. The fitted value is calculated from the fitted values of the parameters $f_0^{(i)}$ (i = 1, ..., 8).

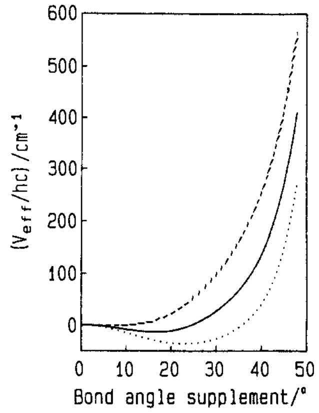

Figure 3. Effective bending potential energy functions for C_3 in different (v_1, v_3) stretching states from the nonrigid bender program NRB1.[200a,204] The solid curve (barrier to linearity 13 cm^{-1}) shows the effective bending potential energy in the (0,0) state, the dashed curve (barrier to linearity 0 cm^{-1}) shows that of the (1,0) state, and the dotted curve (barrier to linearity 36 cm^{-1}) shows that of the (0,1) state. The curves are drawn using a common energy scale so that energy at the linear configuration is zero. (Reproduced by permission from ref 207b.)

Jensen's[207b] analysis yields the correct variation of the B constant with vibrational quantum numbers and is in accord with the ab initio calculations of Kraemer et

TABLE VIII. Values of the *B* Constant for $^{12}C_3$ (cm^{-1})[a]

$(v_1,v_2,v_3)^l$	obsd[b]	predicted
$(0,0,0)^0$	0.430445[c]	0.4343
$(0,1,0)^1$	0.4421	0.4451
$(0,2,0)^0$	0.4519	0.4564
$(0,3,0)^1$	0.4600	0.4670
$(0,4,0)^0$	0.4675	0.4738
$(0,6,0)^0$	0.4807[d]	0.4851
$(1,0,0)^0$	0.4257[d]	0.4297
$(0,0,1)^0$	0.435565[c]	0.4418

[a] Reproduced with permission from ref 207b. [b] From Gausset et al.[150] except where otherwise indicated. [c] From Matsumura et al.[161a] [d] From Merer.[151]

al.[205] in indicating a small barrier to linearity in the ground electronic state of C_3. A barrier to linearity of 16.5 (3.6) cm^{-1} and an equilibrium bond angle of 162.5 (1.0)° were obtained, as given at the bottom of Table VII (bond angle = $180 - \rho_e$). He also notes the analogy with C_3O_2 where the barrier to linearity is 28 cm^{-1} and the equilibrium bond angle is 156°.

Application of the Coulomb explosion technique by Goldring et al.[181] and by Plesser, Vager, and Na'aman[182] has attempted to measure the structure of neutral C_3. This method is regarded as an alternative for structural verification when small amplitudes of vibration do not prevail so that "floppy" C_3 was chosen as a test case. The experiment is highly sensitive to the bond angle and the data are fit well for an ensemble of linear C_3 molecules with the above vibrational frequencies at thermal equilibrium at 500 K. For linear C_3 with two equal bonds, this fitting also yields a bond length of 1.25 ± 0.05 Å, consistent with the rotational analyses. Since this method measures a vibrationally averaged structure, one cannot expect it to be sensitive to a small barrier to linearity.

D. Detection of ν_3 in a Carbon Star

Hinkle, Keady, and Bernath[161b] observed the vibration–rotation lines of the ν_3 = 2040 cm^{-1} band of C_3 in the circumstellar shell of the carbon star IRC+10216. This vibrational mode is ideal for monitoring since it has a strong transition dipole moment (0.44 D)[205] and occurs in a spectral region where the atmosphere is relatively transparent. Fifteen *P* and *R* branch lines were measured from which were derived B_e = 0.41767 cm^{-1} and C–C bond length r_e = 1.297 Å. (r_0 = 1.277 Å, because of the large-amplitude vibrational motion.) As mentioned above, ν_3 = 2040.02113 (62) cm^{-1} and the other rotational parameters also agree with recent laboratory data.[161a] Interestingly, unlike CO, C_2H_2, etc., C_3 appears not to originate in the warmer inner photosphere but is observed at temperatures not greater than about 70 K. Hinkle et al.[161b] also considered several possible sources for its origin in the circumstellar shell and its potential importance in circumstellar chemistry.

E. Renner–Teller Effect in the $A^1\Pi_u$ State

The $A^1\Pi_u$ state of C_3 exhibits large rovibronic effects, but the classic theory of the Renner–Teller effect as espoused by Renner[152] in 1934 is able to account for the major features of the spectra observed by GHLR,[150] by Merer,[151] and in matrices.[156–158] Gausset et al.[150] applied Renner's theory to the analysis of the $A^1\Pi_u \leftrightarrow X^1\Sigma_g^+$ transition of C_3 and obtained the Renner parameter ϵ = +0.537 in the upper state which is a measure of the electrostatic perturbation when the molecule is bent, with the bending frequency ω_2' = 307.9 cm^{-1}. (This value of ϵ, the same as for CNC with the same electronic configuration, is at present the highest among Renner–Teller molecules.) However, a closer examination of the agreement of theoretical calculations and experimental observations indicated that the application of more exact theory was needed. The most recent reviews of the Renner–Teller effect and advances made in theory have been given by Duxberry[201] and Jungen and Merer.[159,209–211]

The vibronic interaction in the $^1\Pi$ state causes a splitting of bending vibrational levels into an upper set (+) and a lower set (−) given by Renner[152] as

$$E_{v_2,K=0} = \nu_2(v_2 + 1)(1 \pm \epsilon)^{1/2}$$

$$E_{v_2,K\neq 0} = \nu_2(v_2 + 1)(1 - \epsilon^2/8) \pm \frac{\epsilon\nu_2}{2}[(v_2 + 1)^2 - K^2]^{1/2}, \quad K < v_2 + 1$$

$$E_{v_2,K=v_2+1} = \nu_2(v_2 + 1) - \frac{\epsilon^2}{8}\frac{K(K + 1)}{2}$$

where the vibronic quantum number $K = l + \Lambda$. Since $\epsilon \simeq 0.5$ for C_3 it is seen that the energy level spacings are very irregular. These energy levels are derived by using second-order perturbation theory, with also the approximations of a two-dimensional harmonic oscillator and a simple form, depending only on ρ^2, for the electrostatic coupling. To extend this theory further one must include the following. (1) Spin–orbit effects, as considered by Pople and Longuet-Higgins[212] and later by Aarts,[213] must be included. (2) It is necessary to include *K*-type doubling (Johns[214] and Brown[162]) due to electronic–rotation Coriolis coupling between the $^1\Pi$ state and the $^1\Sigma$ electronic states. This is a complicated mixture of Λ-type and *l*-type vibration–rotational Coriolis coupling between the bending vibration ν_2 and the antisymmetric stretching vibration ν_3. (It was referred to above as providing evidence for a low value of ν_3 in the $^1\Pi_u$ state of C_3.) (3) One must consider the *K* dependence of mixing of the levels of the Π electronic state with those of Σ and Δ electronic states as shown by Carrington et al.[215] and Brown[216] and applied by Aarts.[213] It introduces a contribution to the vibrational energy levels of the form $g_k|K|$. The magnitude of g_k for C_3 is 2.3 (1) cm^{-1}.[163] (4) Anharmonic corrections as considered by Hougen and Jesson,[217] or if large-amplitude bending motion is involved, by Barrow et al.[218] and by Jungen and Merer,[163,209] must be included. (5) Renner's theory also ignores coupling between vibronic levels of the two Renner–Teller (±) components in linear molecules. For C_3 there occurs a near coincidence of the $v = 2$ (upper) and the $v = 4$ (lower) level in the $A^1\Pi_u$ state for $K = 1$ so that the second-order formulas do not account for GHLR's data. An "exact" calculation[159,163] does reproduce the observed levels to better than 1 cm^{-1}. In fact, C_3 is the only known example of the observation of this interaction because the experimental data for most linear orbitally degenerate molecules does not reach high enough vibrational levels.

A unified theory considering all of the above effects has been given by Jungen and Merer[209–211] and specif-

TABLE IX. Parameters Used To Fit the Bending Levels of the $\tilde{A}^1\Pi_u$ State of C_3[a]

parameters held fixed	
equilibrium bond length, $r(\rho = 0)$	1.308 Å
variation of bond length with ρ, d	0.15 Å
equilibrium bond angle, CCC	180°
parameters varied by least squares	
minimum of bending potentials, T_0	24393.06 ± 0.27 cm^{-1}
variation of $\langle L_z \rangle$ with ρ, g_K	2.28 ± 0.12 cm^{-1}
lower component potential, k^-	4491.9 ± 7.6 cm^{-1} rad^{-2}
lower component potential, k_4^-	355.1 ± 8.3 cm^{-1} rad^{-4}
upper component potential, k^+	15033.8 ± 9.0 cm^{-1} rad^{-2}
overall standard deviation	0.15 cm^{-1}

[a] Error limits are one standard deviation. Reproduced with permission from ref 163; copyright 1980 Taylor & Francis Ltd.

ically applied to C_3.[163] They chose a potential function in the $A^1\Pi_u$ state

$$V^{\pm}(\rho) = T_0 + \frac{1}{2}k^{\pm}\rho^2 + k_4^{\pm}\rho^4$$

where T_0 is the zero-point energy, $k^{\pm}$ are the force constants for the upper and lower Born–Oppenheimer components, and $k_4^{\pm}$ are quartic anharmonicity coefficients. ρ is the bending parameter and the bond distance is assumed to have the form

$$r(\rho) = r(\rho = 0) + d \tan^2 \frac{1}{2}\rho$$

$V^{\pm}$ and d were established by iterative fitting of the bending levels analyzed rotationally by Gausset et al.[150] The derived parameters are given in Table IX. The size of the g_k parameter, introduced by Brown,[216] gives a measure of the relative admixtures of the Σ and Δ electronic states of the linear molecule. Including this parameter was essential to a good fit to the experimental data. As mentioned earlier, the vibrational contribution to K-type doubling, first considered by Johns[214] and extended by Brown[162] (within the harmonic approximation), provides information about ν_3'. Jungen and Merer include it in their theory, demonstrate that the approaches are equivalent,[163] and compare their K-type doublings with those of Brown for C_3. C_3 is the only linear molecule for which the local Coriolis resonances between levels of the two Born–Oppenheimer components have been observed.

Perić and Radić-Perić have reviewed their theoretical work,[194b] in collaboration with Romelt, Peyerimhoff, Buenker, and others at Bonn,[194a–e] on the lowest lying $^1\Pi_u$ (and $^3\Pi_u$) state of C_3. The ab initio MRD–CI calculation of Perić-Radić et al.[194a] was mentioned earlier. They calculated the potential curves corresponding to the three vibrational modes for the ground and $^{1,3}\Pi_u$ states including only s and p functions. The Renner–Teller effect in the $^1\Pi_u$ state was further studied by Perić and Radić-Perić and, including CI and consideration of large bending amplitude, by Perić, Peyerimhoff, and Buenker.[194d] The most recent work[194b] used the ab initio bending potential surfaces[194a] (except for the ground state where the experimentally compatible potential function of Jungen and Merer[163] was used) and a kinetic energy operator for large-amplitude bending vibrations,[198] and included coupling of the electronic and bending motions in the $^1\Pi_u$ state. Calculated intensity distributions in the $^1\Pi_u$–$^1\Sigma_g^+$ bending progressions were compared with the experimental data and with those obtained by Jungen and Merer.[163] A similar quality of fit was obtained.

TABLE X. Molecular Constants of C_3 in the $X^1\Sigma_g^+$ and $A^1\Pi_u$ States

	$X^1\Sigma_g^+$	$A^1\Pi_u$
T_0,[a] cm^{-1}	0	24,675.5
B_{000}, cm^{-1}	0.4305[a–c]	0.4124[a]
r_0, Å	1.277[a–c]	1.305[a]
B_e,[b] cm^{-1}	0.41767	
α_1, cm^{-1}	+0.0048[b]	0.0030[d]
α_2 ($\alpha_{2'}$),[b] cm^{-1}	−0.01345 (+0.00071)	
α_3,[b,c] cm^{-1}	−0.00512 (5)	
r_e,[b] Å	1.2968	
ν_1, cm^{-1}	1224.5[d,e]	1085.9[d]
x_{11},[d] cm^{-1}	3.25	0.95
ν_2,[a] cm^{-1}	63.1	307.9 $\epsilon = +0.537$[f]
ν_3, cm^{-1}	2040.02[b,c]	~840[e]

[a] GHLR, ref 150. [b] Reference 161b. [c] Reference 161a. [d] Reference 151. [e] Reference 157 (see text). [f] Renner parameter.

Table X (and Table VIII) brings up to date the molecular constants of C_3 in the $X^1\Sigma_g^+$ and $A^1\Pi_u$ states.

F. Other Electronic States

1. $a^3\Pi_u$

Experimental evidence for this excited state was provided by the emission studies of Weltner and McLeod[156] in neon and argon matrices and better spectra were obtained by Bondybey and English.[158] Excitation by either 3650- or 4047-Å mercury light yielded a long-lived emission with the (0,0) band at 5856 Å in neon and 5905 Å in argon.[156] Bondybey and English,[158] exciting with a nitrogen-pumped dye laser, observed this same emission spectrum, regardless of which upper state vibrational levels were excited. Vibrational relaxation in the $A^1\Pi_u$ state is then very fast and crossing into the $^3\Pi_u$ state occurs from the vibrationless 000 level of the $^1\Pi_u$ state. Vibrational structure in the emission corresponded with the bending mode in the $X^1\Sigma_g^+$ state and in addition also included a weak band assignable to the previously unobserved symmetric stretching frequency $\nu_1'' = 1235$ cm^{-1} in the ground state. It was also noted that the line widths of transitions involving the low-frequency bending were severely broadened due to matrix phonon interaction, in accord with the low value of ν_2''.[158] The lifetime of the emission was found to be 0.02 s. The overall evidence then indicated that the transition is the forbidden $^3\Pi_u \rightarrow X^1\Sigma_u^+$.

This assignment has been supported by at least two ab initio calculations: Peric-Radić et al.[194a] calculated that the $^3\Pi_u$ state lies at 2.04 eV (compared to 2.10 eV = 5900 Å observed) and found the bond distance to be only slightly larger than in the ground state. (The calculated excitation energy of the $^1\Pi_u$ state was found to be in almost exact agreement with the observed, 3.03 vs 3.06 eV.) Vibrational frequencies were calculated to be $\nu_1 = 1209$, $\nu_2 = 440$, and $\nu_3 = 1344$ cm^{-1}. Williams,[219] using the equation-of-motion method, predicted the $^3\Pi_u$ state to lie at 1.73 eV, which the author considered as support for the assignment of the matrix emission. The accuracy of calculation is indicated by the $^1\Pi_u \leftrightarrow {}^1\Sigma_g^+$ transition energy, which was calculated to be 3.63 eV as compared to the observed 3.06 eV. Perić and Radić-Perić[194b] also predicted the vibronic energy levels of the $a^3\Pi_u$ state.

This triplet excited state has not as yet been detected in the gas phase.

2. ${}^1\Sigma_u{}^+$

Chang and Graham[220] assigned a band system, observed in absorption, originating at 1890 Å (6.6 eV) in a solid argon matrix at 8 K to the long-sought ${}^1\Sigma_u{}^+ \leftarrow X^1\Sigma_g{}^+$ transition of C_3. The intensity of the observed bands correlated with the appearance of the 4050-Å system of C_3. A vibrational analysis, which presumably is somewhat tentative, yielded $\nu_1' \simeq 1080$, $\nu_2' \simeq 300$, and $\nu_3' \simeq 780$ cm^{-1} in the upper state.

The ${}^1\Sigma_u{}^+ \leftarrow X^1\Sigma_g{}^+$ transition is the first optically allowed transition beyond the 4050-Å system, and it is expected to be easily observed since it is strongly allowed [a V–N transition in Mulliken's terms[156]], assuming that the upper state is stable.[157] Early theory predicted it to lie at 5.5[221] or 4.7 eV[222] but two searches that had been made[157,223] in rare-gas matrices failed to find any strong absorptions out to 1950 Å (6.4 eV), even though the 4050-Å bands were very strong. More recent calculations by Williams[219] placed this transition much further into the ultraviolet at 7.68 eV with an oscillator strength $f = 0.92$. MRD–CI calculations by Romelt et al.,[195] placed it at even higher energy (8.00 eV) and with a vertical f value of 0.92. The latter authors also calculated potential curves for symmetric and asymmetric stretching and, less thoroughly, for the bending motion in the ${}^1\Sigma_u{}^+$ state. Although the curves show genuine minima, the bending curves are found to be complicated by mixing, primarily with ${}^1B_2$ components of other states. Their interesting conclusion was that the high intensity of this transition might be distributed over quite a large energy range, with the implication that the higher energy C_3 spectrum might be more complex than originally supposed. There then remains an interesting disagreement between the theoretical predictions and Chang and Graham's findings.

3. Other Excited States

Although the transition to the ${}^1\Sigma_u{}^+$ state is the first optically allowed beyond that to the ${}^1\Pi_u$, there are predicted to be seven other singlet and triplet states with energies up to about 4 eV, excluding the low-lying ${}^3\Pi_u$ state discussed above.[195] Rydberg states are calculated to lie well above the ${}^1\Sigma_u{}^+$ state. The ordering of states when calculated by the equation-of-motion method[219] is about the same as that obtained in the MRD–CI calculations.[195] Also, Sunil et al.[224] calculated the vertical excitation energies of the lowest ten states of C_3 using a 6-31G basis set and limited CI. The ordering of the energy levels was essentially the same as that of Romelt et al.[195] The most recent calculation of Chabalowski, Buenker, and Peyerimhoff[225] extended their earlier calculations[194,195] by utilizing a large AO basis containing two primitive d functions on each atom and s- and p-type functions at the center of each bond to allow for additional polarization. The MRD–CI treatment was again employed. The $A^1\Pi_u$ state is calculated at $T_0 = 3.13$ eV (experiment 3.06 eV).[150] The $C^1\Pi_g$ state is at 4.10 eV (of interest is the $C^1\Pi_g \leftrightarrow A^1\Pi_u$ transition).

TABLE XI. Experimentally and Theoretically Determined Electronic Oscillator Strengths (Absorption) f_{lu} for the $C_3({}^1\Pi_u \leftarrow X^1\Sigma_g)$ Transition[f]

investigator	year	method	f_{lu}	ref
Brewer and Engelke	1962	gas phase, absorption	0.045[a]	143, 232
Barger and Broida	1965	matrix, absorption	0.06[b]	153
Williams	1975	theory	0.129	219
Perič-Radič et al.	1977	theory	0.061	194
Arnold and Langhoff	1978	theory	0.049	233
Römelt et al.	1978	theory	0.0492	195
Cooper and Jones	1979	gas phase, shock tube	0.033[c]	232
Becker et al.	1979	gas phase, fluorescence	0.0246[d]	231
Monyakin and Kuznetsova	1983	gas phase, shock tube	0.044[e]	234
Chabalowski et al.	1986	theory	0.052	225

[a] Given as 0.13, adjusted by Cooper and Jones.[232] [b] Uncertainty factor = 3. [c] ±25%, plus a C_3 concentration uncertainty of ±40%. [d] ±0.0010. [e] ±0.020. [f] Radiative lifetime and square of the electronic transition dipole moment are determined as follows: radiative lifetime = τ (s) = $2(1.5)/f_{lu}\bar{\nu}^2$; square of the electronic transition dipole moment = $\sum|R_e|^2 = ({}^3/{}_2 f_{lu})/\Delta E$, where $\Delta E = 3.06$ eV or $\bar{\nu} = 24\,685$ cm^{-1}.

Lemire et al.[226] recently observed in jet-cooled C_3 a complicated band system in the range 266–302 nm (4.7–4.1 eV) having lifetimes between 0.4 to 2.5 μs. They concluded that the new band system(s) were electric-dipole forbidden and tentatively assigned the upper state(s) as ${}^1\Pi_g$ and/or ${}^1\Delta_u$, the transition being made observable through Herzberg–Teller vibronic coupling. There is evidence of a weak transition in this region in earlier matrix spectra.[157]

G. Electron Affinity (EA) and Ionization Potential (IP)

Sunil et al.[224] used multiconfigurational self-consistent field (MC–SCF) and CI procedures, and for smaller basis sets, Møller–Plesset perturbation theory to calculate EA and IP. They obtained a most probable value of 11.5 eV for the IP, which is not consistent with the older experimental values of 12.1 (0.3)[227] and 12.6 (0.6) eV[122] but is consistent with the more recent values 9.98–11.61[228] and 11.1 (0.5) eV.[229]

The theoretical estimate for the EA is 2.0 eV, not in agreement with 2.5 eV from sublimation of graphite studies[172] but in agreement with a recent photodetachment measurement of 2.05 eV for the IP of $C_3{}^-$.[230]

H. Electronic Oscillator Strength and Franck–Condon Factors for the $A^1\Pi_u \leftarrow X^1\Sigma_g{}^+$ Transition

A recent comparison of the theoretical and experimental values of the absorption oscillator strength (f_{lu}) or radiative lifetime (τ) of the $A^1\Pi_u \leftrightarrow X^1\Sigma_g{}^+$ transition of C_3 has been reviewed by Becker, Tatarczyk, and Radič-Perič[231] and by Chabalowski, Buenker, and Peyerimhoff.[225] A collection of all of the presently measured and calculated values is given in Table XI. Most of the theoretical calculations that have been done by Buenker, Peyerimhoff, and co-workers have now converged on $f_{lu} = 0.05$ and $\tau = 100$ ns, whereas the presumed most reliable experimental value was obtained from gas-phase fluorescence, $f_{lu} = 0.025 \pm 0.001$, $\tau = 200 \pm 8$ ns.[90] This factor of 2 discrepancy is not presently understood.[225] Apparently, a discrepancy of this magnitude also occurs in the ${}^1\Pi_u$–${}^1\Sigma_g{}^+$ Phillips system of C_2, although for five other well-known systems of C_2 there is agreement within 10–20% between experiment and theory.[225] The only other experimental values are of the absorption oscillator strength for the 000–000 transition determined in matrices:[156] f_{00} = 0.0007 in neon, f_{00} = 0.0037 in argon. This difference probably reflects the uncertainty in the determination of the number of molecules trapped.

Franck–Condon factors for this transition were calculated by Jungen and Merer[163] using the potential functions that they generated for the two states (see above). They are found to generally agree with experiment[150] and with unpublished calculations of Morgan and Kroto,[235] who used a harmonic oscillator basis with linear displacements for the bending coordinate. This indicates that the band intensities, as opposed to their positions, are not very sensitive to whether a large-amplitude formalism is used.

The large change in the bending vibrational frequency in the two electronic states leads to very long progressions in the upper state bending frequency in absorption, observed clearly in the neon matrix spectra.[156] Jungen and Merer[163] found that their calculations fit the crude relative intensities measured for the matrix bands surprisingly well for the upper (+) components but less for the lower (−) components. This difference is reasonably explained as due to increased matrix perturbations for the large amplitude of bending of the lower components.

Perič and Radič-Perič improved the earlier ab initio MRD–CI calculations[194] using the operator derived by Hougen et al.[198] to account for the large-amplitude vibration and the potential function of Jungen and Merer[163] and including the coupling between electronic bending motions in the $^1\Pi_u$ state.[194a–d] A comparison between intensity distributions in the bending progression calculated in this way and experiment agrees well with the comparison made by Jungen and Merer.[163]

VI. $C_3{}^+$ and $C_3{}^-$ Ions

There is much interest in these ions, but presently there is no spectroscopic information. The only experimental data are those of Faibis et al.[236] from application of the Coulomb explosion method to determine the geometric structure of $C_3{}^+$. Although not definitive, the results strongly indicate that the molecule is bent, probably into a ring structure. Note that this method was applied to neutral C_3 (see above) by Goldring et al.[181] and by Plesser et al.[182] and supported a floppy linear structure.

A MINDO/3 calculation by Kühnel, Gey, and Spangenberg[237] found $C_3{}^+$ and $C_3{}^-$ to be linear (and neutral C_3 to be bent at an angle of 104.7°). Ab initio calculations by Sunil et al.[224] and by Raghavachari and Binkley,[261] presumably assuming $C_3{}^+$ to be linear, both found its ground state to be $^2\Sigma_u{}^+$. The former authors found that the ground state of linear $C_3{}^-$ is $^2\Pi_g$ and is stable by 1.74 eV.[224] There is apparently more recent unpublished ab initio theoretical support for a bent $C_3{}^+$ structure.[238]

VII. C_4 through C_{10} Molecules and Ions

A. Overview

These molecules constitute a very minor fraction of the saturated vapor over graphite up to 3000 K,[94,122,174,176] and none of them has been detected in the gas phase except via mass spectrometry. Their proportion in carbon vapor can be increased by laser vaporization of graphite[177] or of thin carbon foil[239] or by supersonic expansion of carbon vapor.[240–245]

Many theoretical calculations of their electronic properties and structures have been made, beginning with those of Pitzer and Clementi.[221] Using a refined Hückel π-electron model they predicted that C_n molecules would be linear and that those with n odd would have $^1\Sigma$ ground states and be more stable than those with n even, which would have $^3\Sigma$ ground states. They suggested that at about n = 10 rings might be formed since the strain energy would then be small and forming another bond would be energetically favorable. Clementi[188,246] made an SCF–LCAO calculation for a linear C_4 molecule with fixed bond distances and confirmed the triplet ground state and a double-bonded cumulene-like structure.

Müller[247] applied a novel free-electron model to the linear chains where the electrons were confined to a potential of cylindrical symmetry with radius equal to the van der Waals radius of a carbon atom. There was a clear correlation with LCAO–MO methods for C_3 and C_4.

In 1964 Strickler and Pitzer[248] improved their earlier calculation using a semiempirical LCAO–MO method and concluded in the case of C_4 that an acetylenic structure $\cdot C{\equiv}C{-}C{\equiv}C\cdot$ ($^3\Sigma_u{}^+$) would be more stable. They were uncertain about whether C_6 and higher even-membered species should be polyacetylene- or cumulene-type. Cyclic species would probably not make a large contribution to the vapor since they have much lower entropies than the corresponding chains. Hoffmann,[192] in an extended-Hückel calculation, found linear chains to be more stable than rings up through C_9 but there was a periodicity in the ring stability of $4n + 2$ making rings for C_{10}, C_{14}, and C_{18} more stable than chains. The bond distances alternated; for example, in linear C_{16} they were calculated to be (in Å) 1.233, 1.407, 1.267, 1.366, 1.291, 1.341, 1.306, and 1.332. Extrapolating to large n, he concluded that bond alternation in the linear chains would not persist but that the "end effect" would be great; i.e., "one will have to look quite far into the interior of the carbon chain before the bond distances settle down to a constant value". He found this persisting "mixed behavior" paradoxical since complete alternation or the absence thereof seems intuitively more to be expected. The calculations are perhaps made more significant when one notes that, at this level of theory, Hoffmann made (and discarded!) the prediction that C_3 would be slightly bent [present evidence now supports quasi-linear C_3 (see the above section on the C_3 molecule)].

A significant paper appeared in 1977 in which Slanina and Zahradník[249] considered the C_n (n = 4–7) molecules more generally, using Dewar et al.'s MINDO/2 method,[250] by examining the stabilities of additional geometries. For C_4, for example, they considered eight possible structures ranging from linear ($D_{\infty h}$) to planar (D_2, D_{2h}, D_{4h}) to nonplanar (D_{2d}, T_d). The results of extensive MINDO/2 geometry optimization indicated (1) that the C_n aggregates have at least two isomers and (2) the energetically most favorable isomer is, in all cases, nonlinear. These provocative conclusions brought

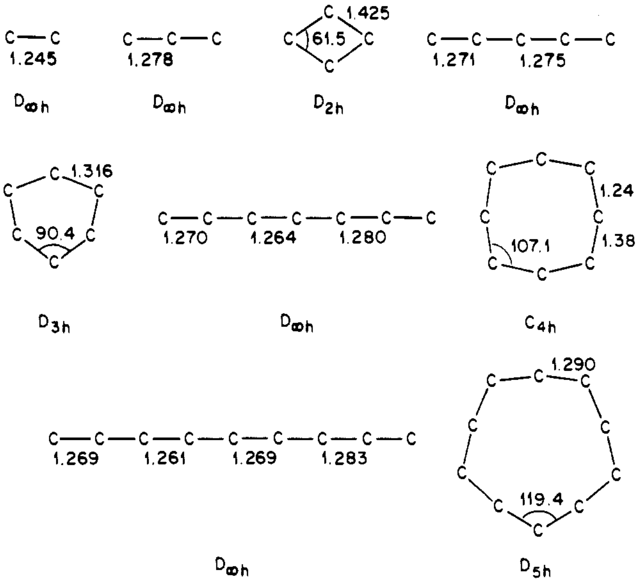

Figure 4. Calculated ground-state geometries of the C_2 through C_{10} molecules. Bond lengths are shown in angstroms and bond angles in degrees. Note that there are also low-lying linear structures that are close in energy to the cyclic forms in the case of C_4, C_6, and C_8. (Reprinted from ref 261; copyright 1987 American Institute of Physics.)

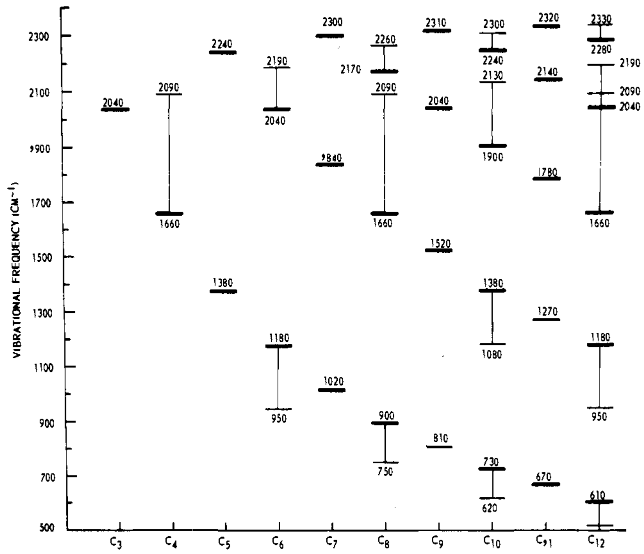

Figure 5. Approximate infrared-active stretching frequencies of linear carbon molecules. Heavy horizontal lines indicate frequencies for $(C{=}C{=})_n$ molecules, and light horizontal lines are for $(C{\equiv}C{-})_n$ molecules. (Reprinted from ref 157; copyright 1966 American Institute of Physics.)

the problem to the attention of other theorists and suggested more exact ab initio treatments of polycarbon species. [A recent similar calculation by Bernholc and Phillips[251,252] used Dewar's self-consistent modified neglect of differential overlap (MNDO) program[250] with the constraint of all C–C bonds equal. However, there, linear chains were found to be most stable up through C_{12} (except C_{10}) and monocyclic rings from C_{13} to C_{25}. The most stable neutral clusters were C_{10}, C_{14}, C_{15}, C_{18}, C_{19}, and C_{23}].

The first of the ab initio calculations by Whiteside et al.[253] considered the linear form and two cyclic forms of C_4, concluding that indeed a bicyclic (D_{2h}) form of C_4 was more stable than the linear form by approximately 6 kcal/mol. This was followed by many good theoretical papers on C_4,[254-264] C_5,[254,257,261,262,265,266] C_6,[254,261,262,266,267] and $n = 7$ to about 10.[261,262] All of these published calculations agree as to the two lowest energy structures of C_4, but cannot always agree as to which is more stable. The other n-even molecules C_6 and C_8 are somewhat controversial. Most calculations find C_5, C_7, and C_9 to be linear and singlet. For $n > 9$, rings are favored. Ab initio calculations including the larger molecules have been made recently by Raghavachari and Binkley[261] and by Ott and Ray.[262] The most stable forms of C_n (n = 2–10) molecules as found by the former authors are shown in Figure 4. One sees that the ground states of all n-odd molecules are predicted to be linear and all n-even to be monocyclic (except C_4, which is bicyclic; however, see below). Also, the monocycles are not found to be regular polygons. However, in some cases for n even, the linear and cyclic structures, with corrections for spin contamination, are projected to be very close in energy, perhaps within the accuracy of the calculations. Figure 4 does not explicitly show these isomeric possibilities. This is the case for C_4 and C_8, and for C_6 the cyclic structure is only about 9 kcal/mol more stable than the linear form. However, at C_{10} the energy difference becomes quite large and the cyclic structure is predicted to be more stable than the linear form by more than 1 eV. Above C_{10} cyclic structures will probably be the most stable isomers. We will discuss these and other ab initio calculations in more detail when considering the individual molecules.

Are there any experimental data to corroborate these theoretical findings? The only spectroscopic measurements of C_n ($n > 3$) molecules have been made in rare-gas matrices at low temperatures. These include infrared, UV–visible, and electron spin resonance (ESR) studies of the neutral polycarbons.

The infrared spectra of the molecules vaporized from ^{12}C- and ^{13}C-enriched graphite were observed in argon matrices by Thompson, DeKock, and Weltner[160] and recently largely corroborated by Ortman[268] and Krätschmer and Nachtigall.[269] A striking feature was the very reactive nature of the small C_n molecules, since raising the matrix temperatures from 4 K to only 30 K caused the essential disappearance of the strong C_3 band at 2040 cm^{-1} and the appearance of a dozen new bands between 1800 and 2200 cm^{-1}. Figure 5, taken from Weltner and McLeod,[157] models the expected variation of the ungerade, i.e., infrared-active, stretching frequencies of linear carbon chains either with equivalent bonds (cumulenic bonding) or with alternating bonds (acetylenic bonding). A force constant $f = 10.3 \times 10^5$ dyn/cm from $\nu_3 = 2040$ cm^{-1} for C_3 was used for equal bonds and $f_1 = 15.6 \times 10^5$ and $f_2 = 4.68 \times 10^5$ dyn/cm for alternating bonds. Both experiment and theory now agree that linear carbon molecules approach closest to cumulene-type bonding; i.e., the heavy lines in Figure 5 are most relevant. At that time cyclic forms were not considered. Efforts were made by Thompson et al.[160] to assign the stretching frequencies (1100–2200 cm^{-1}) to the higher polymers C_4–C_9 using limited normal coordinate treatments and mixed isotopes, assuming all molecules were linear. The most reliably assigned molecule was considered to be C_6, and from the two observed σ_u^+ frequencies at 1997 and 1197 cm^{-1}, approximate values of the three σ_g^+ frequencies were predicted. Bending frequencies were not assigned; however, Sanborn[270] extended the correlation of the filling of the π_g and π_u orbitals with bending force constants, discussed in the C_3 section, to estimate the bending frequencies in linear C_4, C_5, and C_6. There are presently no experimental data on those vibrational modes.

Recently, Krätschmer and Nachtigall[269] remeasured the IR spectra of argon matrix isolated carbon molecules and obtained data in essential agreement with those of Thompson et al., but found the C_6 assignments to be in doubt. Also, lines in the range 1600–1800 cm^{-1} are considered as possibly due to cyclic species.

Wdowiak,[271] in attempting to reproduce the source of the diffuse interstellar bands (DIBs) trapped the discharge products of a dilute methane-in-argon mixture at 16 K. In absorption, he found eight bands in the visible and near-infrared that correlate with DIBs. It is inferred that some of these may be due to long-chain carbon molecules, as suggested by Douglas.[272]

Krätschmer et al.[269,273] also observed the UV–vis absorption spectra of argon matrices and assigned a series of bands between 247 and 600 nm to C_4–C_9 molecules on the basis of growth and decay during annealing. Extrapolating from C_3 and C_4, they assigned bands at increasingly longer wavelengths to (most likely linear) C_5 (311 nm), C_6 (394 nm), C_7 (447 nm), C_8 ($\sim$500 nm), and C_9 ($\sim$600 nm).

The most positive data on these molecules were obtained from ESR spectra where the magnetic triplet species are selectively observed and where ^{13}C hyperfine splittings aid in identification. C_4 was thoroughly studied in this way (and via optical spectroscopy) by Graham, Dismuke, and Weltner,[274] and recently, using laser vaporization, Weltner et al. studied the larger polycarbons C_6, C_8, and C_{10}.[275,276] The small resolved ^{13}C hfs in the C_4 and C_6 spectra, unresolved in C_8, establishes that the bonding in these linear molecules is cumulene-like and not acetylene-like so that they are in their lowest triplet ($^3\Sigma_g^-$) states. C_{10} appears to be trapped as two near-linear triplet isomers. Ab initio theory does not necessarily conflict with the ESR findings for C_4–C_8, since if triplet linear and singlet cyclic forms are in each case almost isoenergetic, both forms could be trapped in the matrices but only the triplet would be detected. This might seriously complicate any attempt to assign infrared or optical spectra. However, as first pointed out by Pitzer et al.[221,248] and again by Van Zee et al.,[276] if equilibrium prevails, the dominant molecular species vaporizing from graphite will be the linear ones, at least up to C_{10}, because of their larger entropy contributions.

B. C_4

As with the other carbon molecules larger than C_3, C_4 is a minor species ($\sim$0.1%) in the saturated vapor over graphite at 2500 K; laser vaporization does increase the proportion of C_4 to about 3%.[177] This was established mass spectrometrically.[94,122,174,176] From these measurements it was also found that the binding energy of the C_4 molecule is 19.4 (4) eV.[122,261,277]

The C_4 molecule has not been observed spectroscopically in the gas phase but has been observed in the infrared and visible regions and via ESR, all in neon and argon matrices. However, most of the research effort has been on theoretical calculations of its properties and has resulted in the prediction of two almost isoenergetic structural isomers.

TABLE XII. Molecular Constants[a] Derived for Linear C_4 from Matrix Data[b]

state	parameter	value
$^3\Sigma_u^-$	T_0	19564 (50)[c]
	ν_1'	2100 (10)
$^3\Pi_g$	T_0	<6000
$X^3\Sigma_g^-$	λ''	0.128 (3)[d]
	γ''	−0.0006 (2)
	$\lvert A_\perp(^{13}C)\rvert$[e]	28.7 (3) MHz
	$\lvert A_\parallel(^{13}C)\rvert$[e]	13.0 (3) MHz
	$g_\perp$	2.0041 (5)

[a] All constants are given in cm^{-1} except A and g. [b] Revised Table 3 in ref 274. [c] Quantities in parentheses indicate uncertainties in gas-phase values predicted from matrix values. [d] The spin-coupling parameter λ is related to the zero-field splitting by $\lambda = D/2$. [e] Observed hf splitting (from ref 276), not definitely assigned to interaction with inner or outer carbon atoms.

1. Experiment

The most positive data on C_4 were obtained by Graham, Dismuke, and Weltner[274] from ESR spectra in neon and argon matrices at 4 K. The molecule was formed both by photolytic dissociation of diacetylene (C_4H_2) and by resistance-heated vaporization of graphite. The characteristic ESR spectrum of a randomly oriented linear triplet molecule was observed with a zero-field-splitting parameter $|D|$ = 0.238 (3) cm^{-1} in solid neon. It is significant that substitution of 98% ^{13}C-enriched carbon produced only an 11-G hyperfine splitting, eliminating an acetylenic-bonded molecule ($\cdot C{\equiv}C{-}C{\equiv}C\cdot$) as a possibility. Such bonding would place the unpaired spins in essentially spσ-hybridized orbitals, but the small observed hfs establishes that the unpaired spins possess negligible s character. Thus the molecule has a $^3\Sigma$ ground state with cumulene-type bonding (crudely depicted as $:C{=}C{=}C{=}C:$) with the two spins in pπ orbitals.

The departure of the measured $g_\perp$ = 2.0041 (5) from the free-electron value g_e = 2.0023 suggests the presence of a low-lying inverted $^3\Pi_g$ state at $<\sim$6000 cm^{-1} = 0.8 eV, which contributes angular momentum to the ground electronic state.[274,278] Also, from Curl's relationship,[278,279] the $g_\perp$ shift yielded a spin-rotation constant of γ'' = −0.0006 (2).

Optical transitions were observed at 5110 and 4617 Å (2.426 and 2.685 eV) in neon, and the $\Delta\nu$ = 2089 cm^{-1} from these bands was assigned as the symmetric stretching frequency (σ_g^+) in the upper electronic state of the linear C_4 molecule. This brief progression was considered to correspond to the electronic transition $^3\Pi_u$ or $^3\Sigma_u^- \leftarrow X^3\Sigma_g^-$. (Theory is in accord with this if the upper state is $^3\Sigma_u^-$; see below.) Krätschmer, Sorg, and Huffman[273] also assigned a band at 247 nm (5.02 eV) to C_4, from the observation that its growth in the argon matrix correlates with that of the above two bands. Making small adjustments for matrix effects, Graham et al.[274] predicted the gas-phase molecular constants of C_4 given in Table XII.

In separate experiments, Thompson, DeKock, and Weltner[160] observed the infrared spectra of argon matrices containing ^{12}C- and ^{13}C-polycarbon molecules. Isotopic shifts and relative rates of growth of bands during diffusion were used to make assignments to particular C_n molecules, assuming they were linear, a procedure obviously fraught with uncertainties. (At that time, a rhombic isomer of C_4 had not yet been proposed.) A band at 2164 cm^{-1} was incorrectly assigned to C_4 (it is now definitely known to be a σ_u vibration of C_5; see below) and considered at the time as support for the acetylenic form. Others[259,260,263,264] noted that this frequency is too high for a cumulene-type C_4 vibration, where a frequency near 1600–1700 cm^{-1} is expected.[270] Thompson et al.[160] observed several bands, with the proper isotopic shifts, in the 1500–1700-cm^{-1} region. Ortman[268] suggested that the 1544-cm^{-1} band assigned to C_5 by those authors may belong to C_4; however, the recent work by Vala et al.[282] supports the earlier assignment (see below). The latest calculations of the vibrational frequencies of C_4 (discussed in the next section) yield ungerade frequencies for the linear molecule at 1586 and 187 cm^{-1}. Infrared spectra have not been measured in the low-frequency bending region. Thus, at this time, none of the ground-state vibrational frequencies of C_4 has been determined.

2. Theory

Clementi[248] made a minimum-basis ab initio SCF–LCAO calculation with all bond distances fixed at 1.28 Å in linear C_4. Among the three states of configuration $1\sigma_g{}^2 1\sigma_u{}^2 2\sigma_g{}^2 2\sigma_u{}^2 3\sigma_g{}^2 3\sigma_u{}^2 4\sigma_g{}^2 4\sigma_u{}^2 5\sigma_g{}^2 1\pi_u{}^4 1\pi_g{}^2$, the order of increasing energy was $^3\Sigma_g{}^-$, $^1\Delta_g$, and $^1\Sigma_g{}^+$. It was concluded that in the $X^3\Sigma_g{}^-$ state the structure corresponds to :C=C=C=C:, as he and Pitzer had previously reported.[218]

After Slanina and Zahradník's[249] semiempirical calculations indicated the possibility that other conformations of C_4 should be considered, Whiteside et al.[253] made an ab initio treatment (using a 6-31G* basis and fourth-order MBPT with single, double, and quadruple excitations) of linear and two planar forms of C_4. They found the bicyclic structure **1** about 30 kcal/mol more stable than **2**, but only marginally more stable than the linear form.

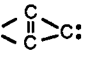

D_{2h}

1

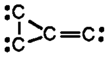

C_{2v}

2

The principal configuration of the ^1A_g ground state of **1** is $1a_g{}^2 1b_{3u}{}^2 2a_g{}^2 1b_{2u}{}^2 3a_g{}^2 2b_{3u}{}^2 2b_{2u}{}^2 4a_g{}^2 1b_{1g}{}^2 1b_{1u}{}^2 3b_{3u}{}^2 5a_g{}^2$. When account was taken of spin multiplicity, it was reasoned that the singlet bicyclic form is more stable than triplet linear C_4 by approximately 6 kcal/mol. The latter value depends somewhat upon a choice for the singlet–triplet energy spacing. Regardless of the exact energy difference between the singlet bicyclic and triplet linear forms, it is clear that they should be, according to this calculation, almost isoenergetic geometrical isomers.

Ab initio calculations comparing the stabilities of optimized structures for these two forms of C_4 were also carried out by Magers, Harrison, and Bartlett[259] using CC–MBPT, by Ritchie, King, and Young[260] using SRCI, by Rao, Khanna, and Jena[258] using UHF–CI, by Koutecký and Pacchioni[257] using MRD–CI, by Raghavachari and Binkley[261] using UHF-CCD+, by Ott and Ray[262] using HF with 6-31G* basis, by Michalska et al.[263] using UHF–UMP2 (or RHF–UMP2), and Nemukhin et al.[280] using HF–CI. Wang, Diffenderfer, and Shavitt[256] made unpublished calculations using MR–CI–DZP. [Calculations on the linear C_4 molecule only were made by Ewing and Pfeiffer[254] (SCF–DZP) and by Nemukhin, Stepanov, and Safonov[255] (small CI, minimum basis + d).] Most of these authors were in essential accord with Pople's group[253] in placing the singlet rhombic form of C_4 lower in energy than the triplet linear form by about 5 kcal/mol. The optimum geometries (varying slightly among the authors) as given by Magers et al.[259] in angstroms are

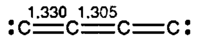

$^3\Sigma_g{}^-$

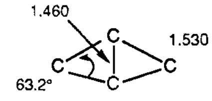

^1A_g

However, Nemukhin et al.[280] and the unpublished work of Shavitt's group[256] found the linear triplet form to be the most stable one. Recent calculations of Bernholdt, Magers, and Bartlett[264] using a 5s3p1d basis at various levels of coupled-cluster and many-body perturbation theory find that the two isomers are essentially isoenergetic.

The possible "fluxional" character of the rhombic form was examined to a limited extent by Magers et al.[259] They found the planar square form quite high in energy, which implies that if any such pseudorotation did occur, it would pass through a nonplanar transition state. Since bonds must be broken to convert the rhombus to the linear structure and vice versa, interconversion between the two isomers would be expected to be slow regardless of the thermodynamics.

Recent calculations,[264,276] assuming equilibrium vaporization of graphite, indicate that the linear form of C_4 is favored over the cyclic form by a factor of about 7, due to the larger entropy of the linear isomer. Partition functions in these calculations were obtained by using the above theoretically derived structures and vibrational frequencies of the two forms and assuming $\Delta H_0° \cong 0$ for the linear to cyclic equilibrium. This dominance of the linear form in the gas phase over graphite would then be expected to be the same when the molecules are quenched in matrices. However, it is not obvious that reactions at low temperature between C and C_3 or $2C_2$ will not form C_4 in the rhombic form in the matrices. As mentioned earlier, this causes some worry about the assignments of infrared and electronic transitions of C_n molecules in matrices. The observed electronic transitions in matrices[274] assigned to C_4 do appear to be in complete accord with the theoretical expectations for the linear isomer. Of course, inferences made from ESR spectra apply only to the linear triplet isomer.

As Table XIII indicates, the electronically allowed transition $^3\Sigma_u{}^- \leftarrow X^3\Sigma_g{}^-$ is calculated to lie at ~2.8 eV (22 600 cm^{-1}) for the linear molecule. Graham et al.[274] observed a progression with the 0–0 band at 2.426 eV (19 570 cm^{-1}) and 1–0 at 2.685 eV (21 660 cm^{-1}) in a neon matrix which was assigned to this transition [or to $^3\Pi_u \leftarrow X^3\Sigma_g{}^-$; however, theoretically that transition should appear in the red or near-infrared (see below)]. The two bands had the correct relative intensities to constitute a vibrational progression in the upper state with symmetric stretching frequency $\nu_1' = 2089$ cm^{-1}. A $\sigma_g{}^+$ frequency of this magnitude is about what one might expect if the corresponding ground-state value is ~2149 cm^{-1}, as is also theoretically predicted[263] (see below).

The $\Delta g_\perp$ shift of the triplet molecule derived from the ESR spectra[274] indicates that there is probably a

TABLE XIII. **Calculated Electronic States (eV) of the Rhombic and Linear Isomers of C_4**[a]

rhombus				linear					matrix data
state	MHB	RKY	PK	state	MHB	RKY	PK	NDKSP	
$^1B_{2u}$			7.03						
$^1B_{3u}$			6.88	$^1\Sigma_u^-$				3.56	
$^3B_{3g}$	3.325			$^1\Sigma_u^{-\,b}$	3.049	2.640	2.86	3.62	2.685
									2.426
$^1B_{2g}{}^e$	3.023		2.41	$^3\Sigma_u^{+\,d}$	(2.611)		2.21	2.05	
$^1B_{1u}{}^b$	2.398	2.451	2.39	$^1\Pi_u$			2.05	2.35	
$^3B_{2g}$	2.312			$^1\Pi_g$			1.73	2.05	
				$^3\Pi_u{}^b$	1.299	1.920	1.54	1.98	
$^3B_{1u}$	0.974			$^3\Pi_g{}^c$	0.971		1.00	1.69	<0.8
				$^1\Sigma_g^+$	(0.256)		0.68	0.73	
				$^1\Delta_g$	(0.253)		0.41	0.45	
X^1A_g	0.00	0.00	0.00	$X^3\Sigma_g^-$	0.00	0.00	0.00	0.00	

[a] MHB, ref 259; RKY, ref 260; PK, ref 257; NDKSP, ref 280; matrix data, ref 274. [b] Electronically allowed transition. [c] Vibronically allowed (σ_u, π_u) transition. [d] Vibronically allowed (π_g) transition. [e] Vibronically allowed (b_{1u}, b_{3u}) transition.

TABLE XIV. **Calculated Harmonic Vibrational Frequencies (cm^{-1}) of Rhombic and Linear Isomers of C_4**[a]

rhombus (^1A_g)			linear ($^3\Sigma_g^-$)	
sym	MCHS[b]	MHB, BMB[b]	sym	MCHS[b]
b_{3u}	374	359	π_u	187
b_{2u}	712	716	π_g	419
a_g	934	912	σ_g	951
b_{3g}	1103	1079	σ_u	1586
a_g	1298	1255	σ_g	2149
b_{1u}	1428	1389		

[a] Ungerade (u) are IR active; gerade (g) are Raman active. [b] MCHS (ref 263) calculations are MBPT (2)/6-31G*; MHB (ref 259) and BMB (ref 264) are MBPT (2)/4s2p1d.

low-lying $^3\Pi_g$ state at $<\sim$0.8 eV above the ground state which is coupled via its orbital angular momentum with the $X^3\Sigma_g^-$ state. As shown in Table XIII, theory places this excited state at ~1.0 eV, which may be taken as support for the experimental finding, considering the inaccuracies in both the experimental and theoretical values.

The harmonic vibrational frequencies of both isomers of C_4 have been calculated by several authors, and the most recent ones are given in Table XIV. As stated earlier, there is at present no experimental confirmation of any of these frequencies. Sanborn's[270] early estimates of the bending frequencies in the linear molecule, 200 cm^{-1} (π_u) and 440 cm^{-1} (π_g), are in good agreement with the calculated values.

3. *Spin Densities*

Graham et al.[274] observed each "perpendicular" line of the $^{12}C_4$ ESR spectrum to be split into a triplet [$|A_\perp(^{13}C)| = 28.7$ MHz] in the $^{13}C_4$ spectrum with a 1:2:1 intensity ratio. This implies that the hyperfine interaction is observable with two equivalent carbon nuclei and is small, within the line widths, for interaction with the other two nuclei. From the relatively small value of the zero-field-splitting parameter, D (varying approximately as $\langle 1/r_{ij}^3 \rangle$, r_{ij} being the electron spin–spin distance), it was reasoned that most of the spin was on the two equivalent *outer* carbon atoms. In later work, Van Zee et al.[276] measured $|A_\parallel(^{13}C)| = 13.0$ MHz, thus allowing $|A_{iso}| = |2A_\perp + A_\parallel|/3$ to be calculated as either 8.4 or 5.3 G, depending upon the relative signs of $A_\parallel$ and $A_\perp$. The spin density on the inner carbon pair would then have to be perhaps one-third of that for the outer carbons in order to match the observations. [Note that it may be difficult to distinguish between possible small spin distributions since an equal distribution of spin over the four ^{13}C nuclei would lead to a quintet having a 1:4:6:4:1 intensity pattern, in which the weaker outer lines might be indistinct.]

The important feature here is the magnitude of $|A_{iso}(^{13}C)|$, implying very small s character in the wave function for the unpaired electrons and requiring that they are not in sp hybrid orbitals as in the acetylenic form, but rather in pπ orbitals in a cumulene-like C_4. The theoretical calculations of Bernholdt et al.[264] confirm the experimental finding of very small isotropic splitting (~5–7 G) although the inner-carbon splitting is slightly larger than the outer, but that may be within the calculational error.

C. C_5 Molecule

Ab initio theorists generally agree that C_5 is linear with a $^1\Sigma_g^+$ ground state.[254,257,265,261,262] Ewing and Pfeiffer's[254] first calculation was restricted to linear C_5. Their later calculation[265,281] and that of Raghavachari and Binkley[261] considered the possibility of a variety of nonlinear structures, similar to Slanina and Zharadnik's[249] approach with MINDO/2. However, they found the linear singlet form to be the most stable by more than 60 kcal/mol, whereas the approximate treatment[249] found the trigonal bipyramid to be most stable. The electron configuration is $...(^1\pi_u)^4(6\sigma_g)^2(5\sigma_u)^2(^1\pi_g)^4$. The bond distances were 1.271 and 1.275 Å[261] or 1.277 and 1.280 Å,[265] consistent with a model :C=C=C=C=C:. A singlet trapezium (C_{2v}) structure, with carbon atom bridging the middle two carbon atoms of linear C_4, was next but considerably higher in energy.[265] Ott and Ray[262] also found, for optimized geometries, the linear form to be more stable than the cyclic, in the form of a ring.

With bond distances fixed at 1.31 Å (from C_4) in the linear structure, Pacchioni and Koutecký[257] calculated the energies of the excited singlet and triplet states. The $^1\Pi_u(6\sigma_g{}^1 2\pi_u{}^1) \leftarrow X^1\Sigma_g^+$ and the $^1\Sigma_u^+(1\pi_g{}^3 2\pi_u{}^1) \leftarrow X^1\Sigma_g^+$ are the lowest energy allowed transitions with T_e (oscillator strengths) of 3.18 eV ($f = 0.016$) and 6.76 eV ($f = 3.02$), respectively. Five triplet states lie in the 2.54–2.64-eV range.

The spectrum of C_5 is then expected to be very similar to that of C_3 in that both molecules have $^1\Pi_u \leftarrow {}^1\Sigma_g^+$ transitions at ~3 eV with comparable f values (0.03 vs 0.016) and intense $^1\Sigma_u^+ \leftarrow {}^1\Sigma_g^+$ transitions in the near-ultraviolet.[255] This is quite different from C_4, and

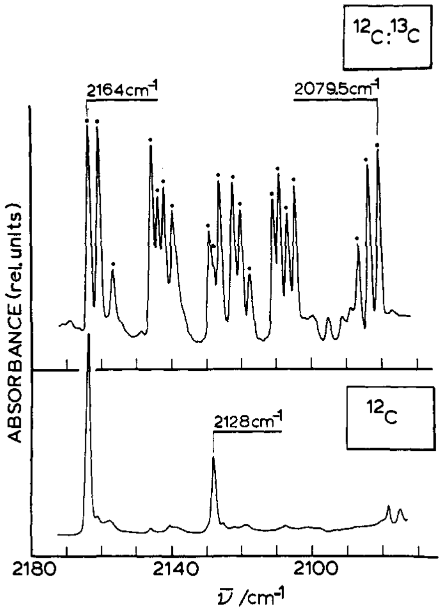

Figure 6. Evidence for a 2164-cm^{-1} vibrational frequency for linear $^{12}C_5$ from observation of its 20 isotopically substituted isomers: infrared bands in the 2070–2180-cm^{-1} region of laser-vaporized graphite in an argon matrix at 12 K. Bottom: vaporization of pure ^{12}C graphite. The 2128-cm^{-1} band has been ascribed to a larger carbon molecule, possibly $^{12}C_9$.[160] Top: vaporization of a 1:1 mixture of ^{12}C:^{13}C graphite; black dots indicate the 20 bands assigned to the 20 isotopically substituted C_5 molecules. The 2164-cm^{-1} band is from $^{12}C_5$ and the 2079.5-cm^{-1} band is from $^{13}C_5$.

probably other small n-even species, where transitions occur below 3 eV.

Thompson, DeKock, and Weltner,[160] from IR studies of matrix-isolated $^{12,13}C_n$ species, assigned the frequencies 1952 and 1544 cm^{-1} to σ_u vibrations of the $^{12}C_5$ molecules. However, Vala et al.[282] (as mentioned in the discussion of C_4) when observing the IR spectra of molecules produced by the vaporization of a 50% mixture of ^{12}C and ^{13}C graphite powders (as done for C_3) definitely identified the 2164-cm^{-1} band previously assigned to C_4[160] as due to linear C_5. The proof rests upon detection of 20 bands spanning 2164 ($^{12}C_5$) to 2080 ($^{13}C_5$) cm^{-1} due to all possible isotopically substituted isomers of C_5 (see Figure 6). Cyclic forms of C_5 would give far fewer isotopomers. Then if the 2164-cm^{-1} and the less definite 1544-cm^{-1} bands are assigned as the σ_u stretching frequencies, force constants can be calculated and from them σ_g frequencies (785 and 1904 cm^{-1}). Harmonic vibrational frequencies have been calculated by Raghavachari and Binkley[261] to be 112 (π_u), 222 (π_g), 648 (π_u), 863 (σ_g), 1632 (σ_u), 2220 (σ_g), and 2344 (σ_u) cm^{-1}. As for C_4, these are expected to be high and the "experimental" values confirm that. Sanborn's[270] estimates of the bending frequencies, from correlation of MO and bending force constants, were 130 (π_u), 330 (π_g), and 520 (π_u) cm^{-1}.

Pickett and Strauss[283] specifically chose C_5 as a possible example of a molecule which in analogy with C_3O_2 (and C_3; see the earlier discussion) might exhibit large-amplitude vibrations contributing significantly to its thermodynamic properties. The treatment was made assuming that the potential function for bending at each of the three inner carbon atoms in C_5 could be taken the same as that at the central atom in C_3O_2 where a very low frequency and anharmonic behavior occurs. The thermodynamic functions for the linear molecule with C–C bond lengths of 1.28 Å were predicted on this basis between 298 and 6000 K. This model probably exaggerates the floppiness and therefore the entropy of the real molecule.

The adiabatic ionization potential of C_5 was calculated to be 10.7 eV.[261] The electron that is removed on ionization comes from a σ orbital and not a π orbital, the $^2\Sigma_u^+$ state of C_5^+ being ~0.4 eV more stable that the $^2\Pi_u$. The dominant fragmentation path is found to involve the loss of C_3, which is common among the neutral polycarbons because of the stability of the triatomic.

D. C_7 and C_9 Molecules

C_7 and C_9 are also linear with $^1\Sigma_g^+$ ground states according to ab initio theory, with bond distances 1.271 (outer) and 1.275 Å (inner).[261] Predicted vibrational frequencies (cm^{-1}) at the HF/6-31G* level in the ground state are as follows[261] C_7, 73 (π_u), 157 (π_g), 240 (π_u), 598 (π_g), 631 (σ_g), 710 (π_u), 1206 (σ_u), 1745 (σ_g), 2132 (σ_u), 2281 (σ_u), and 2376 (σ_g); C_9, 49 (π_u), 114 (π_g), 187 (π_u), 252 (π_g), 496 (σ_g), 567 (π_u), 658 (π_g), 783 (π_u), 960 (σ_u), 1393 (σ_g), 1803 (σ_u), 2084 (σ_u), 2134 (σ_g), 2338 (σ_u), and 2415 (σ_g).

The stretching frequencies are expected to be about 10% larger than experimental frequencies. One might then realistically predict the highest IR-active σ_u fundamental, extrapolating from the C_5 value of 2164 cm^{-1}, to be 2100 and 2160 cm^{-1} for C_7 and C_9, respectively.

Thompson et al.[160] observed three bands in the IR of argon matrix isolated carbon molecules at 2128, 1893, and 1447 cm^{-1} which could be attributed to C_7, C_8, and/or C_9. Isotope shifts did not allow a clear choice. On the basis of the initial high concentration of C_3 and the formation of these bands by subsequent diffusion, C_9 was considered as the most likely candidate. The recent calculated σ_u frequencies for C_9[261] given above, when lowered by a few hundred cm^{-1}, are in approximate agreement with the experimental assignment.

Ionization energies have been estimated[261] to be 10.0 eV (C_7) and 9.4 eV (C_9) where the lowest state of the ions, different from C_3^+ and C_5^+, is probably $^2\Pi_u$.

The lowest energy fragmentation channel of C_7 and C_9, like C_5, is expected to be through loss of C_3.[261,284]

E. C_6, C_8, and C_{10} Molecules

Most information has been obtained on the triplet linear forms of these molecules from ESR spectra, but ab initio theory has predicted the existence of more stable cyclic isomers.

The most recent ab initio studies of Raghavachari and Binkley[261] find that the singlet cyclic forms of these molecules (see Figure 4) are more stable than the triplet cumulenic forms by approximately 0.1–0.2 eV/atom. In these calculations geometries were optimized in each linear, cyclic, or three-dimensional form considered. The calculated minimum-energy cyclic structures are not regular polygons but have in-plane distortions allowing more overlap of the π orbitals. As for C_4, the cyclic and linear isomers of C_8 are found to be almost isoenergetic, but the cyclic forms of C_6 and C_{10} become progressively more stable as n increases. Harmonic vibrational frequencies were calculated at the HF/6-31G* level for each of these most stable structures. The computed frequencies given in Table XV can be ex-

TABLE XV. Harmonic Vibrational Frequencies Calculated for Neutral Carbon Clusters[a]

cluster[b]	vibrational freq, cm^{-1}
C_2	1940 (σ_g)
C_3	154 (π_u), 1367 (σ_g), 2311 (σ_u)
C_4	350 (b_{2u}), 450 (b_{3u}), 1088 (a_g), 1103 (b_{3g}), 1431 (a_g), 1568 (b_{1u})
C_5	112 (π_u), 222 (π_g), 648 (π_u), 863 (σ_g), 1632 (σ_u), 2220 (σ_g), 2344 (σ_u)
C_6	458 (a_2''), 575 (e''), 738 (e'), 888 (a_1'), 1269 (a_1'), 1285 (e'), 1349 (a_2'), 1764 (e')
C_7	73 (π_u), 157 (π_g), 240 (π_u), 598 (π_g), 631 (σ_g), 710 (π_u), 1206 (σ_u), 1745 (σ_g), 2132 (σ_u), 2281 (σ_u), 2376 (σ_g)
C_8	190 (b_g), 294 (b_u), 344 (b_u), 371 (a_u), 482 (e_g), 512 (b_g), 677 (e_u), 738 (a_g), 1014 (a_g), 1097 (e_u), 1276 (b_g), 1957 (b_g), 2007 (e_u), 2050 (a_g)
C_9	49 (π_u), 114 (π_g), 187 (π_u), 252 (π_g), 496 (σ_g), 567 (π_u), 658 (π_g), 783 (π_u), 960 (σ_u), 1393 (σ_g), 1803 (σ_u), 2084 (σ_u), 2134 (σ_g), 2338 (σ_u), 2415 (σ_g)
C_{10}	184 (e_2'), 253 (e_2''), 419 (a_2''), 497 (e_2''), 555 (e_1''), 568 (e_2'), 577 (a_2'), 661 (a_1'), 690 (e_1'), 946 (a_1'), 1118 (e_1'), 1522 (e_2'), 1971 (e_2'), 2013 (e_1')

[a] Reproduced with permission from ref 261; copyright 1987 American Institute of Physics. [b] All the structures correspond to the ground geometries as shown in Figure 4.

pected to be larger than the experimental frequencies by about 10%, but the low bending frequencies are more uncertain and probably more anharmonic. Sanborn's[270] earlier estimates of the bending frequencies for linear C_6 are 470 and 210 cm^{-1} (π_g) and 360 and 80 cm^{-1} (π_u). These may be compared with the calculated values of Raghavachari et al.:[267] 866 and 228 cm^{-1} (π_g) and 494 and 105 cm^{-1} (π_u).

Using the calculated geometries, vibrational frequencies, and approximate energy differences between the triplet linear and singlet cyclic forms, one can calculate via the harmonic oscillator–rigid rotator approximation the thermodynamic functions for each species and the relative equilibrium concentrations of isomers in the vapor phase over graphite. Slanina[285] calculated the enthalpy difference between the linear cumulenic ($^3\Sigma_g^-$) and the most stable D_{3h} cyclic ($^1A_1'$) forms of C_6 to be 42 kJ/mol, but found that 95 mol % of the saturated vapor will be in the linear form compared to 3% in the cyclic form at 2500 K. He has tabulated the thermodynamic properties of C_6(g) at 1000, 2000, and 3000 K, including the contributions from the isomerism.[286] [Slanina also corrected the estimate of the heat of formation of C_6 at zero temperature from $\geqslant$12.14 eV[122] to $\geqslant$11.4 eV.] Thus, the stability in the enthalpy of the cyclic form is heavily outweighed by the larger relative entropy and its increasing importance at higher temperatures of the linear form, as originally pointed out by Pitzer et al.[248] A similar calculation was made by Van Zee et al.[276] (in essential agreement with Slanina), who found K_p = linear/cyclic $\cong$ 200 at 4000 K, considered to be the effective temperature during laser vaporization.[177] The latter calculations indicate that for molecules up through C_8, and possibly C_{10}, the vapor phase over graphite can be considered to a good approximation to be composed of only linear (singlet for n odd, triplet for n even) molecules.[276] Of course, the proportions of the larger species C_4, C_5, etc. relative to C, C_2, and C_3 will always be small when in equilibrium with graphite.

Experimental data on these molecules are again derived only from matrix isolation spectral studies. As in the case of C_4, there is at present no definite experimental evidence for the existence of the singlet cyclic neutral carbon molecules even though they are the most stable isomers of C_6, C_8, and C_{10}. This is probably because the source of these molecules is usually graphite vapor where, as indicated above, the linear triplet isomers are dominant. These larger carbon molecules are formed in the matrices, usually solid argon, either by diffusion of the smaller species, C, C_2, and C_3,[160] or by trapping directly from laser-vaporized graphite.[276] They have been observed in the infrared and UV–visible spectral regions and via ESR spectroscopy.

In the IR, bands were assigned by Thompson et al.[160] on the basis of their location and their relative rate of growth as diffusion proceeded and by ^{13}C spectral shifts. They assigned, with relatively high confidence, the bands at 1997 and 1197 cm^{-1} to the σ_u stretching frequencies of C_6. These are not out of line with the calculated "too high" frequencies 2184 and 1289 cm^{-1} of Raghavachari et al.[267] Krätschmer and Nachtigall,[269] in repeating the ^{12}C argon matrix study, are doubtful of this assignment since they "found that the growing behavior of the 1997-cm^{-1} line does not at all correlate with that of the band at 1197 cm^{-1}". Other bands at 1447, 1893, and 2128 cm^{-1} were ascribed to C_7, C_8, or C_9, but isotopic shifts did not provide a definite assignment.[160] [Note that the calculated highest IR-active bands of the cyclic species are 1764 (e') (C_6), 2007 (e_u) (C_8), and 2013 (e_1') (C_{10}) cm^{-1} relative to those for the linear species, 2184 (σ_u) (C_6) cm^{-1}, ...]. Induced diffusion in these matrices was used to produce the larger species, and it is possible that the cyclic isomers were formed during that process. Krätschmer and Nachtigall indicated that bands in the IR at 1804 and 1844 cm^{-1} may be due to an (unidentified) cyclic species.

Electronic transitions between 250 and 550 nm were observed in these matrices by Thompson et al.[160] and between 200 and 700 nm by Krätschmer and co-workers.[269,273] The latter authors assigned what appears to be a regular pattern of bands to successively longer linear molecules: C_4 (247 nm), C_5 (311 nm), C_6 (394 nm), C_7 (447 nm), C_8 (529 nm), and C_9 (586 nm), i.e., correlating the larger species with longer wavelengths. These assignments are, of course, highly uncertain, particularly since the n-even and n-odd species can be expected to have distinct absorption spectra.[257]

ESR signals of triplet C_6, C_8, and C_{10} species in neon and argon matrices at 4 K were observed in a similar way to the previous study of C_4,[272] except that the concentrations of the larger molecules were increased through laser vaporization of graphite and ^{13}C-enriched graphite.[276] C_4 signals were stronger than those observed during thermal vaporization of graphite. These signals were then attributed to linear C_6, C_8, and C_{10} in their lowest $^3\Sigma_g^-$ states. There is evidence of two forms of the triplet C_{10} molecule, perhaps suggesting two slightly bent structural isomers. Hyperfine interaction in the $^{13}C_n$ molecules was small and resolved only for C_6, indicating cumulene-type bonding with the unpaired electrons principally in pπ orbitals on the carbon chains, as in C_4, and in agreement with the ab initio calculations.

The zero-field-splitting parameters, $|D|$, form an interesting series among the C_4–C_{10} $^3\Sigma_g^-$ molecules: 0.236, 0.363, 0.783, and 0.190 cm^{-1}, respectively. One expects a monotonically decreasing value as the chains become longer if only electron spin–spin interaction were contributing. The variation observed at least from C_4 to C_8 then indicates an additional sizeable contribution of spin–orbit effects tending to reverse the trend. This has been rationalized[276] by ab initio calculations to locate the lowest excited $^1\Sigma_g{}^+$ state, which is considered to be the principal contributor to this contribution to $|D|$ (as in O_2). The $^1\Sigma_g{}^+$–$X^3\Sigma_g{}^-$ energy gap was calculated to decrease from approximately 1.3 to 0.3 eV from C_4 to C_{10}. But C_{10} is then anomalous in having a relatively low zero-field splitting and also in apparently being trapped in two similar forms. It is suggested that both of these anomalies may be due to the nonlinearity of C_{10} in two structural isomers, analogous to cis and trans forms. There are no obvious indications of nonlinearity or isomers in the ESR signals of the C_4 to C_8 species as found for C_{10}.

Thus, the ESR results, taken alone, indicate that triplet linear C_6, C_8, and nearly linear C_{10} are the ground states of these molecules since they are all observed at 4 K. Ab initio theory indicates otherwise and the experimentalist is challenged to observe the more stable singlet cyclic isomers.

F. Electron Affinities of C_2 to C_{10} via Photoelectron Spectroscopy

In some significant research Smalley and co-workers found, through ultraviolet photoelectron spectroscopy, further evidence for even–odd alternation and an abrupt transition to ring structures at $n = 10$.

Cheshnovsky et al. applied a magnetic time-of-flight photoelectron spectrometer[287] for mass-selected negative cluster ions to C_n^- (n = 2–84).[288,289] Carbon clusters were prepared in the usual way by laser vaporization of a rotating graphite disk in a pulsed supersonic nozzle using helium carrier gas. Negative clusters were obtained either from the laser-induced plasma or by multiphoton ionization to provide free electrons for attachment to carbon neutrals. The ultraviolet photoelectron spectra (UPS) for C_2^- to C_9^- are shown in Figure 7.[288,290] The arrows in each panel indicate the authors' estimates of the vertical photodetachment threshold from the negative cluster ion, corresponding to the vertical electron affinity (EA) of the neutral cluster at the geometrical configuration of the negative ion. Note that the patterns for n-odd clusters are alike and different from those of the n-even clusters. Presuming that these are linear molecules, the n-odd neutral clusters have closed shells with $^1\Sigma$ ground states and relatively low electron affinities, here varying smoothly from 2.0 eV for C_3 to 3.6 eV for C_9. The n-even neutrals have open-shell $^3\Sigma$ ground states and higher EA's varying from 3.2 eV for C_2 to 4.4 eV for C_8. Also in accord with this picture are the indications of larger HOMO–LUMO gaps in the n-odd (neutral) clusters. [There is no apparent indication of the n-even cluster ions being formed from the more stable singlet cyclic neutral isomers, particularly for C_6 and C_8. This is in accord with the preferential vaporization of linear C_n neutrals from graphite up to $n \cong 9$.[276]]

At C_{10}^-, not shown in Figure 7, there is an abrupt change in the even–odd alternation and the pattern looks like that of C_7^- or C_9^-. Also, instead of having an extrapolated n-even electron affinity of perhaps 4.5 eV, it is closer to 2.3 eV. Yang et al.[288,290] proposed that this is the beginning of the transition to monocyclic rings. As discussed in section VIII, C_{10} is then considered as the initial member of a series of especially stable rings obeying the $4n + 2$ rule.

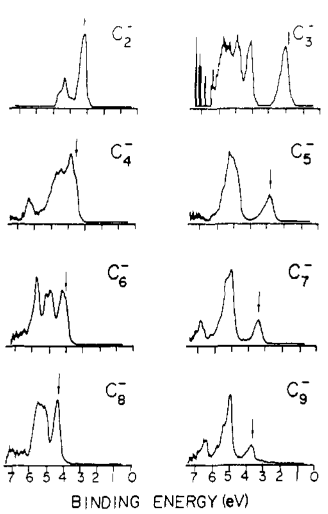

Figure 7. Ultraviolet photoelectron spectra (UPS) of mass-selected C_n^- clusters in the n = 2–9 range taken with a F_2 photodetachment laser (7.9 eV). Arrows mark estimates of the photodetachment threshold (the vertical electron affinity), corrected roughly for thermal and instrument resolution effects. (Reprinted from ref 288; copyright 1988 Elsevier Science Publishers.)

Other support for anomalous behavior at $n = 10$ comes from the experiments of Geusic et al.[291] They photofragmented mass-resolved C_6^+ to C_{20}^+ and found the formation of $C_{n-3}^+ + C_3$ as the dominant channel. (This dominance of the fragment C_3 was also observed by Rohlfing, Cox, and Kaldor.[240]) The total cross section for fragmentation depends upon the cluster size: it rises smoothly to $n = 9$, drops abruptly at $n = 10$, and then rises again up to $n = 20$. Similar indications of rapid change in properties at $n = 10$ are derived from the variation of the reactivities of the C_n^+ ions (see below).

G. Evidence for Isomers of C_7^+, C_8^+, and C_9^+

McElvany et al.[292,293] employed ICR/FTMS to study the reactions of selected ions C_n^+ (n = 1–19) with D_2 and O_2. A similar study was made by McElvany[294a] of the reactivities of C_n^+ ions with the hydrocarbons CH_4, C_2H_2, and C_2H_4 and by Parent and McElvany[294b] with HCN. The ions are laser vaporized from a graphite surface located flush with the bottom ICR cell plate. Specific ions can then be isolated within the cell and allowed to react with the neutral background gas. With D_2, they found for n = 3–10 that (1) relative reaction rate decreased as the cluster size increased, with an abrupt decrease between $n = 9$ and 10, (2) even clusters appeared to be less reactive than odd, and (3) the reaction went to completion, for sufficiently long times, for all C_n^+ except C_7^+. From these observations it was inferred that a structural change from linear to monocyclic ring occurs between $n = 9$ and 10. C_7^+ is postulated to exist in two structural isomeric forms, one reactive and the other relatively unreactive to D_2 (and O_2), and again attributed to linear and cyclic forms. MNDO calculations were performed to attempt to explain the trends in the observed ion/molecule reactions.

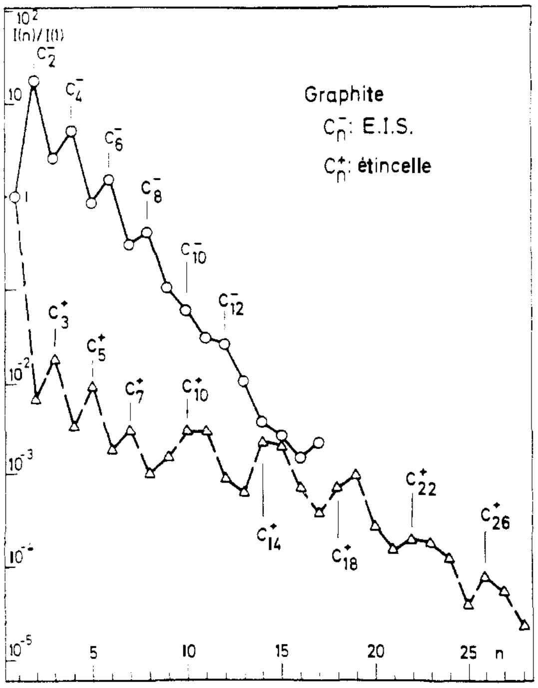

Figure 8. Intensities of the C_n^+ and C_n^- ions emitted from a graphite target. C_n^+, spark source;[296] C_n^- secondary ion emission (SIMS). (Reproduced with permission from ref 312.)

The later study of the reactions with hydrocarbons[294a] and HCN[294b] reinforced the evidence for a change in reactivity at $n \geq 10$ and for the presence of isomers of C_7^+ and also C_8^+ and C_9^+ with different reactivities.

VIII. Carbon Ions and Molecules Produced by Vaporization of Graphite; Magic Numbers

A. Ions and Alternations in Mass Spectral Signals

As early as 1943 Mattauch et al.[295] identified positive and negative C_n ions up to $n = 15$ produced in high-frequency spark discharges between graphite electrodes. In the early sixties Hintenberger, Franzen, and coworkers,[296] using the spark source, published abundance distributions of ions up to over $n = 30$. Recently, there has been a revival of interest in the mass spectrometric (MS) identification of the carbon neutrals and ions produced during laser-induced (LIMS),[297-299] spark-source (SSMS),[296,298] secondary ion emission (SIMS),[300] and laser microprobe mass analysis (LAMMA).[301,302] Figure 8 illustrates, in the cases of SSMS and SIMS, the variation of relative intensities of C_n^+ and C_n^- ions emitted by graphite (abundances normalized to C_1 in each case). Similar variations in intensities are found in LIMS and LAMMA but the peak intensities occur at different n depending upon the laser power (10^8–10^{10} W/cm^2).[299] In LAMMA experiments the target was a 500-Å-thick carbon foil.[301] Also, doubly charged ions up to C_{20}^{2+} have been observed in spark sources.[296,303]

Again in all of these experiments there is observed an alternation of intensities among the C_n^+ ions, illustrated very clearly in Figure 8. Among the negative ions up to about C_8^- those with n even are more intense than the adjacent n-odd molecules, while in the C_n^+ series it is just the opposite; n-odd signals up to about C_7^+ are more intense than adjacent n-even signals. The explanation of these variations always employs Pitzer and Clementi's[221] MO theory of such variations among the neutral carbon molecules for $n \leq 9$. For those molecules, assumed linear and at thermodynamic equilibrium, the simple theory indicates increased relative stabilities and vapor concentrations of the n-odd members. Removal of an electron from the filled MO of a neutral does not disturb the dominance of the odd members in the C_n^+ series; however, the higher electron affinity of the n-even clusters leads to relative maxima for these species in the C_n^- series.[304] As indicated in the earlier sections, other than C_2^+ and C_2^-, there are little definitive experimental data on the structural and electronic properties of these polycarbon ions, although the recent photoelectron spectroscopic studies (see sections VII.F and IX.B) are informative.[288,289]

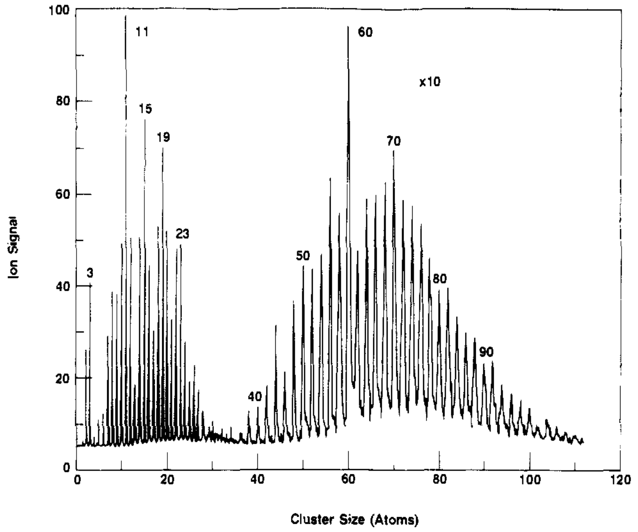

Figure 9. Photoionized, time-of-flight, mass spectrometrically detected (PI-TOF-MS) carbon clusters obtained with 40-mJ doubled Nd-YAG vaporizing laser energy and with 1.6-mJ unfocused ArF (193 nm) ionizing laser energy. This spectrum is a combination of two different spectra. For C_n^+ ($1 \leq n \leq 30$), the vertical deflection plate voltage used 300 V, which optimizes C_{20}^+ collection, while for C_{2n}^+ ($20 \leq n \leq 50$), 600 V was used, optimizing C_{100}^+. The gain in the latter instance was also increased by a factor of 10. The signal intensities of the two distributions cannot be compared directly since the small clusters are two-photon ionized while the large clusters are single-photon ionized. (Reprinted from ref 240; copyright 1984 American Institute of Physics.)

B. Neutral Molecules

Large ($n \geq \sim 10$) C_n molecules were detected in the gas phase, after explicit ionization, by Rohlfing, Cox, and Kaldor[240] by supersonic expansion of carbon vapor from laser-heated graphite quenched in high-pressure helium gas. The graphite target rod was continuously rotated and translated during the experiment to always expose a fresh surface to the vaporization laser. The carbon clusters were photoionized by 193- or 248-nm laser radiation about 1 m downstream from the nozzle, and the ions were detected by a time-of-flight mass spectrometer. The ion signal distribution, unusual because of its bimodal structure, is shown in Figure 9. (Note that in Figure 9 the conditions of detection of the two distributions are not the same.) In the range of 1–30 atoms all possible ions are observable but with alternations in intensity. Above about 40 atoms only *even* ion signals are observed, C_{2n}^+, for $20 \leq n \leq 90$. Surprisingly, the distribution for $n \leq 30$ is qualitatively the same, even to a periodicity in the ion signal every four atoms (maxima at $n = 11, 15, 19$, and 23), as in the laser microprobe (LAMMA) vaporization of carbon foil mentioned above where positive (and negative) ions are directly detected. The implication is that nearly the same neutral carbon clusters for $n \leqslant 30$ are produced in each case, but with the carbon ions being formed by hot plasma electrons in the LAMMA process instead of by photoionization.

There are now several indications that the high-mass cluster ions ($n > 30$) are produced from a different kind of source, one in which small clusters are not entrained and grown in a quenching gas:

(1) Essentially the same pattern as in Figure 9 was observed by O'Keefe, Ross, and Baronavski[305] when carbon cluster positive ions were detected directly above a laser irradiation fixed spot on a stationary graphite target, but only after a long enough time (>5 min) for a pit or channel to form. Before this channel formed the distribution of ions only included those with $n < 30$. It is postulated that the channel provides the confined space and higher particle densities for the plasma in which reactions occur to yield the high-mass ions.

(2) In a follow-up of the earlier work, Cox, Reichmann, and Kaldor[306] found that the revaporization of prior vaporized material on the inside surface of the nozzle/extender produced the high-mass neutrals. Further evidence came from comparing the effect of different nozzle configurations on the time of arrival spectra for small and large clusters, suggesting that some confinement of vaporized carbon is required [as in (1) above] in order to generate the large $n > 30$ clusters.

Phillips[252] refers to the region of n where crossover of structure occurs as a "dead" region (no peaks in C_n) as in Figure 9 for $30 \leqslant n \leqslant 40$. It is not clear what the structures are beginning at $n \cong 40$ but the magic $n = 60$ peak is identified with the spheroidal cluster, as discussed below.

C. Magic Numbers

In Figure 9 one notes that there are certain cluster ion sizes that are prominent; "magic" numbers such as $n = 3, 11, 15, 19, 60$, and 70 are clearly in that category. This distribution of C_n^+ ions, particularly for $n < 30$, was, in fact, reproduced in three other experiments from different sources where the positive ions are sampled directly by the mass spectrometer and not formed by photoionization of neutrals. The distribution in one of these, the spark-source vaporization of graphite, was shown in Figure 8, and although less distinct, prominent intensities occur at spacings of $\Delta n = 4$, i.e., at $n = 11, 15, 19$, and 23. Bloomfield et al.[241] accelerated and mass-resolved the positive (or negative) ions formed naturally in the laser-vaporized-graphite, helium-expansion source used to produce neutral clusters and also observed this array of magic numbers. As mentioned earlier, O'Keefe, et al.[305] obtained the same distribution as in Figure 9 by direct detection of C_n^+ ions from laser-vaporized graphite. Knight et al.[307] observed the positive (and negative) ions produced by laser vaporization of a graphite sample positioned outside of an ion cyclotron resonance (ICR) cell. Magic numbers for C_n^+ were 7, 11, 15, 19, satisfying the relationship $n = 4m - 1$, $m = 2, 3, ...$, with groupings of four. [Note, however, that this is not the $4n + 2$ distribution 10, 14, 16, 18, predicted as the most stable species for planar aromatic cyclic molecules.] C_n^+ ions of high mass have been produced by growth from laser-generated carbon vapor in a helium flow channel without the aid of subsequent laser ionization. Under these conditions Hahn et al.[308] observed prominent signals at $n = 36, 50, 60$, and 70.

The distributions of C_n^- ions are more variable with experiment, but the magic numbers appear to favor the n-even clusters, whether sampled from a bombarded source (see Figure 8), produced via helium expansion,[241] or directly from laser vaporization.[307] Jet-cooled negative cluster ions with $n > 40$ have been produced by Liu et al.[309] by electron attachment to neutrals and also show this preference for an even number of carbon atoms. The conditions could be arranged such that C_{60}^+ was a dominant species.

Magic numbers are usually interpreted as designating clusters of unusual stability, as demonstrated for the alkali-metal clusters.[310] Kroto et al.[311] in discussions relevant to their observations of an extraordinary C_{60}^+ signal (see section IX), suggested that only the more inert neutral clusters survived during the growth process. On the basis of this reasoning, magic C_n^+ ions are produced from the most stable (magic) C_n neutrals provided that fragmentation and photoionization do not alter the distribution among the neutrals. Since, from the above experiments, all of the C_n^+ distributions appear to be almost the same, whether produced from neutrals or measured directly from the source, it seems likely that this is also the distribution among the C_n species. For the smaller clusters this is supported, as mentioned earlier, by the observed even–odd alternation in signal intensities, approximately accounted for by the calculations of relative stabilities by Pitzer and co-workers[221,248] and Hoffmann.[192]

Several authors have been interested in examining this reasoning by comparing experimental numbers with theoretically derived ones. Joyes and Leleyter[312] (extension of Pitzer et al.'s one-electron method), Bernholc and Phillips[251] (self-consistent, geometry-optimized MNDO), Seifert[313] (LCAO-Xα), and Ray[314] (all-electron HF/31-G minimal basis) have made calculations for $n \lesssim 25$ assuming only chain or monocyclic ring structures. Ray's calculation was made only for the neutral C_n clusters.

It is not too surprising that for neutral molecules these procedures all find chains most stable for $n \leqslant 9$ and monocyclic rings most stable for larger n. Magic numbers occur at 10, 14, and 18 among the monocycles in analogy with Hückel's $4n + 2$ rule for aromatic hydrocarbons. However, Bernholc and Phillips[251] and Seifert[313] calculate the most stable positive ions in the form of planar rings to occur at odd n values of 11, 15, and 19, which is also observed experimentally. The implication then is that fragmentation of the (n-even) neutrals must be occurring to account for the observations, e.g., $C_{14}^+ \rightarrow C_{11}^+ + C_3$. Bernholc and Phillips[251] treated the formation of the larger clusters more realistically as a kinetic growth problem but arrived at essentially the same conclusion: the distribution of neutrals is affected by the photoionization process.

In the above rationale for the magic numbers, the clusters with $n > 10$ were always assumed to be monocyclic rings. However, Van Vechten and Keszler[315]

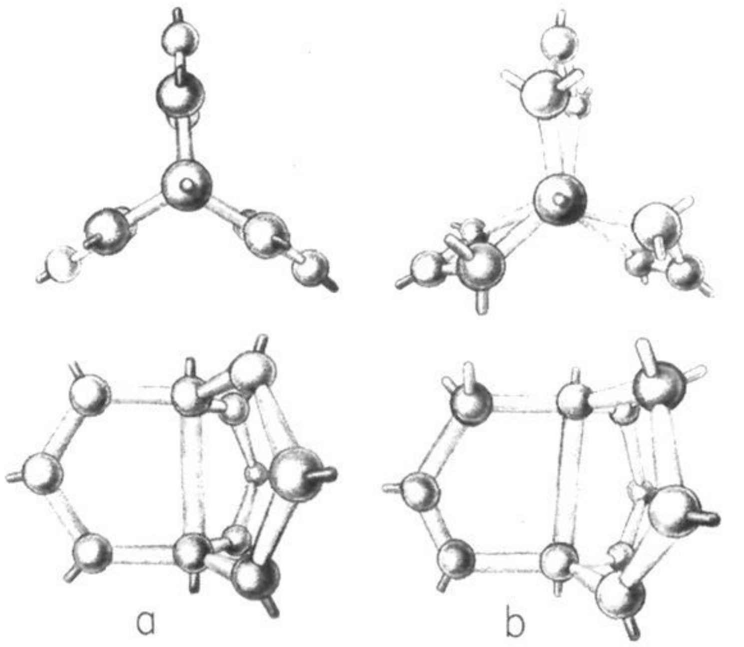

Figure 10. (a) The all-sp^2-bonded, 11-carbon-atom cluster (chemical name abbreviated to TUTT) proposed for the $n = 11$ magic number cluster. TUTT units are also found in sputter-induced carbon whiskers. (b) TUT, derived from TUTT by converting the three atoms bonded to one of the hub atoms from sp^2 to sp^3 bonding. TUT is less stable in free space but allows for much denser packing in a condensed phase. Sputter-induced carbon whiskers contain many TUT units. (Reprinted from ref 315; copyright 1987 American Physical Society.)

proposed the more novel polycarbons of the form shown in Figure 10 as the beginning of a series of "magic number" clusters. These arise from their carbon whisker studies and are considered to be possibly present in the laser ablation produced plasma or even in the original target. Extended-Hückel calculations indicate that the neutral C_{11} cluster in this form has a cohesive energy within 1% of that for a C_{10} carbyne chain or ring and a C_{11} cumulene ring. The extension of these structures by the successive addition of four-atom units produces hexagonal rings yielding C_{15}, C_{19}, and C_{23} as particularly stable. Ionization occurs from nonbonded orbitals so that these magic numbers are sustained in the positive ions, but not in the negative ions. The absence of $n = 27$ or 31 magic numbers is attributed to destabilization of these units beyond the formation of three hexagons. Other support for these clusters is given based on their expected photofragmentation and chemical reactivity behavior.

For C_n^- clusters where the experimental observations are more variable and magic numbers sometimes less distinct, theory via the kinetic treatment including electron transfer[251] apparently matches experiment.

IX. Large Clusters

A. C_{60}

The unique stability of this magic molecule[240] was first suggested by Kroto et al.[311] The latter authors proposed that it has a truncated icosahedron structure (resembling a soccer ball; see Figure 11) containing 20 hexagons and 12 pentagons on its almost spherical surface (I_h symmetry) and called it "buckminsterfullerene" or "footballene". Carbo-*s*-icosahedron[316] and follene-60[317] (derived from the latin "follis" for football) have also been proposed.

Under certain clustering conditions Kroto et al.[311] discovered that the C_{60}^+ mass peak in laser vaporization, supersonic expansion experiments could be enhanced by a factor of 40 over that of neighboring clusters. This occurs at high helium density and prolonged time between graphite vaporization and expansion. It was proposed that the fragments torn from the solid surface equilibrate in the dense helium to form the most stable species, which is a unique cluster of 60 atoms. Subsequent experiments by this group supported the spheroidal structure and stability by demonstrating that its inner cavity could trap a La atom,[320] that it was relatively inert toward reactants NO, SO_2, and CO,[245] and that its prominence was not an artifact of the ionization conditions.[309]

Figure 11. Proposed structure for the C_{60} cluster "buckminsterfullerene".

Efforts by other groups[306,309] have also been made to establish whether C_{60}^+, not neutral C_{60}, is the "magic" entity and that the source of the special behavior might be its electronic (e.g., unique high ionization cross section), rather than geometric, structure. However, it does appear that neutral C_{60} has special stability and therefore that the proposed closed-shell structure is probable.[321]

Heath et al.[318,319] and Smalley[290] recently reviewed the discovery of buckminsterfullerene (Bf) and the efforts that have been made to establish its properties. Although the evidence for a cluster of this structure and stability is largely circumstantial, it is nevertheless very convincing. Spectroscopic data are obviously difficult to obtain and are rather meager at present.

Iijima[322] (see also Kroto and McKay[323]) has observed spherical particles during electron microscopic observation of graphitized carbon particles and proposed that C_{60} is visible as their nuclei. Zhang et al.[245] and Kroto and McKay[323] suggested that the growth of soot and circumstellar dust may be nucleated in this way.

In the interest of clarity, it seems best to first discuss what the theoretical calculations predict for the properties of C_{60} and then to present the experimental data.

1. Theory

The possible existence of such a highly symmetric ultrastable carbon molecule has provoked a great deal of interest among theoreticians. As pointed out by Heath et al.[318] and Kroto,[324] such hollow molecules had been postulated and considered prior to the discovery of C_{60}, most notably by Jones,[325] Osawa,[326] Bochvar and Gal'pern,[316] Davidson,[327] and Haymet.[328] Presently, it is the fascination of theoreticians that has provided the details of bonding, aromaticity, and the projected spectra of C_{60}.

Many theoretical calculations of the properties of C_{60} have been made and have progressed from semi-empirical to ab initio methods. However, planar Hückel theory, assuming all carbon atoms are sp^2 hybridized with neighboring parallel π orbitals interacting, provides the essence of its electronic properties, in the context of I_h symmetry (Bochvar and Gal'pern,[316] Davidson,[327] Haymet,[328] Klein et al.,[329] Ozaki and Takahashi,[330] Haddon, Brus, and Raghavachari,[331] Brown,[332] Coulombeau and Rassat[333]). Thus, truncated icosahedrane C_{60} (Figure 10) contains 20 six-membered rings and 12 five-membered rings, and the 60 π electrons fill up through the highest occupied fivefold degenerate h_u (HOMO) level lying 0.757β below the lowest unoccupied threefold degenerate t_u (LUMO) level. The lowest allowed electronic transition ($h_u \rightarrow t_{1g}$) is equal to 1.000β. The resonance energy (ethylene based) is 0.553β/carbon atom relative to 0.333β/carbon atom in benzene and 0.576β/carbon atom in graphite. Then the ground state is ^1A_g with much aromatic character. The two independent bond types have bond orders 0.476 for edges separating hexagonal and pentagonal (6–5) faces and 0.601 for edges separating two hexagonal (6–6) faces, implying bond lengths of 1.426 and 1.405 Å, respectively. (The in-plane bond length in graphite is 1.42 Å.)

There have been a series of semiempirical calculations extending the planar Hückel theory and including the three-dimensional character of the structure. The latter places the π orbitals at an angle of 23° with respect to each other and requires rehybridization of the carbon atoms. These calculations include the free-electron model, Coulson–Golebiewski self-consistent Hückel theory (Ozaki and Takahashi[330]), Kekulê structure analysis, Herndon–Simpson resonance theory or the conjugated-circuit method (Klein et al.,[334,335] Otto[336]), MNDO with geometry optimization (Newton and Stanton,[337] McKee and Herndon[338]), π-orbital axis vector–three dimensional Hückel (POAV/3D HMO) [Haddon, Brus, and Raghavachari[331,339]] DV–Xα (Hale[340]), the linear muffin-tin orbital method in its atomic sphere approximation (LMTO ASA) [Satpathy[341]], partial retention of diatomic differential overlap (PRDDO) [Marynick and Estreicher[342]], Stone's tensor surface harmonic theory [Fowler and Woolrich[343]], the Pariser–Parr–Pople method with CI [Lâszlô and Udvardi[344]], INDO [Shibuya and Yoshitani[345]], CNDO/S including CI (Larsson, Volosov, and Rosên[317]), and the tight-binding model with electron–phonon coupling (Hayden and Mele[348]).

These calculations generally agree on the probable stability of the truncated icosahedrane structure of C_{60}. The 6–6 bond distance is found to vary from 1.36 to 1.42 Å and to be 0.02–0.08 Å shorter than the 6–5 bond distance. The HOMO–LUMO energy gap was found to be somewhere between 2.2 and 9.2 eV and the IP varied from 5.5 to 8.4 eV. The lowest optical transition is between 2.6 and 4.2 eV. Thus, there are wide quantitative differences, but the qualitative ordering of levels and bond character are in general agreement.

Elser and Haddon[365] examined theoretically the ring-current magnetic susceptibility provided by the 60 π electrons on the surface of C_{60} and concluded, surprisingly, that the diamagnetic and paramagnetic characters will largely cancel, leading to probable weak diamagnetism. Correspondingly, the shielding effect on a central atom will be less than 1 ppm.

Two ab initio calculations have been done. The first by Disch and Schulman[347] is an SCF calculation at the STO-3G level yielding bond distances of 1.376 and 1.465 Å (distance between diametrically opposed carbon atoms is 7.1 Å). The HOMO–LUMO gap is 8.7 eV. Later considerations by Schulman et al.[348] find the vertical ionization energy to be ~7.4 eV (at the upper end of the experimental range[240]) and $\Delta H_f \cong 582$ kcal/mol. Lüthi and Almlöf[349] performed a large-scale restricted Hartree–Fock calculation (7s3p basis contracted to double ζ 7s3p/4s2p) on icosahedral C_{60} and compared its stability to a 60-atom sheet of graphite. Optimized bond distances were 1.369 and 1.453 Å and the estimated ΔH_f was 415–490 kcal/mol (relative to graphite sheet). The ionization potential was calculated to be 7.92 eV. Also, an electron affinity of 0.80 eV was obtained, reflecting the slightly negative orbital energies of the LUMOs (but contradicting an earlier postulate of an exceptionally high EA[331] and a calculated value of 2.4 eV by Larsson et al.[317]).

There have also been several calculations of the expected vibrational frequencies of buckminsterfullerene. Of the 174 normal modes, because of the high symmetry only four fundamentals (t_{1u}) can appear in the infrared and ten (eight h_g plus two a_g) in the Raman. Values for some or all of these frequencies were calculated from theory or from estimated force constants by Newton and Stanton,[337,350] Disch and Schulman,[347] Coulombeau and Rassat,[333] Wu, Jelski, and George,[350] and Weeks and Harter.[351] The agreement among these methods can perhaps best be judged by comparing the calculated two a_g frequencies: 1667, 676;[337,350] 1772, 510;[347] 1423, 676;[333] 1830, 510[351] cm^{-1}.

There is also the possibility of other structural isomers of truncated icosahedrane C_{60} having greater or comparable stability. One of these forms would be the truncated dodecahedron obtained by truncating the vertices, to form small triangles, of a regular dodecahedron with 20 vertices and 12 faces of regular pentagons. Hückel calculations yield a closed-shell ground state but the highest occupied levels are antibonding (Fowler and Woolrich[343]). Klein et al.[334] in their quantitative resonance-theoretic treatment also found it to be unstable. However, INDO calculations by Shibuya and Yoshitani[345] found its highest occupied levels to be bonding with a HOMO–LUMO gap of 8.86 eV, but its potential energy was 1.6 eV/atom higher than that of buckminsterfullerene. They reasoned that it might still exist as a stable, not just a transient, configuration of C_{60}. Schmalz et al.[352] considered the five alternative structures for C_{60} by simple MO and quantitative resonance theory and found Bf to be significantly more stable. A maximum number of hexagonal rings and a minimum number of adjoining pentagonal rings are required for the most stable structure.

On the other hand, Stone and Wales[353] considered the stability of isomers obtained from Bf by transformations involving the movement of only two atoms such as to interchange hexagons and pentagons. They are effected through a thermally forbidden four-electron Hückel transition state but nevertheless formally lead to the generation of many isomers. Hückel calculations indicated that many of these structures are likely to be as stable as Bf. Thermal interconversion is unlikely, but under the experimental conditions where Bf is observed[311] it is reasoned that the detected C_{60} mass peak may arise from a mixture of isomers.

2. *Experiment*

As mentioned earlier there is good evidence for the inertness of C_{60} and for its ability to accommodate an internal La ion. Its experimental ionization potential (IP) has been found to lie between 6.42 and 7.87 eV, but closer to the higher energy; in fact, it may be that 7.87-eV photons produce near-resonant ionization.[245,306,354,355] Most of the calculated IP values lie in the range 7.4–8.4 eV. Most relevant for comparison with experiment are presumably the CNDO/S calculations of Larsson et al.[317] and the two ab initio calculations of Lüthi and Almlöf[349] and Schulman et al.,[348] which yield IP values of 7.55, 7.92, and ~7.4 eV, respectively, in good agreement with expectations.

From the photoelectron spectrum of C_{60}^-, the vertical electron affinity (EA) of C_{60} is measured to be ~2.8 eV. Larsson et al. calculated the EA to be 2.4 eV, in good agreement with the experimental value. The other ab initio calculation by Lüthi and Almlöf gives the much lower value of 0.8 eV. The experimental value appears to be rather well determined here, indicating that the CNDO/S calculation is the better one in this case. It is expected that bond length changes in going from C_{60} to C_{60}^- will be small[317] and not appreciably affect the comparison.

Initial indications are that C_{60} is nearly transparent in the visible region since over 60 mJ/cm^2 irradiation at 532 nm was required before any fragmentation could be seen.[356] In the ultraviolet a transition at 3.22 eV (3860 Å) has been tentatively assigned as the 0,0 band of the allowed $^1T_{1u} \leftarrow {}^1A_g$ transition. The absorption was measured by Heath, Curl, and Smalley[357] using "laser depletion spectroscopy" based upon the absorption and depletion of the C_{60}–adduct$^+$ signals, the adduct being either a C_6H_6 or CH_2Cl_2 molecule. The experimental oscillator strength is judged to be ~0.004. The calculations by Larsson et al.[317] place this absorption at 3.6 eV, which is close to the measured band position, but they also indicate that the band should be much stronger, with an oscillator strength near 0.08. Other calculations place this optical transition at ~2.6 eV (DV-Xα[340]) and 4.2 eV (PPP CI[344]).

Although predicted, there are no data on bond distances or vibrational frequencies.

B. Photoelectron Spectroscopy of C_{11}^- to C_{84}^-

The most direct experimental information about these C_n clusters has been obtained by Smalley and co-workers from ultraviolet photoelectron spectroscopy (UPS) as discussed in section VIII for the smaller clusters. Yang et al.[289] extended those measurements to C_{84}^-. The spectra up to $n = 29$ are given in Figure 12. Those findings are summarized as follows:[289,290]

(1) There appear to be two distinct types of C_{11} that can be selectively prepared and have different vertical electron affinities,[288] 4.00 and 2.85 eV. The former is attributed to an extension of the linear molecules, the $n = 7$ and $n = 9$ series, whereas the latter, along with C_{10} (see section VII), is proposed to fit into the larger n monocyclic ring series.

(2) As shown in Figure 13 for $n \geqslant 10$ the EA's are much lower and form at least two distinct branches, particularly as n approaches 30. There actually appear to be four series beginning with C_{10}, C_{11}, C_{12}, and C_{13} (see Figure 12), with each progressing in steps of $\Delta n = 4$.[288] This is in accord with the $4n + 2$ rule originally proposed for monocyclic rings.[192,221]

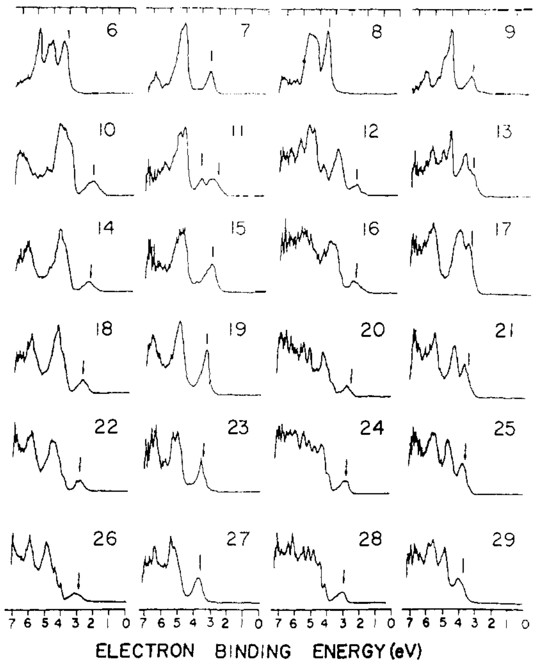

Figure 12. Ultraviolet photoelectron spectra (UPS) of mass-selected C_n^- clusters in the $n = 6$–29 range. (See Figure 7.) (Reprinted from ref 288; copyright 1988 Elsevier Science Publishers.)

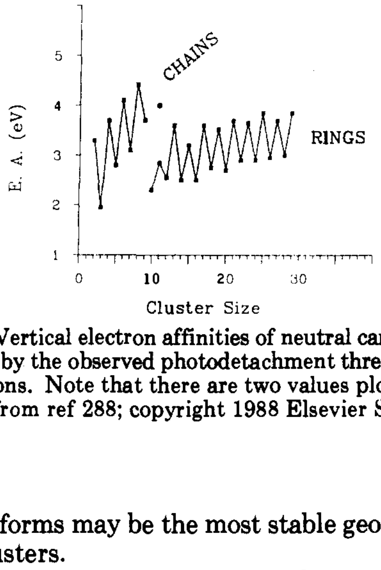

Figure 13. Vertical electron affinities of neutral carbon clusters as measured by the observed photodetachment thresholds of the C_n^- cluster ions. Note that there are two values plotted for C_{11}. (Reprinted from ref 288; copyright 1988 Elsevier Science Publishers.)

(3) Ring forms may be the most stable geometries for neutral clusters.

(4) Clusters in the range of C_{30} to C_{40} are difficult to study because their reactivity causes them to have abnormally low concentrations (see Figure 9). They are therefore difficult to generate and the UPS patterns were ill-defined.

(5) In the 40–80 size range n-even negative ion clusters were roughly 10 times more abundant than n-odd clusters, and 50, 60, and 70 were favored. This was when a second laser was used to generate a shower of electrons for attachment to the neutrals. If the vaporization laser alone was used to generate C_n^- ions, the intensities of odd clusters approached those of even clusters and C_{60}^- was not prominent.

(6) UPS of these high-mass C_n^- clusters showed only broad, sloping spectra, except for $n = 50$, 60, and 70 where a LUMO bump at low binding energy appeared. The EA of most clusters was generally between 3.0 and 3.5 eV.

TABLE XVI. Spectroscopic Constants for the 2169-cm^{-1} Band of C_5

	source		
	carbon star	laboratory	
constant	BHK[374]	HCGSS[376]	MMA[375]
ν_0, cm^{-1}	2169.44205 (40)	2169.4404 (18)	2169.4432 (2)
B'', MHz	2557.48 (19)	2557.38 (93)	2557.66 (11)
D'', kHz			0.17 (2)
B', MHz	2544.88 (18)	2545.24 (96)	2545.01 (11)
D', kHz			0.16 (2)

(7) For C_{60}^-, UPS was characteristic of a closed-shell neutral species with a HOMO–LUMO gap and an EA of 2.6–2.8 eV, lower than any other carbon cluster in this size range.

(8) There appear to be at least two forms of these C_n^- clusters prepared in different ways and having different UPS patterns. These are attributed to open-shell and closed-shell electronic structures, with the latter formed only after extensive reaction and annealing processes in the nozzle.

C. Other Possible Spheroidal Clusters

Although there are not experimental data on other large clusters, except as they are detected as magic numbers, icosahedral C_{60} has also led to the contemplation by theorists of a broad range of "fullerenes",[323,324] Archimedean solids,[328] and Goldberg polyhedra.[358] Among many,[352] C_{24},[333,348] C_{30},[338] C_{50},[337] C_{70}[337,339,343,364] and C_{120}[333,343,339] have been specifically considered. "Fullerenes"[324] is suggested as the generic name for the class of all closed carbon cages composed of 12 five-membered rings and an unrestricted number of six-membered rings. Kroto[324] predicted those with $n = 24$, 28, 32, 36, 50, 60, and 70 should have enhanced stability relative to near neighbors. Polyhedra[358] containing 180, 240, and 540 atoms are also predicted to be closed shells. Schmalz et al.[335,352] considered all possible icosahedral-symmetry cages and made explicit calculations on over 50 cages to check their proposed criteria for stability.

X. Conclusion

The spectroscopy of C_2 and C_3 is well advanced, although there is particular need for more information on the excited electronic states of C_3. Many states of C_2^- have now been characterized, but the elusive C_2^+ has only just been observed in matrices and characterized in the gas phase. C_3^+ and C_3^- are complete unknowns, except for Coulomb explosion studies on the former. Ab initio calculations considering possible bent structures of these ions would be of great value.

Theory indicates that C_4, C_6, C_8, and C_{10} exist in two isomeric forms, one linear ($^3\Sigma$) and the other cyclic (^1A). These isomers are predicted to be essentially isoenergetic for C_4 (linear and rhombic), but singlet monocyclic forms are proposed to be increasingly more stable from C_6 to C_{10}. (However, entropy considerations dictate that the vapor over hot graphite should contain predominantly the linear triplet species.)

ESR spectra of linear C_4 have shown it to be cumulene-like and have provided some electronic and magnetic parameters in the ground ($^3\Sigma_g^-$) state. An electronic transition was also observed in matrices. Extensive ab initio theoretical calculations on the C_4 isomers have yielded their structures, electronic states, vibrational frequencies, and spin densities (for the $^3\Sigma$ isomer). Where overlapping, theory and experiment are in good agreement.

C_5, C_7, and C_9 are predicted to have linear singlet ($^1\Sigma_g^+$) ground states, cyclic forms lying at much higher energy; however, there is evidence for isomeric forms of C_7^+, C_8^+, and C_9^+. Matrix IR spectra have identified a σ_u frequency of C_5 at 2164 cm^{-1} and confirmed that it is a linear molecule.

IR and electronic spectra of these molecules in matrices have been observed but are largely unassigned; gas-phase data are badly needed.

Photoelectron spectroscopy of mass-selected C_n^- ions has yielded the electron affinities of C_2 to C_{84} and suggests a change in structure at $n = 10$. Those measurements above $n = 10$ also indicate an alternation varying as $\Delta n = 4$ in the molecular properties, confirming such variations in intensities of mass spectral signals of C_n^+ from sparks and laser-heated graphite sources. These extraabundant "magic" C_n species are attributed to monocyclic rings obeying the Hückel $4n + 2$ rule of aromaticity; however, this is controversial since there are no accurate theoretical calculations or spectroscopic studies of C_n species above $n = 10$.

For high masses, magic numbers occur at $n = 36$, 50, 60, and 70, and conditions during supersonic expansion can be found that make C_{60} the dominant vapor species. C_{60} is found to be chemically unreactive and is proposed to have an almost spherical truncated icosahedral structure with a closed-shell (^1A_g) ground state. The photoelectron spectrum indicates that it has an exceptionally low electron affinity. Perhaps a $T_{1u} \leftarrow {}^1A_g$ electronic transition has been observed; there are no other experimental spectroscopic data.

Other ultrastable spheroidal clusters with $n = 36$, 50, 70, and 120 have been proposed.

The polycarbons form a fascinating series of molecules, ions, and clusters for both the spectroscopist and theorist. They may have increasing importance in many areas, already implied by their probable involvement in the mechanism of formation of long chains and dust in circumstellar and interstellar space[290,359–362] and in the formation of soot on earth.[245,323,363]

Acknowledgments. We are grateful to many authors for discussions and for permission to reproduce preprints, reprints, and figures for publication here: Drs. T. Amano, R. J. Bartlett, P. F. Bernath, D. E. Bernholdt, P. R. Bunker, D. M. Cox, D. W. Ewing, W. R. M. Graham, P. Jensen, P. Joyes, L. B. Knight, W. C. Lineberger, A. R. W. McKellar, D. H. Magers, S. W. McElvany, J. P. Maier, A. J. Merer, T. Oka, M. Perić, J. C. Phillips, K. Raghavachari, R. J. Saykally, I. Shavitts, Z. Slanina, R. E. Smalley, M. Vala, and J. A. Van Vechten. We thank Ms. Shari Strain for her expert efforts in preparing the manuscript. Research on carbon species in our laboratory has extended over many years. We thank the contributors R. L. DeKock, K. I. Dismuke, R. F. Ferrante, W. R. M. Graham, K. R. Thompson, and K. J. Zeringue. Recent support has come from the National Science Foundation under Grant No. CHE-8514585 and CHE-8814297 and from the Petroleum Research Fund, administered by the American Chemical Society. We also thank H. L.

Flanagan for proofreading and helpful comments.

XI. Addendum: Recent Developments (up to April 1989)

Since the completion of this review there have been new developments; particularly noteworthy is the observation of a vibration–rotation spectrum of C_5 in the laboratory and in a carbon star. However, here we will keep the order of contents in the review, that is, proceeding from small to large molecules.

C_2 Molecule. Curtis and Sarre[366] have reported a detailed analysis of their sub-Doppler laser spectroscopy of $^{13}C_2$ in the $a^3\Pi_g$ and $d^3\Pi_u$ states and the relation of the nuclear hyperfine parameters to its electronic structure and bonding. This thorough experimental study points up the need for ab initio calculations of these parameters.

The new $1^1\Delta_u$ electronic state of C_2 (besides the two recently discovered by Douay et al.[10] (see section II)) was observed and characterized by Goodwin and Cool via the transition $1^1\Delta_u \leftarrow A^1\Pi_u$ using laser-based resonance-enhanced multiple photon ionization (REMPI) spectroscopy.[20] This state had been predicted by ab initio calculations. These authors have now observed six vibronic bands of a new transition to that state $1^1\Delta_u \leftarrow B^1\Delta_g$ with ν_{00} = 45 507 cm^{-1}.[367]

Rohlfing[368] has observed direct emission in three band systems (Swan, Deslandres–d'Azambuja, Mulliken) from free-jet-expanded C_2 formed by laser vaporization of graphite into a pulsed helium flow. These experiments extend those of Anselment et al.[369] into the UV and VUV.

Davis et al.[370] have observed three new bands corresponding to (v'–v'') = (1–3), (2–4), and (2–3) of the Phillips system using high-resolution Fourier transform spectroscopy. In conjunction with other data, this has led to improved molecular parameters and extension to higher vibrational levels resulting in a global fit to all vibrational bands with v' and v'' between 0 and 4, with a variance of 0.018 cm^{-1}.

C_3 Molecule. Rohlfing and Goldsmith[371] report dispersed fluorescence from, and stimulated emission pumping through, the Σ_u^+–Σ_g^+ vibronic band at 33 588 cm^{-1}. Progressions in the bending mode in the ground $^1\Sigma_g^+$ state are observed for each set of the stretching quantum numbers v_1 and v_3 and B_v, q_v values obtained. Strong coupling between bending and stretching is evident. Rotational levels $J \leqslant 8$ were observed.

Snow, Seab, and Joseph[372] have made a new sensitive search for interstellar C_3 resulting in upper limits in a few diffuse clouds of 10^{10} cm^{-2}, or about 10^{-11} with respect to H_2. Measurements were made at 4050 Å. The shock model for the production of C_3 and constraints on linear carbon molecules as carriers of the diffuse interstellar bands are discussed.

C_4 Molecule. Theoretical arguments by Martin, Francois, and Gijbels[373] place the infrared-active (σ_u) stretching of linear C_4 at 1544 cm^{-1}, in disagreement with Vala et al.[282] The latter authors assigned this band to C_5, but it is reasoned that the C_5 frequency lies nearer to 1368 cm^{-1} (see discussion of C_5 below).

The structure of C_4 has been studied by the Coulomb explosion method by Algranati et al.[390] (extending their earlier work on C_3;[182] see section V.C). The two-dimensional projection of the "exploded" structure indicates that the neutral C_4 enters the foil as a rhombus, "proving unambiguously that many of the neutrals measured have the rhombic form". Inconsistency with the photoelectron spectroscopy of Yang et al.,[288] interpreted in terms of linear species, is rationalized by noting that there is no discrimination against low electron affinity species in the explosion experiments so that rings will more probably be observed.

C_5 Molecule. Great progress has been made here, very much paralleling recent observations on C_3. At essentially the same time two groups have observed the high-resolution vibration–rotation spectrum of C_5 in the laboratory, and Bernath, Hinkle, and Keady,[374] following their C_3 work, have observed the corresponding infrared spectrum in circumstellar absorption in a carbon star. Moazzen-Ahmadi, McKellar, and Amano detected C_5 in the laboratory using a cooled hollow cathode discharge in C_2H_2 + He and C_2H_4 + He mixtures with a tunable diode laser spectrometer.[375] They measured 59 lines with J values rangingf from 0 to 72. Heath et al.[376] have also observed C_5 using diode laser spectroscopy but with an entirely different source. Graphite is laser vaporized in the throat of a supersonic nozzle and the plasma entrained in argon or neon. The rotational temperature of the beam is of the order of 8 K. Thirty-six rovibrational lines of the v_3 band were measured. The resulting molecular parameters from all three sources are given in Table XVI. The observed band origin of 2169.44 cm^{-1} agrees well with the neon matrix value of 2167 cm^{-1} [160] and argon matrix value of 2164 cm^{-1}.[282]

In contrast with C_3, the change in the rotational parameter upon excitation is quite normal and indicates that C_5 is a more rigid linear molecule than C_3. If the bonds were of identical length, as is almost the case in a cumulenic structure, B$''$ predicts an average r_o = 1.283 Å, close to that of C_3 where r_o = 1.277 Å.

In the theoretical paper by Martin et al.,[373] referred to above, the MP2/6-31G* program of Michalska et al.[263] was used to calculate the geometry, harmonic frequencies, and infrared intensities of the vibrational modes of linear C_5. Using a general scaling factor, the σ_u stretching frequencies were predicted to be 2193 and 1368 cm^{-1}. The predicted frequency 2193 cm^{-1} is only slightly higher than the observed band at 2164 cm^{-1} so that it is suggested that 1368 cm^{-1} is too low to correspond to an assignment of the 1544-cm^{-1} band to C_5, and it should be assigned to C_4. However, the reasoning that the low calculated intensity of the 1368-cm^{-1} band (about 1/20th of that at 2193 cm^{-1}) provides support for this assignment does not seem valid since the 1544-cm^{-1} band is also relatively weak.

C_6 Molecule. A theoretical calculation has been carried out by Parasuk and Almlöf[377] that departs widely from other recent ab initio theoretical results. Energies and equilibrium geometries, including consideration of linear and monocyclic rings, were calculated for C_6 using MCSCF and multireference CI methods with large basis sets of ANO type. According to these calculations the linear cumulene ($^3\Sigma_g^-$) form has the lowest energy with the triacetylenic structure higher by about 20 kcal/mol and the cyclic form even higher by 40 kcal/mol. These differences are considered to be well outside the error bars for the predicted relative energies. (However, a note added in proof to the pub-

lished article indicates that perhaps the energy difference between the two structures "might crucially depend on the number of electrons correlated".)

Carbon Cluster Ions. Seifert, Becker, and Dietze[378] have continued their work on the neutral and ion clusters by mass spectrometric detection of $C_n^{\pm}$ ions in laser-vaporized graphite plasmas. The abundance distribution data have been interpreted on the basis of LCAO–Xα calculations of binding energies. The crossover from odd–even alternation to "four periodicity" in the cluster ion intensities could be explained as a transition from linear to cyclic C_n clusters, as suggested by other authors (see section VIII.C).

Large Clusters. Radi et al.[379] directly sampled the positive cluster ions C_n^+ from the plume formed during laser vaporization of a rotating, translation carbon rod (i.e., "pits" were not formed; see section VIII.B,C). Fragmentation of mass-selected metastable ions occurred to release predominantly C_3 neutrals for $5 < n < 30$ and C_2 neutrals for $30 \leq n \leq 60$. In addition to C_3 loss, other neutral fragments C_1, C_5, C_{10}, and C_{14} were detected. The patterns support the stability of odd-n linear chains for $n < 10$, monocyclic rings C_{10} and C_{14} with $4n + 2$ enhanced stability, and a transition around $n = 30$ perhaps to carbyne[240] or spheroidal-shell[319,356] structures.

Rohlfing,[368] in addition to emission from C_2 formed from laser vaporization of graphite into a confined helium flow (see above), has observed a long-lived continuum attributed to the incandescence of hot carbon particles. This is the first direct evidence that carbon particles are being produced in this cluster source (not by sputtering of a carbon overlayer on the walls[306]), and the author addresses the questions of why and how this occurs.

Using the restricted Hartree–Fock (RHF) method, Almlöf and Lüthi[380] have investigated planar, single-sheet graphite fragments containing 6–54 atoms with high-spin and low-spin systems of dangling bonds. There is slow convergence to bulk values. Also by treating a C_{20} polyyne ring it was concluded that large clusters would not be expected to be observed experimentally in a cyclic (or linear) chain structure.

C_{60} and Proposed Spheroidal Clusters. Calculations on buckminsterfullerene (Bf) by Lüthi and Almlöf[349] (see section IX.A.1) were extended to the bowl-shaped corannulene molecule $C_{20}H_{10}$ containing only six-membered rings to estimate the effect of inclusion of d orbitals on the calculated stability of C_{60}.[380] The calculations suggest that Bf is thermodynamically unstable with respect to graphite by about 23 eV.

On the basis of MNDO theory,[337] Stanton and Newton[381] have computed the normal modes of vibration of buckminsterfullerene and predicted the intensities of its four infrared-active (F_{1u}) frequencies at 577, 719, 1353, and 1628 cm^{-1}.

Rosén and Wästberg[382] have applied the local density approximation (LDA) with the discrete variational method (DVM) to analyze the electronic structures of C_{60}, C_{60}^+, and C_{60}^-. Xα exchange correlation ($\alpha = 0.7$) and von Barth–Hedin potentials were used. The latter, considered more accurate, yielded electron affinities (EA) of C_{60}^+ as 7.8 eV (expt 6.4–7.9 eV) and of C_{60} as 2.7 eV (expt 2.6–2.8 eV) and ionization potentials (IP) of C_{60} as 7.8 eV (expt 6.4–7.9 eV) and of C_{60}^- as 2.7 eV (expt 2.6–2.8 eV). All are in good agreement with present experimental data (see section IX.A.2).

Brendsdal[383] has calculated the 174 symmetry coordinates of C_{60}, and Brendsdal et al.[384] have used an approximate force field developed for (planar) aromatics to calculate its 46 vibrational frequencies. These have been compared with other calculated frequencies (see section IX.A.1).

Kroto[385–387] has reviewed the possible role of C_{60}, fullerenes, and "icospiral" nucleation in soot and cosmic particle formation. Wright[388] has calculated, via the discrete dipole approximation, the ultraviolet extinction curves of small spherical particles arranged in onion-like structures.[323] The model does not fit the interstellar absorption feature of 2200 Å well; the width of the absorption is too large. Lêger et al.[389] have reasoned in favor of the polyhedral carbon ions C_{60}^+, C_{70}^+, etc., as possible carriers of the diffuse interstellar bands.

Registry No. C, 7440-44-0.

References

(1) Some recent observations of C_2, for example, are (a) during shock-induced decomposition of liquid benzene [Nicol, M.; Johnson, M. L.; Holmes, N. C. *Physica B+C* 1986, *139, 140*, 582], (b) during photodissociation of acetylene at 193 nm [Wodtke, A. M.; Lee, Y. T. *J. Phys. Chem.* 1985, *89*, 4744], (c) from IR multiphoton dissociation of ethylene [Grunwald, R.; Lademann, J.; Homan, G.; Shibanov, A. N. *Khim. Fiz.* 1985, *4*, 46], (d) in a helium + acetylene diffusion flame [Winicur, D.; Hardwick, J. L. *Chem. Phys.* 1985, *94*, 157], and (e) in an organic halide–alkali metal flame [Curtis, M. C.; Sarre, P. J. *J. Mol. Spectrosc.* 1985, *114*, 427].

(2) Fujita, Y. *Mem. Soc. R. Sci. Liege, Collect. 4°* 1957, *18*, 297; McKellar, A. *J. R. Astron. Soc. Can.* 1960, *54*, 97; *Astron. J.* 1960, *65*, 350.

(3) Brault, J. W.; Delbouille, L.; Grevesse, N.; Roland, G.; Sauval, A. J.; Testerman, L. *Astron. Astrophys.* 1982, *108*, 201.

(4) Gural'chuk, A. L.; Dement'ev, M. S.; Klimenko, V. M. *Kinematika Fiz. Nebesnykh Tel* 1986, *2*, 91.

(5) Van Dishoeck, E. F. *Ned. Tijdschr. Natuurkd., A* 1985, *A51*, 38.

(6) Huber, K. P.; Herzberg, G. *Molecular Spectra and Molecular Structure IV. Constants of Diatomic Molecules*; Van Nostrand Reinhold: New York, 1979; Appendix IX.

(7) Ballik, E. A.; Ramsay, D. A. *Astrophys. J.* 1963, *137*, 61; 1963, *137*, 84.

(8) Roux, F.; Wannous, G.; Michaud, F.; Verges, J. *J. Mol. Spectrosc.* 1985, *109*, 334.

(9) Douay, M.; Nietmann, R.; Bernath, P. F. *J. Mol. Spectrosc.* 1988, *131*, 250.

(10) Douay, M.; Nietmann, R.; Bernath, P. F. *J. Mol. Spectrosc.* 1988, *131*, 261.

(11) Fongere, P. F.; Nesbet, R. K. *J. Chem. Phys.* 1966, *44*, 285. Barsuhn, J. *Z. Naturforsch. A: Phys., Phys. Chem. Kosmophys.* 1972, *A27*, 1031. Kirby, K.; Liu, B. *J. Chem. Phys.* 1979, *70*, 893.

(12) Chauville, J.; Maillard, J. P.; Mantz, A. W. *J. Mol. Spectrosc.* 1977, *68*, 399.

(13) Davis, S. P.; Abrams, M. C.; Phillips, J. G.; Rao, M. L. P. *J. Opt. Soc. Am. B: Opt. Phys.* 1988, *5*, 2280.

(14) Pesic, D. S.; Vujisic, B. R.; Rakotoarijimy, D.; Weniger, S. *J. Mol. Spectrosc.* 1983, *100*, 245.

(15) Amiot, C.; Chauville, J.; Maillard, J. P. *J. Mol. Spectrosc.* 1979, *75*, 19.

(16) Amiot, C. *Astrophys. J., Suppl. Ser.* 1983, *52*, 329. Amiot, C.; Verges, J. *Astrophys. J.* 1982, *263*, 933; *Astron. Astrophys., Suppl. Ser.* 1983, *51*, 257.

(17) Curtis, M. C.; Sarre, P. J. *J. Mol. Spectrosc.* 1985, *114*, 427; *J. Chem. Soc., Chem. Commun.* 1986, 604.

(18) Yan, W. B.; Curl, R. F.; Merer, A. J.; Carrick, P. B. *J. Mol. Spectrosc.* 1985, *112*, 436.

(19) van der Burgt, L. J.; Heaven, M. C. *J. Chem. Phys.* 1987, *87*, 4235.

(20) Goodwin, P. M.; Cool, T. A. *J. Chem. Phys.* 1988, *88*, 4548; 1989, *90*, 1296.

(21) DeFrees, D. J.; Raghavachari, K.; Schlegel, H. B.; Pople, J. A. *J. Am. Chem. Soc.* 1982, *104*, 5576.

(22) Raghavachari, K. *J. Chem. Phys.* 1985, *82*, 4607.

(23) Rohlfing, C. M.; Martin, R. L. *J. Phys. Chem.* 1986, *90*, 2043.

(24) Dunlap, B. I. *J. Chem. Phys.* 1983, *78*, 4997.

(25) Dunlap, B. I. *Phys. Rev. A* 1984, *A29*, 2902.

(26) Painter, G. S.; Averil, F. W. *Phys. Rev. B: Condens. Matter* **1982**, *B26*, 1781.
(27) Averill, F. W.; Painter, G. S. *Phys. Rev. B: Condens. Matter* **1986**, *B34*, 2088.
(28) Fukushima, K.; Mizuno, J.; Fujima, K.; Adachi, H. *J. Phys. Soc. Jpn.* **1982**, *51*, 4028.
(29) Becke, A. D. *Phys. Rev. A* **1986**, *A33*, 2786.
(30) Heera, V.; Seifert, G.; Ziesche, P. *J. Phys. B* **1984**, *B17*, 519.
(31) Bauschlicher, C. W., Jr.; Langhoff, S. R. *J. Chem. Phys.* **1987**, *87*, 2919.
(32) Walvekar, A. P.; Rama, M. A. *Indian J. Phys. B* **1984**, *58B*, 390.
(33) Brown, C. W. *J. Chem. Phys.* **1982**, *77*, 5379.
(34) Kuz'menko, N. E.; Chumak, L. V. *J. Quant. Spectrosc. Radiat. Transfer* **1986**, *35*, 419.
(35) Sauval, A. J.; Tatum, J. B. *Astrophys. J., Suppl. Ser.* **1984**, *56*, 193.
(36) Rossi, S. C.; Maciel, W. J.; Benevides-Soares, P. *Astronom. Astrophys.* **1985**, *148*, 93.
(37) Padial, N. T.; Collins, L. A.; Schneider, B. I. *Astrophys. J.* **1985**, *298*, 369.
(38) Pouilly, B.; Robbe, J. M.; Schamps, J.; Roueff, E. *J. Phys. B* **1983**, *B16*, 437.
(39) Tatarczyk, T.; Fink, E. H.; Becker, K. H. *Chem. Phys. Lett.* **1976**, *40*, 126.
(40) Cooper, D. M.; Nicholls, R. W. *Spectrosc. Lett* **1976**, *9*, 139.
(41) Brewer, L.; Hagan, L. *High Temp. Sci.* **1979**, *11*, 233.
(42) Naulin, C.; Costes, M.; Dorthe, G. *Chem. Phys. Lett.* **1988**, *143*, 496.
(43) Curtis, L.; Engman, B.; Erman, P. *Phys. Scr.* **1976**, *13*, 270.
(44) Campbell, J. D.; Yu, M. H.; Wittig, C. *Appl. Phys. Lett.* **1978**, *32*, 413.
(45) McDonald, J. R.; Baronavski, A. P.; Donnelly, V. M. *Chem. Phys.* **1978**, *33*, 161.
(46) Erman, P. *Phys. Scr.* **1980**, *22*, 108.
(47) Arnold, J. O. *J. Quant. Spectrosc. Radiat. Transfer* **1968**, *8*, 1781.
(48) Cooper, D. M.; Nicolls, R. W. *J. Quant. Spectrosc. Radiat. Transfer* **1975**, *15*, 139.
(49) Stark, G.; Davis, S. P. *Z. Phys. A* **1985**, *A321*, 75.
(50) Bauer, W.; Becker, K. H.; Bielefeld, M.; Meuser, R. *Chem. Phys. Lett.* **1986**, *123*, 33.
(51) Arnold, J. O.; Langhoff, S. R. *J. Quant. Spectrosc. Radiat. Transfer* **1978**, *19*, 461.
(52) Chabalowski, C. F.; Buenker, R. J.; Peyerimhoff, S. D. *Chem. Phys. Lett.* **1981**, *83*, 441.
(53) Cooper, D. M. *J. Quant. Spectrosc. Radiat. Transfer* **1981**, *26*, 113.
(54) Roux, F.; Cerny, D.; D'Incan, J. *Astrophys. J.* **1976**, *204*, 940.
(55) van Dishoeck, E. F. *Chem. Phys.* **1983**, *77*, 277.
(56) Chabalowski, C. F.; Peyerimhoff, S. D.; Buenker, R. J. *Chem. Phys.* **1983**, *81*, 57.
(57) Theodorakopoulos, G.; Petsalakis, I. D.; Nicolaides, C. A.; Buenker, R. J. *Chem. Phys.* **1987**, *112*, 319.
(58) O'Neil, S. V.; Rosmus, P.; Werner, H.-J. *J. Chem. Phys.* **1987**, *87*, 2847.
(59) Wentink, T.; Marram, E.; Isaacson, L.; Spindler, R. *Air Force Weapons Lab. Report* **1967**, *AFWL-TR-67-30*, 1.
(60) Sviridov, A. G.; Sobolev, N. N.; Novgorodov, M. Z. *J. Quant. Spectrosc. Radiat. Transfer* **1966**, *6*, 337.
(61) Smith, W. H. *APEA J.* **1969**, *156*, 791.
(62) van Dishoeck, E. F.; Black, J. H. *Astrophys. J.* **1982**, *258*, 533.
(63) van Dishoeck, E. F. *Chem. Phys.* **1983**, *77*, 277.
(64) Krishna Swamy, K. S.; O'Dell, C. R. *Astrophys. J.* **1981**, *251*, 805.
(65) Lambert, D. L.; Danks, A. C. *Astrophys. J.* **1983**, *268*, 428.
(66) Pouilly, B., unpublished, 1983; cited in ref 67.
(67) Le Bourlot, J.; Roueff, E. *J. Mol. Spectrosc.* **1986**, *120*, 157.
(68) Fowler, A. *Mon. Not. R. Astron. Soc.* **1910**, *70*, 484.
(69) Johnson, R. C.; Asundi, R. K. *Proc. R. Soc. London, A* **1929**, *A124*, 668.
(70) Fox, J. G.; Herzberg, G. *Phys. Rev.* **1937**, *52*, 638.
(71) Herzberg, G. *Astrophys. J.* **1939**, *89*, 290.
(72) Jeunehomme, M.; Schwenker, R. P. *J. Chem. Phys.* **1965**, *42*, 2406.
(73) Savadatti, M. I.; Broida, H. P. *J. Chem. Phys.* **1966**, *45*, 2390.
(74) Kunz, C.; Harteck, P.; Dondes, S. *J. Chem. Phys.* **1967**, *46*, 4157.
(75) Meinel, H.; Messerle, G. *Astrophys. J.* **1968**, *154*, 381.
(76) Gosse, F.; Sadeghi, N.; Pebay-Peyroula, J. C. *Chem. Phys. Lett.* **1972**, *13*, 557.
(77) Faust, W. L.; Goldberg, L. S.; Craig, B. B.; Weiss, R. G. *Chem. Phys. Lett.* **1981**, *83*, 265.
(78) Herzberg, G. *Phys. Rev.* **1946**, *70*, 762.
(79) Setser, D. W.; Thrush, B. A. *Nature (London)* **1963**, *200*, 864.
(80) Little, C. E.; Browne, P. G. *Chem. Phys. Lett.* **1987**, *134*, 560.
(81) Kirby, K.; Liu, B. *J. Chem. Phys.* **1979**, *70*, 893.
(82) Zeitz, M.; Peyerimhoff, S. D.; Buenker, R. J. *Chem. Phys. Lett.* **1979**, *64*, 243.
(83) Rosmus, P.; Werner, H.-J. *J. Chem. Phys.* **1984**, *80*, 5085.
(84) Dupuis, M.; Liu, B. *J. Chem. Phys.* **1980**, *73*, 337.
(85) Nichols, J. A.; Simons, J. *J. Chem. Phys.* **1987**, *86*, 6972.
(86) Corderman, R. R.; Lineberger, W. C. *Annu. Rev. Phys. Chem.* **1979**, *30*, 347.
(87) Vardya, M. S.; Krishna Swamy, K. S. *Chem. Phys. Lett.* **1980**, *73*, 616.
(88) Wallerstein, G. *Astron. Astrophys.* **1982**, *105*, 219.
(89) Sarre, P. J. *J. Chim. Phys. Phys.-Chim. Biol.* **1980**, *77*, 769.
(90) Chupka, W. A.; Berkowitz, J.; Giese, C. F.; Inghram, M. G. *J. Phys. Chem.* **1958**, *62*, 611.
(91) De Maria, G.; Balducci, G.; Capalbi, A.; Guido, M. *Proc. Br. Ceram. Soc.* **1967**, *No. 8*, 127.
(92) Kohl, F. J.; Sterns, C. A. *J. Phys. Chem.* **1970**, *74*, 2714.
(93) Bianchini, J. J.; Van Zee, R. J.; Weltner, W., Jr. *J. Mol. Struct.* **1987**, *157*, 93.
(94) Honig, R. E. *J. Chem. Phys.* **1954**, *22*, 126.
(95) Herzberg, G.; Lagerqvist, A. *Can. J. Phys.* **1968**, *46*, 2363.
(96) Milligan, D. E.; Jacox, M. E.; Abouaf-Marguin, L. *J. Chem. Phys.* **1967**, *46*, 4562.
(97) Milligan, D. E.; Jacox, M. E. *J. Chem. Phys.* **1969**, *51*, 1952.
(98) Lineberger, W. C.; Patterson, T. A. *Chem. Phys. Lett.* **1972**, *13*, 40.
(99) Jones, P. L.; Mead, R. D.; Kohler, B. E.; Rosner, S. D.; Lineberger, W. C. *J. Chem. Phys.* **1980**, *73*, 4419.
(100) Mead, R. D.; Schulz, P. A.; Feigerle, C. S.; Lineberger, W. C. *IEEE Trans. Nucl. Sci.* **1981**, NS-28, 1194.
(101) Hefter, U.; Mead, R. D.; Schulz, P. A.; Lineberger, W. C. *Phys. Rev. A* **1983**, *A28*, 1429.
(102) Mead, R. D.; Stevens, A. E.; Lineberger, W. C. In *Gas Phase Ion Chemistry*; Bowers, M. T., Ed.; Academic: New York, 1984; Vol. III, p 213.
(103) Mead, R. D.; Hefter, U.; Schulz, P. A.; Lineberger, W. C. *J. Chem. Phys.* **1985**, *82*, 1723.
(104) Rehfuss, B. D.; Liu, D.-J.; Dinelli, B. M.; Jagod, M.-F.; Ho, W. C.; Crofton, M. W.; Oka, T. *J. Chem. Phys.* **1988**, *89*, 129. Oka, T. *Philos. Trans. R. Soc. London, A* **1988**, *No. 324*, 81–95.
(105) Cade, P. E.; Wahl, A. C.; Sales, K.; Greenshields, J. B.; Malli, G. *At. Data Nucl. Data Tables* **1974**, *13*, 339.
(106) Barsuhn, J. *J. Phys. B* **1974**, *B7*, 155.
(107) Thulstrup, P. W.; Thulstrup, E. W. *Chem. Phys. Lett.* **1974**, *26*, 144.
(108) Feldmann, D. *Z. Naturforsch. A: Astrophys., Phys. Phys. Chem.* **1970**, *A25*, 621. Locht, R.; Momigny, J. *Chem. Phys. Lett.* **1970**, *6*, 273.
(109) Cederbaum, L. S.; Domcke, W.; von Niessen, W. *J. Phys. B* **1977**, *B10*, 2963.
(110) Bondybey, V. E.; Brus, L. E. *J. Chem. Phys.* **1975**, *63*, 2223.
(111) Leutwyler, S.; Maier, J. P.; Misev, L. *Chem. Phys. Lett.* **1982**, *91*, 206.
(112) Cathro, W. C.; Mackie, J. C. *J. Chem. Soc., Faraday Trans. 1* **1973**, *I2*, 237.
(113) Frosch, R. P. *J. Chem. Phys.* **1971**, *54*, 2660.
(114) Jacox, M. E. *J. Mol. Spectrosc.* **1985**, *113*, 286–301.
(115) Brus, L. E.; Bondybey, V. E. *J. Chem. Phys.* **1975**, *63*, 3123.
(116) Graham, W. R. M.; Dismuke, K. I.; Weltner, W., Jr. *J. Chem. Phys.* **1974**, *61*, 4793.
(117) Bondybey, V. E.; Nibler, J. W. *J. Chem. Phys.* **1972**, *56*, 4719.
(118) Allamandola, L. J.; Nibler, J. W. *Chem. Phys. Lett.* **1974**, *28*, 335.
(119) Allamandola, L. J.; Rojhantalab, H. M.; Nibler, J. W.; Chappell, T. *J. Chem. Phys.* **1977**, *67*, 99.
(120) Allamandola, L.; Rojhantalab, H.; Nibler, J. *Ber. Bunsen-Ges. Phys. Chem.* **1978**, *82*, 126.
(121) Roessler, K.; Manzanares, A. R. *Ber. Kernforschungsanlage Juelich* **1984**, *Juel-1924*, 90.
(122) Drowart, J.; Burns, R. P.; De Maria, G.; Inghram, M. G. *J. Chem. Phys.* **1959**, *31*, 1131.
(123) Dibeler, V. H.; Liston, S. K. *J. Chem. Phys.* **1967**, *47*, 4548.
(124) Petrongolo, C.; Bruna, P. J.; Peyerimhoff, S. D.; Buenker, R. J. *J. Chem. Phys.* **1981**, *74*, 4594.
(125) Krankowsky, D.; Lämmerzahl, P.; Herrwerth, I.; Woweries, J.; Eberhardt, P.; Dolder, U.; Herrmann, U.; Schulte, W.; Berthelier, J. J.; Illiano, J. M.; Hodges, R. R.; Hoffman, J. H. *Nature (London)* **1986**, *321*, 326. Coplan, M. A.; Ogilvie, K. W.; A'Hearn, M. F.; Bochsler, P.; Geiss, J. *J. Geophys. Res.* **1987**, *A92*, 39.
(126) Huntress, W. T. *Astrophys. J., Suppl. Ser.* **1977**, *33*, 495.
(127) Adams, N. G.; Smith, D. *Chem. Phys. Lett.* **1977**, *47*, 383. Smith, D.; Adams, N. G. *Astrophys. J.* **1977**, *217*, 741.
(128) Raksit, A. B.; Bohme, D. K. *Int. J. Mass Spectrom. Ion Processes* **1985**, *63*, 217.
(129) Mackay, G. I.; Vlachos, G. D.; Bohme, D. K.; Schiff, H. I. *Int. J. Mass Spectrom. Ion Phys.* **1980**, *36*, 259.
(130) Meinel, H. *Can. J. Phys.* **1972**, *50*, 158.
(131) Rosmus, P.; Werner, H.-J.; Reinsch, E.-A.; Larsson, M. *J. Electron Spectrosc. Relat. Phenom.* **1986**, *41*, 289.
(132) (a) O'Keefe, A.; Derai, R.; Bowers, M. T. *Chem. Phys.* **1984**, *91*, 161. (b) Rasanen, M.; Liu, J. Y.; Dzugan, T. P.; Bondy-

bey, V. E. *Chem. Phys. Lett.* **1987**, *142*, 308.

(133) (a) Forney, D.; Althaus, H.; Maier, J. P. *J. Phys. Chem.* **1987**, *91*, 6458. (b) Rösslein, M.; Wyttenbach, M.; Maier, J. P. *J. Chem. Phys.* **1987**, *87*, 6770. (c) Maier, J. P.; Rösslein, M. *J. Chem. Phys.* **1988**, *88*, 4614–4620.

(134) Knight, L. B., Jr.; Cobranchi, S. T.; Earl, E. *J. Chem. Phys.* **1988**, *88*, 7348.

(135) Smith, G. R.; Weltner, W., Jr. *J. Chem. Phys.* **1975**, *62*, 4592.

(136) Huggins, W. *Proc. R. Soc. London* **1882**, *33*, 1.

(137) Swings, P.; Elvey, C. T.; Babcock, H. W. *Astrophys. J.* **1941**, *94*, 320. Swings, P. *Rev. Mod. Phys.* **1942**, *14*, 190. Rosen, B.; Swings, P. *Ann. Astrophys.* **1953**, *16*, 82.

(138) McKellar, A. *Astrophys. J.* **1948**, *108*, 453. McKellar, A.; Richardson, E. H. *Mem. Soc. R. Sci. Liege, Collect. 4°* **1955**, *15*, 256.

(139) Swings, P.; McKellar, A.; Rao, K. N. *Mon. Not. R. Astronom. Soc.* **1953**, *113*, 571.

(140) Crampton, D.; Cowley, A. P.; Humphreys, R. M. *Astrophys. J.* **1975**, *198*, L135.

(141) Clegg, R. E. S.; Lambert, D. L. *Mon. Not. R. Astron. Soc.* **1982**, *201*, 723.

(142) Ramsay gives a bibliography of the observations, up to that time, of C_3 produced in discharges, flames, and furnaces and by flash photolysis [Ramsay, D. A. *Adv. Spectrosc.* **1959**. *1*, 1].

(143) Brewer, L.; Engelke, J. L. *J. Chem. Phys.* **1962**, *36*, 992.

(144) Herzberg, G. *Astrophys. J.* **1942**, *96*, 314.

(145) Monfils, A.; Rosen, B. *Nature (London)* **1949**, *164*, 713.

(146) Douglas, A. E. *Astrophys. J.* **1951**, *114*, 466.

(147) Clusius, K.; Douglas, A. E. *Can. J. Phys.* **1954**, *32*, 319.

(148) Kiess, N. H.; Bass, A. M. *J. Chem. Phys.* **1954**, *22*, 569.

(149) Kiess, N. H.; Broida, H. P. *Can. J. Phys.* **1956**, *34*, 1471.

(150) Gausset, L.; Herzberg, G.; Lagerqvist, A.; Rosen, B. *Discuss. Faraday Soc.* **1963**, *35*, 113; *Astrophys. J.* **1965**, *142*, 45.

(151) Merer, A. J. *Can. J. Phys.* **1967**, *45*, 4103.

(152) Renner, R. *Z. Phys.* **1934**, *92*, 172–193.

(153) Barger, R. L.; Broida, H. P. *J. Chem. Phys.* **1962**, *37*, 1152–1153; **1965**, *43*, 2364.

(154) Weltner, W., Jr.; Walsh, P. N. *J. Chem. Phys.* **1962**, *37*, 1153–1154.

(155) Weltner, W., Jr.; Walsh, P. N.; Angell, C. L. *J. Chem. Phys.* **1964**, *40*, 1299–1305.

(156) Weltner, W., Jr.; McLeod, D., Jr. *J. Chem. Phys.* **1964**, *40*, 1305–1316.

(157) Weltner, W., Jr.; McLeod, D., Jr. *J. Chem. Phys.* **1966**, *45*, 3096–3105.

(158) Bondybey, V. E.; English, J. H. *J. Chem. Phys.* **1978**, *68*, 4641–4643.

(159) Jungen, Ch.; Merer, A. J. *Molecular Spectroscopy: Modern Research*; Rao, K. N., Ed.; Academic Press: New York, 1976; Vol. II, pp 127–164.

(160) Thompson, K. R.; DeKock, R. L.; Weltner, W., Jr. *J. Am. Chem. Soc.* **1971**, *93*, 4688–4695.

(161) (a) Matsumura, K.; Kanamori, H.; Kawaguchi, K.; Hirota, E. *J. Chem. Phys.* **1988**, *89*, 3491–3494. (b) Hinkle, K. H.; Keady, J. J.; Bernath, P. F. *Science* **1988**, *241*, 1319–1322.

(162) Brown, J. M. *J. Mol. Spectrosc.* **1973**, *56*, 159–162.

(163) Jungen, Ch.; Merer, A. J. *Mol. Phys.* **1980**, *40*, 95–114.

(164) Walsh, A. D. *Discuss. Faraday Soc.* **1963**, *35*, 223.

(165) Herzberg, G.; Travis, D. N. *Can. J. Phys.* **1964**, *42*, 1658.

(166) Ramsay, D. A. *J. Chem. Phys.* **1965**, *43*, S18.

(167) Smith, W. H.; Leroi, G. E. *J. Chem. Phys.* **1966**, *45*, 1784.

(168) Brewer, L.; Gilles, P. N.; Jenkins, F. A. *J. Chem. Phys.* **1948**, *16*, 797.

(169) Thorn, R. J.; Winslow, G. H. *J. Chem. Phys.* **1957**, *26*, 186.

(170) Goldfinger, P. *Mem. Soc. R. Sci. Liege, Collect. 4°* **1955**, *15*, 378.

(171) Chupka, W. A.; Inghram, M. G. *J. Chem. Phys.* **1953**, *21*, 371; **1953**, *21*, 1313; **1954**, *22*, 1472.

(172) Honig, R. E. *J. Chem. Phys.* **1954**, *22*, 126.

(173) Chupka, W. A.; Inghram, M. G. *J. Phys. Chem.* **1955**, *39*, 100–104.

(174) Zavitsanos, P. D.; Carlson, G. A. *J. Chem. Phys.* **1973**, *59*, 2966.

(175) Kern, D. M. *J. Chem. Educ.* **1956**, *33*, 272.

(176) Zavitsanos, P. D. *Carbon* **1968**, *6*, 731.

(177) Berkowitz, J.; Chupka, W. A. *J. Chem. Phys.* **1964**, *40*, 2735.

(178) Robiette, A. G.; Strauss, H. L. *J. Chem. Phys.* **1966**, 2826, 2827.

(179) Strauss, H. L.; Thiele, E. *J. Chem. Phys.* **1967**, *46*, 2473–2480.

(180) Palmer, H. B.; Shelef, M. *Chem. Phys. Carbon* **1968**, *4*, 85–135.

(181) Goldring, G.; Eisen, Y.; Thieberger, P.; Wegner, H. E.; Filevich, A. *Phys. Rev. A* **1982**, *A26*, 186–198.

(182) Plesser, I.; Vager, Z.; Na'aman, R. *Phys. Rev. Lett.* **1986**, *56*, 1559–1562.

(183) Bunker, P. R. *Annu. Rev. Phys. Chem.* **1983**, *34*, 59–75.

(184) Yamada, K.; Winnewisser, M. *Z. Naturforsch. A: Phys., Phys. Chem., Kosmophys.* **1976**, *31A*, 139–144.

(185) Winnewisser, B. P. *Molecular Spectroscopy: Modern Research*; Rao, K. N., Ed.; Academic Press: New York, 1985; Vol. III, Chapter 6, pp 321–419.

(186) Hansen, C. F.; Pearson, W. E. *Can. J. Phys.* **1973**, *51*, 751–760.

(187) Hansen, C. F.; Henderson, B. J.; Pearson, W. E. *J. Chem. Phys.* **1974**, *60*, 754–759.

(188) Clementi, E.; McLean, A. D. *J. Chem. Phys.* **1962**, *36*, 45–47.

(189) Clementi, E.; Clementi, H. *J. Chem. Phys.* **1962**, *36*, 2824–2833.

(190) Müller, H. *Z. Chem.* **1963**, *10*, 369–378.

(191) Nibler, J. W.; Linnett, J. W. *Trans. Faraday Soc.* **1966**, *64*, 1153–1164.

(192) Hoffmann, R. *Tetrahedron* **1966**, *22*, 521–538.

(193) Liskow, D. H.; Bender, C. F.; Schaefer, H. F., III *J. Chem. Phys.* **1972**, *56*, 5075–5080.

(194) (a) Perić-Radić, J.; Römelt, J.; Peyerimhoff, S. D.; Buenker, R. J. *Chem. Phys. Lett.* **1977**, *50*, 344–350. (b) Perić, M.; Perić-Radić, J. *J. Serb. Chem. Soc.* **1987**, *52*, 389–398. (c) Perić, M.; Perić-Radić, J. *Chem. Phys. Lett.* **1979**, *67*, 138–141. (d) Perić, M.; Peyerimhof, S. D.; Buenker, R. J. *Mol. Phys.* **1983**, *49*, 379–400. (e) Perić, M.; Peyerimhoff, S. D.; Buenker, R. J. *Int. Rev. Phys. Chem.* **1985**, *4*, 85–124.

(195) Römelt, J.; Peyerimhoff, S. D.; Buenker, R. J. *Chem. Phys. Lett.* **1978**, *58*, 1–7.

(196) Jones, R. O. *Phys. Rev. A* **1985**, *A32*, 2589–2594.

(197) Carter, S.; Mills, I. M.; Murrell, J. N. *J. Mol. Spectrosc.* **1980**, *81*, 110–121.

(198) Hougen, J. T.; Bunker, P. R.; Johns, J. W. C. *J. Mol. Spectrosc.* **1970**, *34*, 136–172.

(199) Bunker, P. R.; Stone, J. M. R. *J. Mol. Spectrosc.* **1972**, *41*, 310–332. Hoy, A. R.; Bunker, P. R. *J. Mol. Spectrosc.* **1974**, *52*, 439–452; **1979**, *74*, 1–8.

(200) Jensen, P.; Bunker, P. R. *J. Mol. Spectrosc.* **1983**, *99*, 348–356; **1986**, *118*, 18–39. (a) Jensen, P. *Comput. Phys. Rep.* **1983**, *1*, 1.

(201) Duxbury, G. *Mol. Spectrosc. (Chem. Soc., London)* **1975**, *3*, 497.

(202) Sorenson, G. O. *Top. Curr. Chem.* **1979**, *82*, 99–175.

(203) Jensen, P. *Comput. Phys. Rep.* **1983**, *1*, 1–56.

(204) Beardsworth, R.; Bunker, P. R.; Jensen, P.; Kraemer, W. P. *J. Mol. Spectrosc.* **1986**, *118*, 50–63.

(205) Kraemer, W. P.; Bunker, P. R.; Yoshimine, M. *J. Mol. Spectrosc.* **1984**, *107*, 191–207.

(206) Jensen, P. *J. Mol. Spectrosc.* **1988**, *128*, 478–501; *J. Chem. Soc., Faraday Trans. 2*, **1988**, *84*, 1315.

(207) (a) Jensen, P.; Kraemer, W. P. *J. Mol. Spectrosc.* **1988**, *129*, 172–185. (b) Jensen, P. *Collect. Czech. Chem. Commun.*, in press. (c) Smith, R. S.; Anselment, M.; DiMauro, L. F.; Frye, J. M.; Sears, T. J. *J. Chem. Phys.* **1987**, *87*, 4435; erratum, **1988**, *89*, 2591.

(208) Perić, M.; Buenker, R. J.; Peyerimhoff, S. D. *Mol. Phys.* **1986**, *59*, 1283–1303.

(209) Jungen, Ch.; Merer, A. J. *Mol. Phys.* **1980**, *40*, 1–24.

(210) Jungen, Ch.; Hallin, K.-E. J.; Merer, A. J. *Mol. Phys.* **1980**, *40*, 25–64.

(211) Jungen, Ch.; Hallin, K.-E. J.; Merer, A. J. *Mol. Phys.* **1980**, *40*, 65–94.

(212) Pople, J. A.; Longuet-Higgins, H. C. *Mol. Phys.* **1958**, *1*, 372.

(213) Aarts, J. F. M. *Mol. Phys.* **1978**, *35*, 1785.

(214) Johns, J. W. C. *J. Mol. Spectrosc.* **1965**, *15*, 473–482.

(215) Carrington, A.; Fabris, A. R.; Howard, B. J.; Lucas, N. J. D. *Mol. Phys.* **1971**, *20*, 961.

(216) Brown, J. M. *J. Mol. Spectrosc.* **1977**, *68*, 412–422.

(217) Hougen, J. T.; Jesson, J. P. *J. Chem. Phys.* **1963**, *38*, 1524.

(218) Barrow, T.; Dixon, R. N.; Duxberry, G. *Mol. Phys.* **1974**, *27*, 1217–1234.

(219) Williams, G. R. J. *Chem. Phys. Lett.* **1975**, *33*, 582–584.

(220) Chang, K. W.; Graham, W. R. M. *J. Chem. Phys.* **1982**, *77*, 4300–4303.

(221) Pitzer, K. S.; Clementi, E. *J. Am. Chem. Soc.* **1959**, *81*, 4477.

(222) Julg, A.; Pellégatti, A. *Theor. Chim. Acta* **1964**, *2*, 210–214.

(223) Jacox, M. E.; Milligan, D. E. *Chem. Phys.* **1974**, *4*, 45–61.

(224) Sunil, K. K.; Orendt, A.; Jordan, K. D. *Chem. Phys.* **1984**, *89*, 245–256.

(225) Chabalowski, C. F.; Buenker, R. J.; Peyerimhoff, S. D. *J. Chem. Phys.* **1986**, *84*, 268–274.

(226) Lemire, G. W.; Fu, Z.; Hamrick, Y. M.; Taylor, S.; Morse, M. D., submitted for publication in *J. Phys. Chem.*

(227) Kohl, F. J.; Stearns, C. A. *J. Chem. Phys.* **1970**, *52*, 6310.

(228) See note added in proof in ref 224.

(229) Gupta, S. K.; Gingerich, K. A. *J. Chem. Phys.* **1979**, *71*, 3072.

(230) Oakes, J.; Ellison, G. B., as cited in ref 19 in Sunil et al.[224]

(231) Becker, K. H.; Tatarczyk, T.; Perić-Radić, J. *Chem. Phys. Lett.* **1979**, *60*, 502–506.

(232) Cooper, D. M.; Jones, J. J. *J. Quant. Spectrosc. Radiat. Transfer* **1979**, *22*, 201–208.

(233) Arnold, J. O.; Langhoff, S. R., cited in Cooper et al.[232] Gu, Y.; Lesiecki, M. L.; Bialkowski, S. E.; Guillory, W. A. *Chem. Phys. Lett.* **1982**, *92*, 443–448.

(234) Monyakin, A. P.; Kuznetsova, L. A. *Opt. Spektrosk.* **1983**, *54*, 79–84.
(235) Morgan, T. F.; Kroto, H. W., unpublished as cited by Jungen and Merer.[163]
(236) Faibis, A.; Kanter, E. P.; Tack, L. M.; Bakke, E.; Zabransky, B. J. *J. Phys. Chem.* **1987**, *91*, 6445–6447.
(237) Kühnel, W.; Gey, E.; Spangenberg, H.-J. *Z. Phys. Chem. (Leipzig)* **1982**, *263*, 641–645.
(238) Raghavachari, K., unpublished, cited by Faibis et al., in ref 236.
(239) Fürstenau, N.; Hillenkamp, F.; Nitsche, R. *Int. J. Mass Spectrom. Ion Phys.* **1979**, *31*, 85. Fürstenau, N.; Hillenkamp, F. *Ibid.* **1981**, *37*, 135.
(240) Rohlfing, E. A.; Cox, D. M.; Kaldor, A. *J. Chem. Phys.* **1984**, *81*, 3322–3330.
(241) Bloomfield, L. A.; Geusic, M. E.; Freeman, R. R.; Brown, W. L. *Chem. Phys. Lett.* **1985**, *121*, 33.
(242) Geusic, M. E.; McIlrath, T. J.; Jarrold, M. F.; Bloomfield, L. A.; Freeman, R. R.; Brown, W. L. *Z. Phys. D: At. Mol. Clusters*, in press.
(243) Geusic, M. E.; McIlrath, T. J.; Jarrold, M. F.; Bloomfield, L. A.; Freeman, R. R.; Brown, W. L. *J. Chem. Phys.* **1986**, *84*, 2421.
(244) Kroto, H. W.; Heath, J. R.; O'Brien, S. C.; Curl, R. F.; Smalley, R. E. *Nature (London)* **1985**, *318*, 162.
(245) Zhang, Q. L.; O'Brien, S. C.; Heath, J. R.; Liu, Y.; Curl, R. F.; Kroto, H. W.; Smalley, R. E. *J. Phys. Chem.* **1986**, *90*, 525.
(246) Clementi, E. *J. Am. Chem. Soc.* **1961**, *83*, 4501–4505.
(247) Müller, H. *Z. Chem.* **1963**, *10*, 369–378.
(248) Strickler, S. J.; Pitzer, K. S. In *Molecular Orbitals in Chemistry, Physics, and Biology*; Pullman, B., Löwdin, P.-O., Eds.; Academic: New York, 1964; pp 281–291.
(249) Slanina, Z.; Zahradnik, R. *J. Phys. Chem.* **1977**, *81*, 2252–2257.
(250) Bodor, N.; Dewar, M. J. S.; Harget, A.; Haselbach, E. *J. Am. Chem. Soc.* **1970**, *92*, 3854.
(251) Bernholc, J.; Phillips, J. C. *Phys. Rev. B: Condens. Matter* **1986**, *B33*, 7395–7398; *J. Chem. Phys.* **1986**, *85*, 3258–3267.
(252) Phillips, J. C. *Chem. Rev.* **1986**, *86*, 619–634.
(253) Whiteside, R. A.; Krishnan, R.; DeFrees, D. J.; Pople, J. A.; von R. Schleyer, P. *Chem. Phys. Lett.* **1981**, *78*, 538–540.
(254) Ewing, D. W.; Pfeiffer, G. V. *Chem. Phys. Lett.* **1982**, *86*, 365–368.
(255) Nemukhin, A. V.; Stepanov, N. F.; Safonov, A. A. *Teor. Eksp. Khim.* **1982**, *18*, 608–612.
(256) Wang, Z. Z.; Diffenderfer, R. N.; Shavitt, I., unpublished paper presented at 39th Symposium on Molecular Spectroscopy, Ohio State University, 1984.
(257) Koutecký, J.; Pacchioni, G.; Jeung, G. H.; Hass, H. C. *Surf. Sci.* **1985**, *156*, 650. Pacchioni, G.; Koutecký, J. *Physics and Chemistry of Small Clusters*; Jena, P., Rao, B. K., Khanna, S. N., Eds.; Plenum Press: New York, 1987; pp 439–444. Pacchioni, G.; Koutecký, J. *J. Chem. Phys.* **1988**, *88*, 1066–1073.
(258) Rao, B. K.; Khanna, S. N.; Jena, P. *Solid State Commun.* **1986**, *58*, 53–56; *Ultramicroscopy* **1986**, *20*, 51–54.
(259) Magers, D. H.; Harrison, R. J.; Bartlett, R. J. *J. Chem. Phys.* **1986**, *84*, 3284–3290.
(260) Ritchie, J. P.; King, H. F.; Young, W. S. *J. Chem. Phys.* **1986**, *85*, 5175–5181.
(261) Raghavachari, K.; Binkley, J. S. *J. Chem. Phys.* **1987**, *87*, 2191–2197; *Physics and Chemistry of Small Clusters*; Jena, P., Rao, B. K., Khanna, S. N., Eds.; Plenum Press: New York, 1987; pp 317–322.
(262) Ott, L. S.; Ray, A. K. *Physics and Chemistry of Small Clusters*; Jena, P., Rao, B. K., Khanna, S. N., Eds.; Plenum Press: New York, 1987; pp 95–101.
(263) Michalska, D.; Chojnacki, H.; Hess, B. A., Jr.; Schaad, L. J. *Chem. Phys. Lett.* **1987**, *141*, 376–379.
(264) Bernholdt, D. E.; Magers, D. H.; Bartlett, R. J. *J. Chem. Phys.* **1988**, *89*, 3612.
(265) Ewing, D. W.; Pfeiffer, G. V. *Chem. Phys. Lett.* **1987**, *134*, 413–417.
(266) Ewing, D. W.; Pfeiffer, G. V. *Physics and Chemistry of Small Clusters*; Jena, P., Rao, B. K., Khanna, S. N., Eds.; Plenum Press: New York, 1987, pp 67–72.
(267) Raghavachari, K.; Whiteside, R. A.; Pople, J. A. *J. Chem. Phys.* **1986**, *85*, 6623.
(268) Ortman, B. J. Ph.D. Thesis, Rice University, Houston, TX, 1987, unpublished.
(269) Krätschmer, W.; Nachtigall, K. *Polycyclic Aromatic Hydrocarbons and Astrophysics*; Léger, A., et al., Eds.; Reidel: Dordrecht, 1987; pp 75–83.
(270) Sanborn, R. H. *J. Chem. Phys.* **1968**, *49*, 4219–4221.
(271) Wdowiak, T. J. *Astrophys. J.* **1980**, *241*, L55–L58.
(272) Douglas, A. E. *Nature (London)* **1977**, *269*, 130.
(273) Krätschmer, W.; Sorg, N.; Huffman, D. R. *Surf. Sci.* **1985**, *156*, 814–821.
(274) Graham, W. R. M.; Dismuke, K. I.; Weltner, W., Jr. *Astrophys. J.* **1976**, *204*, 301–310.
(275) Van Zee, R. J.; Ferrante, R. F.; Zeringue, K. J.; Weltner, W., Jr. *J. Chem. Phys.* **1987**, *86*, 5212–5213.
(276) Van Zee, R. J.; Ferrante, R. F.; Zeringue, K. J.; Weltner, W., Jr. *J. Chem. Phys.* **1988**, *88*, 3465–3474.
(277) Stull, D. R.; Prophet, H. *Natl. Stand. Ref. Data Ser. (U.S., Natl. Bur. Stand.)* **1971**, *37*.
(278) Weltner, W., Jr. *Magnetic Atoms and Molecules*; Van Nostrand Reinhold: New York, 1983.
(279) Curl, R. F. *Mol. Phys.* **1965**, *9*, 585.
(280) Nemukhin, A. V. *Ves'tn. Mosk. Univ., Ser. 2: Khim.* **1982**, *23*, 336. Nemukhin, A. V.; Dement'ev, A. I.; Kolesnikov, A. I.; Stepanov, N. F.; Polyakov, V. I. *Teor. Eksp. Khim.* **1983**, *19*, 715.
(281) Ewing, D. W.; Pfeiffer, G. V. *Physics and Chemistry of Small Clusters*; Jena, P., Rao, B. K., Khanna, S. N., Eds.; Plenum Press: New York, 1987; pp 67–72.
(282) Vala, M.; Chandrasekhar, T. M.; Szczepanski, J.; Van Zee, R. J.; Weltner, W., Jr. *J. Chem. Phys.* **1989**, *90*, 595.
(283) Pickett, H. M.; Strauss, H. L. *J. Chem. Phys.* **1969**, *51*, 952–955.
(284) Rao, B. K.; Khanna, S. N.; Jena, P. *Solid State Commun.* **1986**, *58*, 53.
(285) Slanina, Z. *Chem. Phys. Lett.* **1987**, *142*, 512–514.
(286) Slanina, Z. *Thermochim. Acta* **1988**, *127*, 237–246.
(287) Cheshnovsky, O.; Yang, S.; Pettiette, C. L.; Craycraft, M. J.; Smalley, R. E. *Rev. Sci. Instrum.* **1987**, *58*, 2131–2137.
(288) Yang, S.; Taylor, K. J.; Craycraft, M. J.; Conceicao, J.; Pettiette, C. L.; Cheshnovsky, O.; Smalley, R. E. *Chem. Phys. Lett.* **1988**, *144*, 431–436.
(289) Yang, S. H.; Pettiette, C. L.; Conceicao, J.; Cheshnovsky, O.; Smalley, R. E. *Chem. Phys. Lett.* **1987**, *139*, 233–238.
(290) Smalley, R. E. "Down-to-Earth Studies of Carbon Clusters". NASA Conference on "Carbon in the Galaxy", November 1987, NASA Conference Report.
(291) Geusic, M. E.; Jarrold, M. F.; McIlrath, T. J.; Freeman, R. R.; Brown, W. L. *J. Chem. Phys.* **1987**, *86*, 3862–3869.
(292) McElvany, S. W.; Creasy, W. R.; O'Keefe, A. *J. Chem. Phys.* **1986**, *85*, 632.
(293) McElvany, S. W.; Dunlap, B. I.; O'Keefe, A. *J. Chem. Phys.* **1987**, *86*, 715–725.
(294) (a) McElvany, S. W. *J. Chem. Phys.* **1988**, *89*, 2063–2075. (b) Parent, D. C.; McElvany, S. W., submitted for publication in *J. Am. Chem. Soc.*
(295) Mattauch, J.; Ewald, H.; Hahn, O.; Strassmann, F. *Z. Phys.* **1943**, *120*, 598–617.
(296) Dörnenburg, E.; Hintenberger, H. *Z. Naturforsch. A: Astrophys., Phys. Phys. Chem.* **1959**, *14A*, 765. Dörnenburg, E.; Hintenberger, H.; Franzen, J. *Z. Naturforsch. A: Astrophys. Phys. Phys. Chem.* **1961**, *16A*, 532. Franzen, J.; Hintenberger, H. *Z. Naturforsch. A: Astrophys. Phys. Phys. Chem.* **1961**, *16A*, 535. Hintenberger, H.; Franzen, J.; Schuy, K. D. *Z. Naturforsch. A: Astrophys. Phys. Phys. Chem.* **1963**, *18A*, 1236–1237.
(297) Bykovský, Ju. A.; Zuravlev, G. I.; Belousov, V. I.; Gladskoj, V. M.; Degtyarev, V. G.; Kolosov, Ju. N.; Nevolin, V. N. *Fiz. Plasmy (Moscow)* **1978**, *4*, 323.
(298) Dietze, H.-J.; Becker, S.; Opauszky, I.; Matus, L.; Nyâry, I.; Frecska, J. *Mikrochim. Acta* **1983**, 263.
(299) Becker, S.; Dietze, H.-J.; Pompe, W. *Z. Chem.* **1986**, *26*, 453–454.
(300) Leleyter, M.; Joyes, P. *Radiat. Eff.* **1973**, *18*, 105; *J. Phys. (Les Ulis, Fr.)* **1975**, *36*, 343–353.
(301) Fürstenau, N.; Hillenkamp, F. *Int. J. Mass Spectrom. Ion Phys.* **1981**, *37*, 135–151.
(302) Clarke, N. S.; Daver, A. R.; Ruckman, J. C. *Microbeam Anal.* **1984**, *19th*, 40–44.
(303) Cornides, I. *Int. J. Mass Spectrom. Ion Phys.* **1982**, *45*, 219.
(304) Honig, R. E. *Adv. Mass Spectrom.* **1963**, *2*, 25–37.
(305) O'Keefe, A.; Ross, M. M.; Baronavski, A. P. *Chem. Phys. Lett.* **1986**, *130*, 17–19.
(306) Cox, D. M.; Reichmann, K. C.; Kaldor, A. *J. Chem. Phys.* **1988**, *88*, 1588–1597.
(307) Knight, R. D.; Walch, R. A.; Foster, S. C.; Miller, T. A.; Mullen, S. L.; Marshall, A. G. *Chem. Phys. Lett.* **1986**, *129*, 331–335.
(308) Hahn, M. Y.; Honea, E. C.; Paguia, A. J.; Schriver, K. E.; Camerena, A. M.; Whetten, R. L. *Chem. Phys. Lett.* **1986**, *130*, 12–16.
(309) Liu, Y.; O'Brien, S. C.; Zhang, Q.; Heath, J. R.; Tittel, F. K.; Curl, R. F.; Kroto, H. W.; Smalley, R. E. *Chem. Phys. Lett.* **1986**, *126*, 215–217.
(310) Kappes, M. M.; King, R. W.; Schumacher, E. *Chem. Phys. Lett.* **1982**, *91*, 413. Knight, W. D.; Clemenger, K.; de Heer, W. A.; Saunders, W. A.; Chou, M. Y.; Cohen, M. L. *Phys. Rev. Lett.* **1984**, *52*, 2141.
(311) Kroto, H. W.; Heath, J. R.; O'Brien, S. C.; Curl, R. F.; Smalley, R. E. *Nature (London)* **1985**, *318*, 162–163.
(312) Joyes, P.; Leleyter, M. *J. Phys. (Les Ulis, Fr.)* **1984**, *45*, 1681–1688.
(313) Seifert, G. *ZfI-Mitt., Leipzig* **1987**, *134*, 49–64.

(314) Ray, A. K. *J. Phys. B*: **1987**, *20*, 5233–5239.
(315) Van Vechten, J. A.; Keszler, D. A. *Phys. Rev.* **1987**, *B36*, 4570–4573.
(316) Bochvar, D. A.; Gal'pern, E. G. *Dokl. Akad. Nauk SSSR* **1973**, *209*, 610; *Dokl. Chem.* (*Engl. Transl.*) **1973**, *209*, 239–241; Stankevich, I. V.; Nikerov, M. V.; Bochvar, D. A. *Russ. Chem. Rev.* (*Engl. Transl.*) 1984, *53*, 640.
(317) Larsson, S.; Volosov, A.; Rosên, A. *Chem. Phys. Lett.* **1987**, *137*, 501–504.
(318) Heath, J. R.; O'Brien, S. C.; Curl, R. F.; Kroto, H. W.; Smalley, R. E. *Comments Condens. Matter Phys.* **1987**, *13*, 119–141.
(319) Heath, J. R.; O'Brien, S. C.; Curl, R. F.; Kroto, H. W.; Smalley, R. E., submitted for publication in *Acc. Chem. Res.*
(320) Heath, J. R.; O'Brien, S. C.; Zhang, Q.; Liu, Y.; Curl, R. F.; Kroto, H. W.; Tittel, F. K.; Smalley, R. E. *J. Am. Chem. Soc.* **1985**, *107*, 7779–7780.
(321) O'Brien, S. C.; Heath, J. R.; Kroto, H. W.; Curl, R. F.; Smalley, R. E. *Chem. Phys. Lett.* **1986**, *132*, 99–102.
(322) Iijima, S. *J. Phys. Chem.* **1987**, *91*, 3466–3467.
(323) Kroto, H. W.; McKay, K. *Nature* (*London*) **1988**, *331*, 328–331.
(324) Kroto, H. W. *Nature* (*London*) **1987**, *329*, 529–531.
(325) Jones, D. E. H. *New Sci.* **1966**, *245*, 118–119.
(326) Osawa, E. *Kagaku* **1970**, *25*, 854.
(327) Davidson, R. A. *Theor. Chim. Acta* 1981, *58*, 193–231.
(328) Haymet, A. D. J. *Chem. Phys. Lett.* **1985**, *122*, 421; *J. Am. Chem. Soc.* **1986**, *108*, 319–321.
(329) Klein, D. J.; Schmalz, T. G.; Hite, G. E.; Seitz, W. A. *J. Am. Chem. Soc.* **1986**, *108*, 1301.
(330) Ozaki, M.; Takahashi, A. *Chem. Phys. Lett.* **1986**, *127*, 242–244.
(331) Haddon, R. C.; Brus, L. E.; Raghavachari, K. *Chem. Phys. Lett.* **1986**, *125*, 459–464.
(332) Brown, W. B. *Chem. Phys. Lett.* **1987**, *136*, 128–133.
(333) Coulombeau, C.; Rassat, A. *J. Chim. Phys. Phys.-Chim. Biol.* **1987**, *84*, 875–882.
(334) Schmalz, T. G.; Seitz, W. A.; Klein, D. J.; Hite, G. E. *Chem. Phys. Lett.* **1986**, *130*, 203–207.
(335) Klein, D. J.; Seitz, W. A.; Schmalz, T. G. *Nature* (*London*) **1986**, *323*, 703–706.
(336) Otto, A. *Z. Chem.* **1987**, *10*, 380–381.
(337) Newton, M. D.; Stanton, R. E. *J. Am. Chem. Soc.* **1986**, *108*, 2469–2470.
(338) McKee, M. L.; Herndon, W. C. *J. Mol. Struct.* **1987**, *153*, 75–84.
(339) Haddon, R. C.; Brus, L. E.; Raghavachari, K. *Chem. Phys. Lett.* **1986**, *131*, 165–169.
(340) Hale, P. D. *J. Am. Chem. Soc.* **1986**, *108*, 6087.
(341) Satpathy, S. *Chem. Phys. Lett.* **1986**, *130*, 545–550.
(342) Marynick, D. S.; Estreicher, S. *Chem. Phys. Lett.* **1986**, *132*, 383–386.
(343) Fowler, P. W.; Woolrich, J. *Chem. Phys. Lett.* **1986**, *127*, 78–83.
(344) Lâszlô, I.; Udvardi, L. *Chem. Phys. Lett.* **1987**, *136*, 418–422.
(345) Shibuya, T.-I.; Yoshitani, M. *Chem. Phys. Lett.* **1987**, *137*, 13–16.
(346) Hayden, G. W.; Mele, E. J. *Phys. Rev.* **1987**, *B36*, 5010–5015.
(347) Disch, R. L.; Schulman, J. M. *Chem. Phys. Lett.* **1986**, *125*, 465.
(348) Schulman, J. M.; Disch, R. L.; Miller, M. A.; Peck, R. C. *Chem. Phys. Lett.* **1987**, *141*, 45–47.
(349) Lüthi, H. P.; Almlöf, J. *Chem. Phys. Lett.* **1987**, *135*, 357–360.
(350) Wu, Z. C.; Jelski, D. A.; George, T. F. *Chem. Phys. Lett.* **1987**, *137*, 291–294.
(351) Weeks, D. E.; Harter, W. G. *Chem. Phys. Lett.* **1988**, *144*, 366–372.
(352) Schmalz, T. G.; Seitz, W. A.; Klein, D. J.; Hite, G. E. *J. Am. Chem. Soc.* **1988**, *110*, 1113–1127.
(353) Stone, A. J.; Wales, D. J. *Chem. Phys. Lett.* **1986**, *128*, 501.
(354) Cox, D. M.; Trevor, D. J.; Reichmann, K. C.; Kaldor, A. *J. Am. Chem. Soc.* **1986**, *108*, 2457.
(355) Dick, B.; Nickel, B. *Chem. Phys.* **1983**, *78*, 1.
(356) O'Brien, S. C.; Heath, J. R.; Curl, R. F.; Smalley, R. E. *J. Chem. Phys.* **1988**, *88*, 220–230.
(357) Heath, J. R.; Curl, R. F.; Smalley, R. E. *J. Chem. Phys.* **1987**, *87*, 4236.
(358) Fowler, P. W. *Chem. Phys. Lett.* **1986**, *131*, 444–449.
(359) Suzuki, H. *Astrophys. J.* **1983**, *272*, 579–590.
(360) Freed, K. F.; Oka, T.; Suzuki, H. *Astrophys. J.* **1982**, *263*, 718–722.
(361) Kroto, H. W.; Heath, J. R.; O'Brien, S. C.; Curl, R. F.; Smalley, R. E. *Astrophys. J.* **1987**, *314*, 352–355.
(362) Tielens, A. G. G. M. "Carbon in the Galaxy: Studies from Earth and Space". NASA *Conf. Publ.*, in press.
(363) Gerhardt, Ph.; Loffler, S.; Homann, K. H. *Chem. Phys. Lett.* **1987**, *137*, 306–310.
(364) Rudzinski, J. M.; Slanina, Z.; Togasi, M.; Osawa, E. *Thermochim. Acta* 1988, *125*, 155–162.
(365) Elser, V.; Haddon, R. C. *Nature* (*London*) **1987**, *325*, 792–794.
(366) Curtis, M. C.; Sarre, P. J. *Mol. Phys.* **1988**, *65*, 225.
(367) Goodwin, P. M.; Cool, T. A. *J. Mol. Spectrosc.* **1989**, *133*, 230.
(368) Rohlfing, E. A. *J. Chem. Phys.* **1988**, *89*, 6103.
(369) Anselment, M.; Smith, R. S.; Daykin, E.; DiMauro, L. F. *Chem. Phys. Lett.* **1987**, *134*, 444.
(370) Davis, S. P.; Abrams, M. C.; Phillips, J. G.; Rao, M. L. P. *J. Opt. Soc. Am. B*: *Opt. Phys.* **1988**, *5*, 2280–2285.
(371) Rohlfing, E. A.; Goldsmith, J. E. M. *J. Chem. Phys.* **1989**, *90*, 6804.
(372) Snow, T. P.; Seab, C. G.; Joseph, C. L. *Astrophys. J.* **1988**, *335*, 185.
(373) Martin, J. M. L.; Francois, J. P.; Gijbels, R. *J. Chem. Phys.* **1989**, *90*, 3403.
(374) Bernath, P. F.; Hinkle, K. H.; Keady, J. J. *Science* **1989**, *244*, 562.
(375) Moazzen-Ahmadi, N.; McKellar, A. R. W.; Amano, T. *Chem. Phys. Lett.* **1989**, *157*, 1.
(376) Heath, J. R.; Cooksy, A. L.; Gruebele, M. H. W.; Schuttenmaer, C. A.; Saykally, R. J. *Science* **1989**, *244*, 564.
(377) Parasuk, V.; Almlöf, J. *J. Chem. Phys.* **1989**, *91*, 1137.
(378) Seifert, G.; Becker, S.; Dietze, H.-J. *Int. J. Mass Spectrom. Ion Processes* **1988**, *84*, 121–133.
(379) Radi, P. P.; Bunn, T. L.; Kemper, P. R.; Molchan, M. E.; Bowers, M. T. *J. Chem. Phys.* **1988**, *88*, 2809.
(380) Almlöf, J.; Lüthi, H. P. *Supercomputer Research in Chemistry and Chemical Engineering*; ACS Symposium Series 353; American Chemical Society: Washington, DC, 1987; Chapter 3.
(381) Stanton, R. E.; Newton, M. D. *J. Am. Chem. Soc.* **1988**, *92*, 2141.
(382) Rosên, A.; Wâstberg, B. *J. Chem. Phys.* **1989**, *90*, 2525.
(383) Brendsdal, E. *Spectrosc. Lett.* **1988**, *21*, 319–339.
(384) Brendsdal, E.; Cyvin, B. N.; Brunvoll, J.; Cyvin, S. J. *Spectrosc. Lett.* 1988, *21*, 313–318.
(385) Kroto, H. *Science* **1988**, *242*, 1139.
(386) Kroto, H. W. *Proc. R. Inst. G.B.* **1986**, *58*, 45.
(387) Kroto, H. W. *Philos. Trans. R. Soc. London, B* **1988**, *325A*, 405.
(388) Wright, E. L. *Nature* (*London*) **1988**, *336*, 227.
(389) Lêger, A.; d'Hendecourt, L.; Verstraete, L.; Schmidt, W. *Astron. Astrophys.* **1988**, *203*, 145–148.
(390) Algranati, M.; Feldman, H.; Kella, D.; Malkin, E.; Miklazky, E.; Naaman, R.; Vager, Z.; Zajfman, J. *J. Chem. Phys.* **1989**, *90*, 4617–4618.